TOR VERGATA
UNIVERSITÀ DEGLI STUDI DI ROMA

Development of Computational Tools for Cardiovascular Applications

Eirini Kardampiki

Under the supervision of:

Prof. Marco Evangelos Biancolini

Dr. Emiliano Costa

Dr. Karen-Hele Støverud

MEDITATE RINA SINTEF

February 23rd , 2024

XXXVI Ph.D. cycle
Academic Year:

Department of Enterprise Engineering "Mario Lucertini"

My MeDiTATe journey

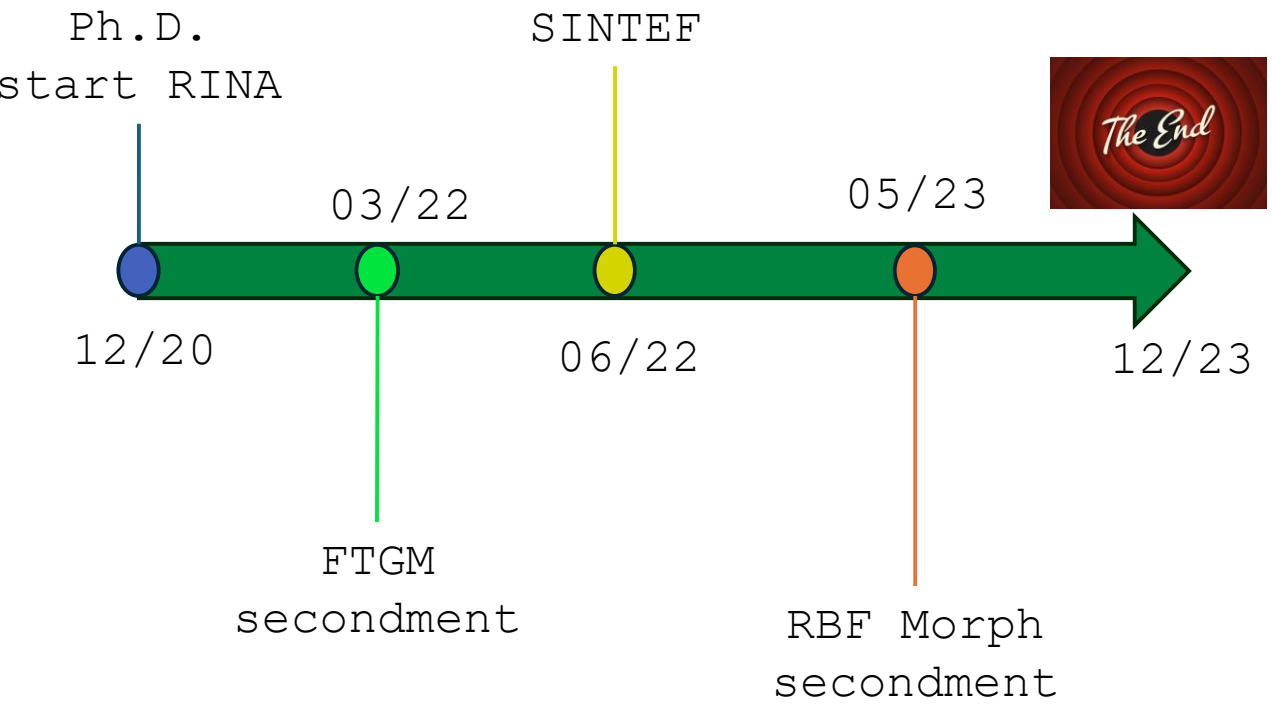

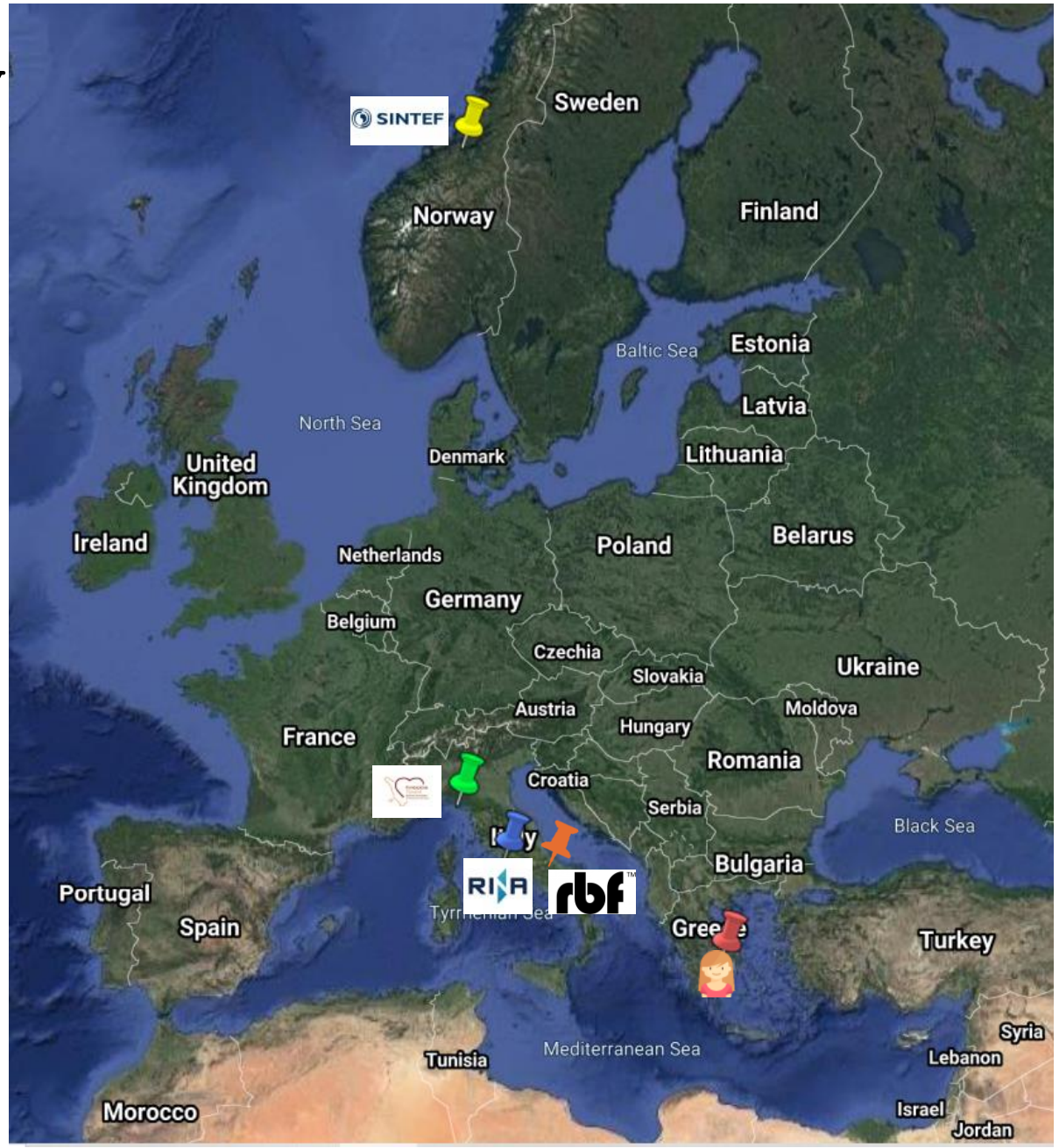

Cardiovascular diseases (CVDs)

Cardiovascular diseases (CVDs) are the leading cause of death globally.

World Health Organization

Financial impact of 282 billion € for the EU economy in 2021

Oxford Population Health's Health Economics Research Centre

1.8 million deaths in Europe in 2020

Eurostat European Commission

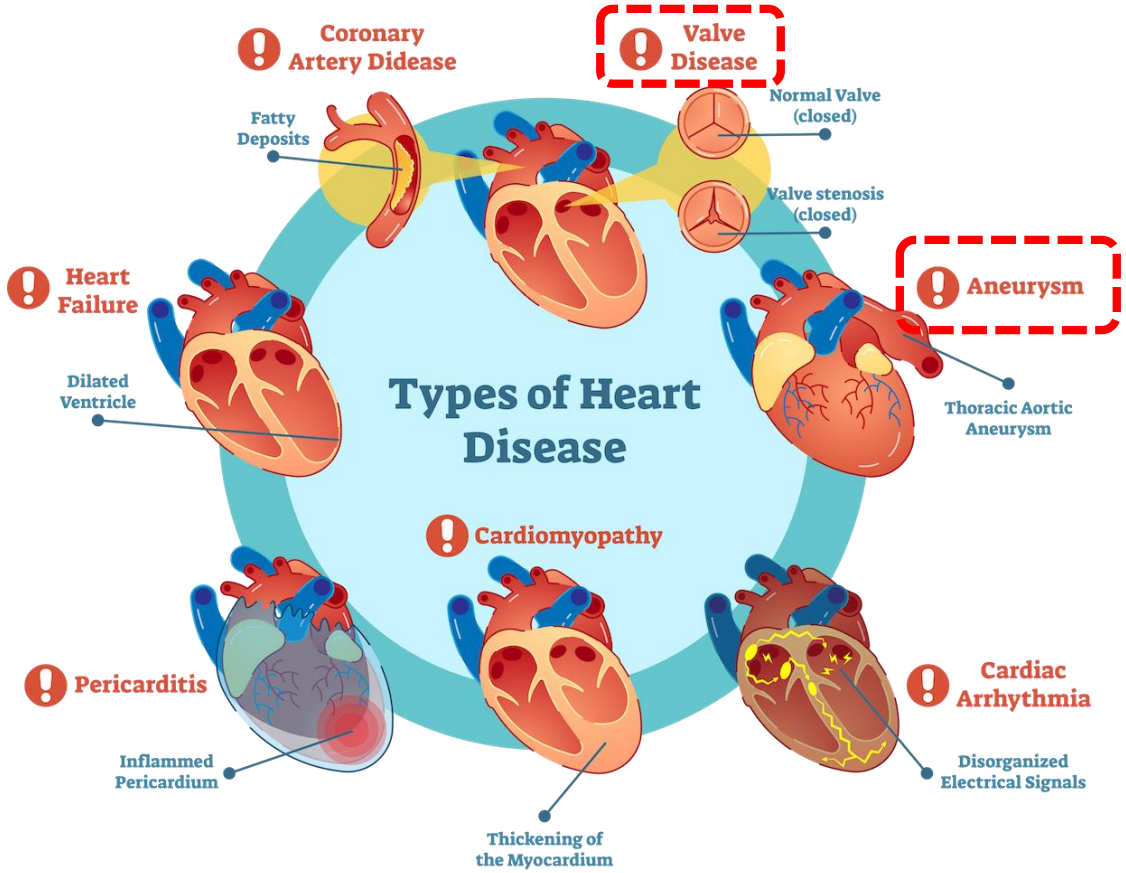

Pulmonary Atresia

Pulmonary atresia is a congenital heart defect where the valve controlling blood flow from the heart to the lungs fails to form.

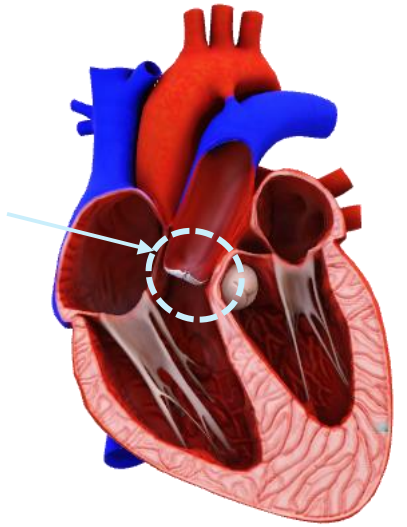

Occurrence rate: 1 in every 7,100 babies born in the United States yearly

Palliative treatment: **Modified Blalock-Taussig Shunt (MBTS) procedure**

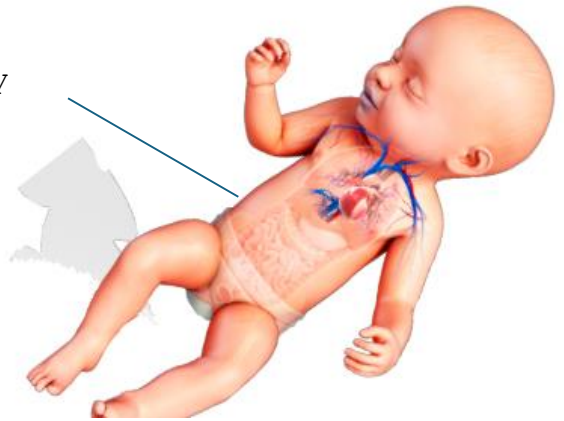

Overall mortality and composite morbidity rates: 7.2% and 13.1% respectively.

Modified Blalock-Taussig Shunt

MBTS Implant
- Synthetic graft providing oxygenated blood to the pulmonary from the systemic circulation
- Choice of size according to surgeon experience

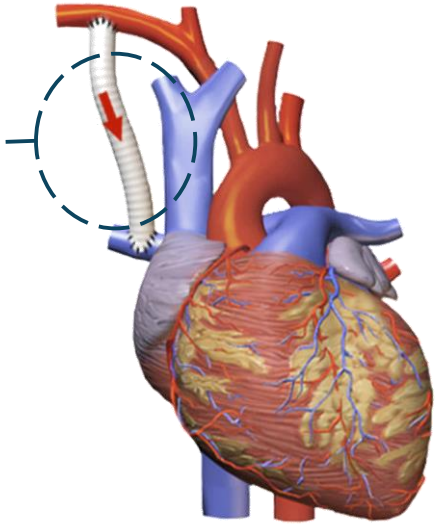

Oversized MBTS → ✗ Pressure and systemic perfusion drop

Undersized MBTS → ✗ Thrombosis risk

Issue: necessity for a reliable tool to predict the MBTS implant outcome

→ Aim: The development of a fast and interactive pipeline for the analysis of different complex implant configurations in a patient-specific case.

Study I

Abdominal Aortic Aneurysms (AAAs)

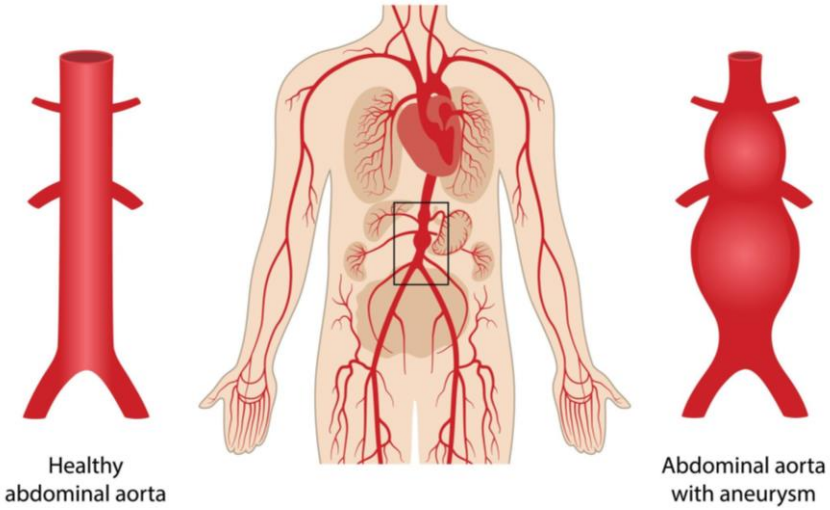

Treatment for abdominal aortic aneurysm: 10^6/year operations worldwide

- Open surgery: 30%
- Endovascular Aneurysm Repair (EVAR): 70%

Abdominal Aortic Aneurysms (AAAs)

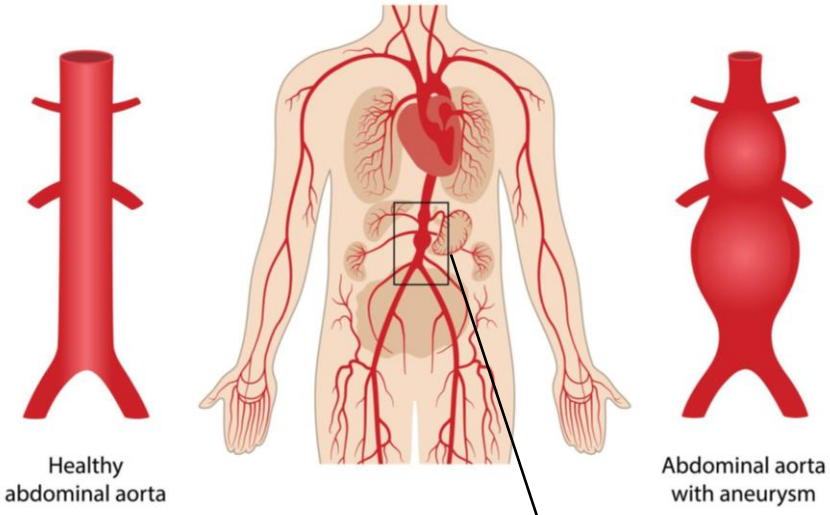

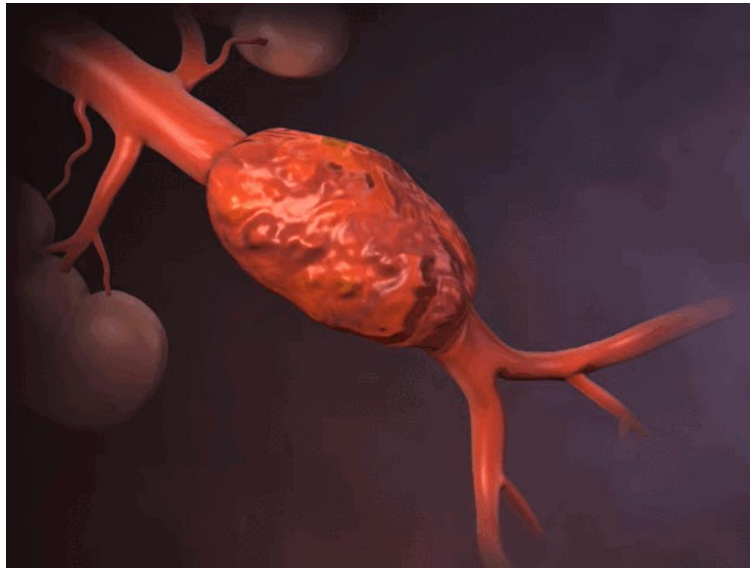

Treatment for abdominal aortic aneurysm: 10^6/year operations worldwide

- Open surgery: 30%
- Endovascular Aneurysm Repair (EVAR): 70%

EVAR Planning and Navigation Challenges

Preoperative volume **Deformed volume**

Stiff guidewire outside of the aortic boundaries

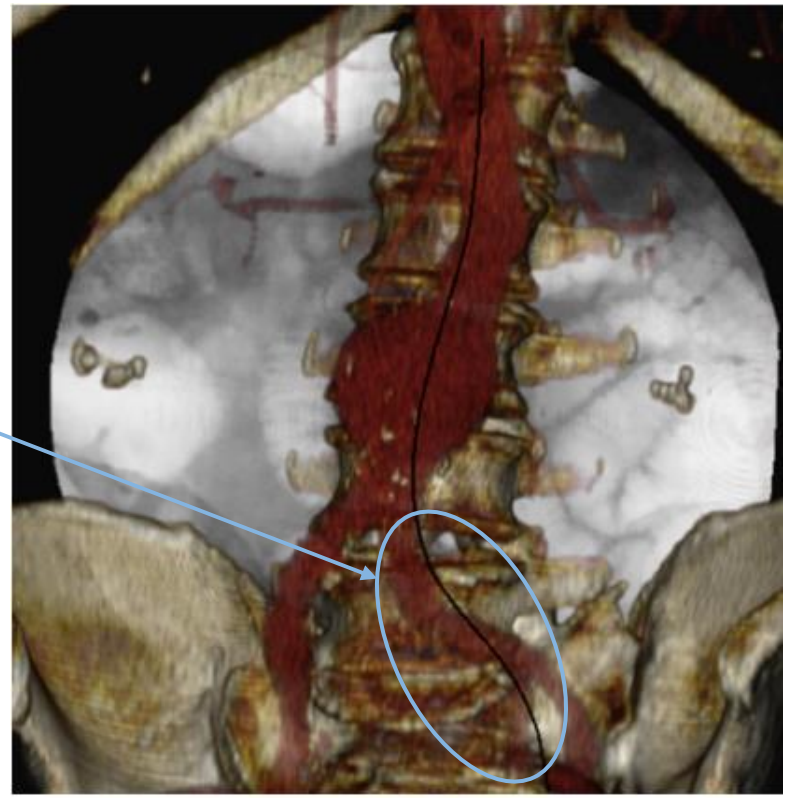

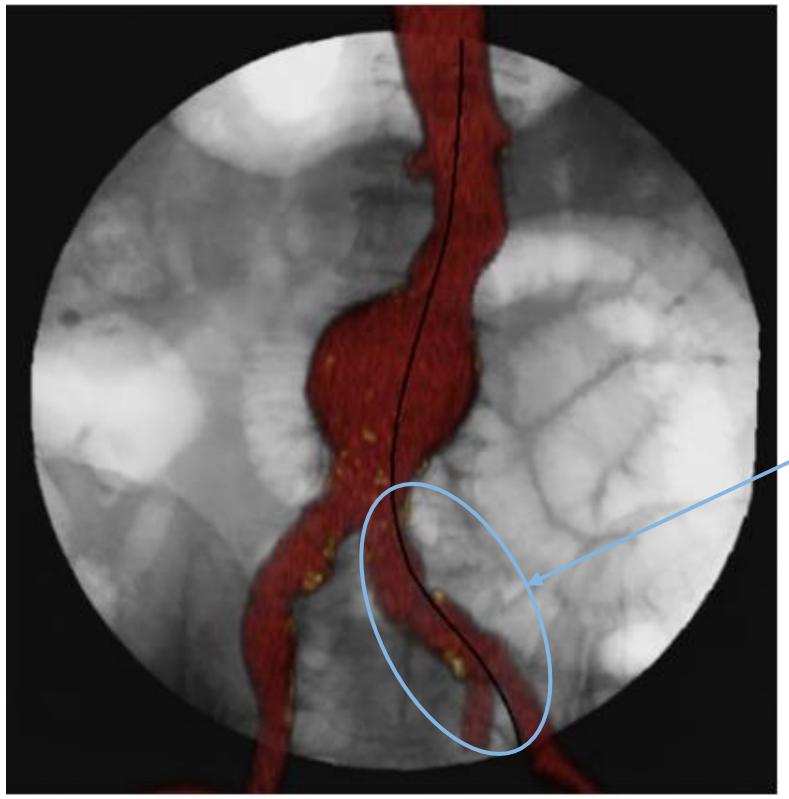

Stiff guidewire within the aortic boundaries

Kaladji A, et al., Comput Med Imaging Graph. 2013

EVAR Planning and Navigation Challenges

Issue: Difficulty in the estimation of guidewire-induced deformations

- Radiations and contrast
- Risk of failure
- Post-operative complications

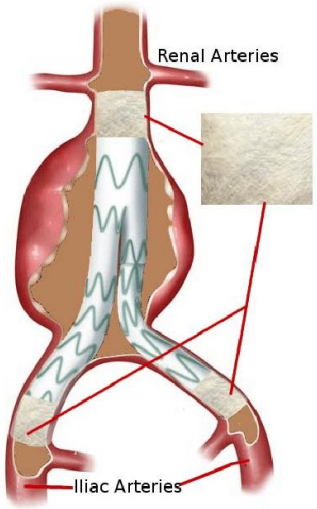

Aim: Provide clinicians with a fast and accurate tool for predicting guidewire-induced deformations

Study II

Post-EVAR Intraluminal Thrombus Formation (IPT)

Varying incidence rate up to 36%

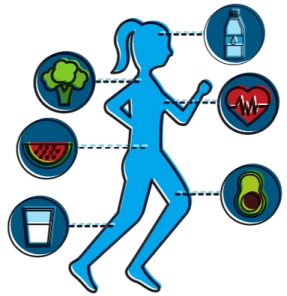

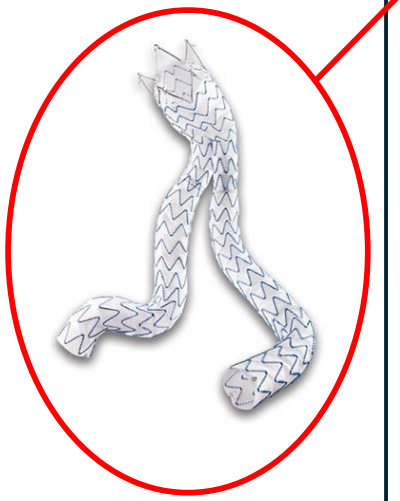

Stent graft type

Factors linked with IPT

Post-EVAR Thrombus formation and stentgrafts

Popular commercial AAA grafts

- Zenith Alpha
- Excluder
- Endurant II

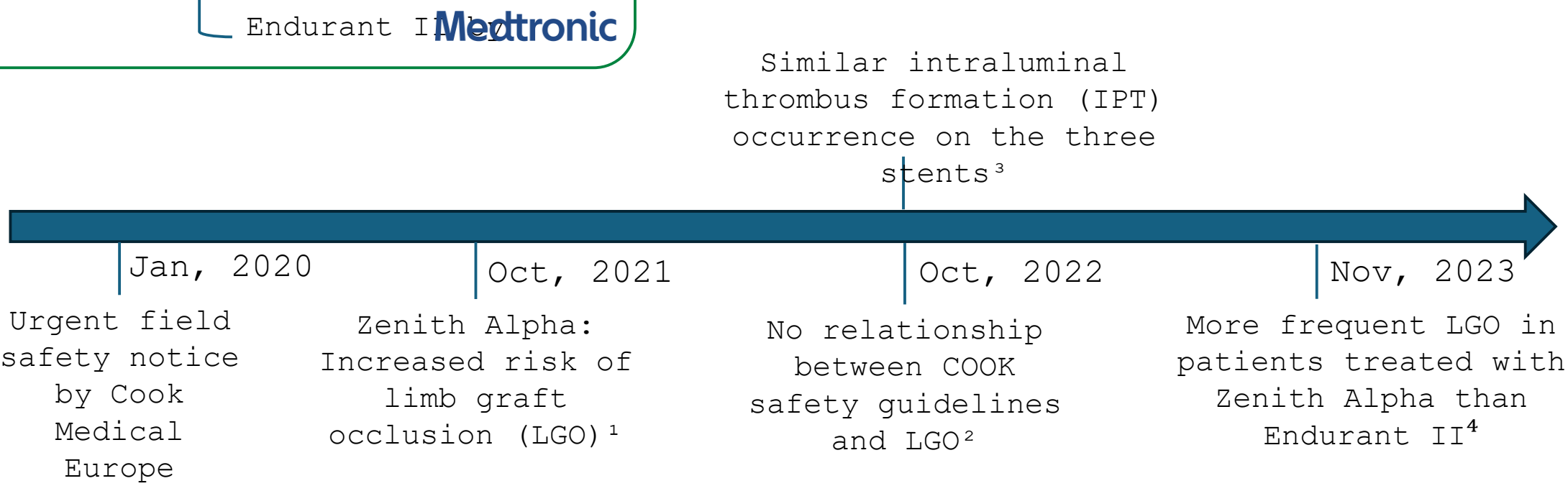

[1] Bogdanovic, Marko, et al. "Limb graft occlusion following endovascular aneurysm repair for infrarenal abdominal aortic aneurysm with the Zenith Alpha, Excluder, and Endurant devices: a multicentre cohort study." *European Journal of Vascular and Endovascular Surgery* 62.4 (2021): 532-539.
[2] Broda, Magdalena, et al. "Limb graft occlusion after endovascular aneurysm repair with the Cook Zenith Alpha abdominal graft." *Journal of Vascular Surgery* 77.3 (2023): 770-777.
[3] Draper, Kian, et al. "Evaluation of factors associated with limb thrombus formation after endovascular aortic aneurysm repair." *Journal of Vascular Surgery* 77.2 (2023): 440-445.
[4] Ulsaker, Håvard, et al. "A retrospective evaluation of intra-prosthetic thrombus formation after endovascular aortic repair in cook zenith alpha and Medtronic endurant II patients." *European Journal of Vascular and Endovascular Surgery* 66.5 (2023): 644-651.

Post-EVAR Thrombus formation and stentgrafts

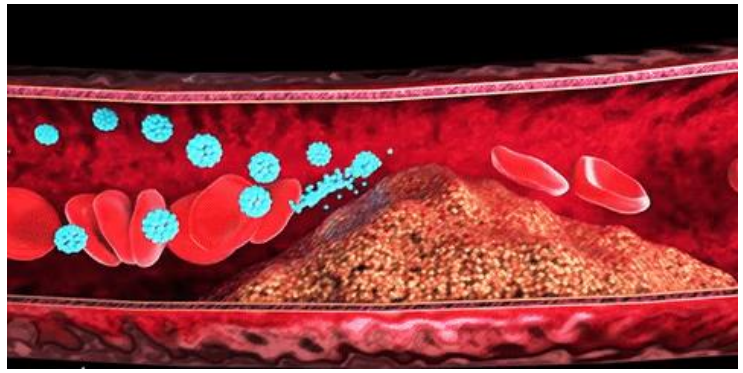

Issue: more frequent thrombotic events of Zenith Alpha stent graft

Aim: Blood flow analysis of three simplified commercial AAA stent grafts for detecting thrombotic predictors

Study III

Overview of the performed studies

- Development of Reduced Order Model for the support of modified Blalock Taussig shunt (MBTS) procedures — Study I
- Development of Reduced Order Model for the assisting of the pre-operative planning and intra-operative EVAR navigation — Study II
- Investigation of the post-EVAR thrombotic events on simplified abdominal commercial stent grafts, through computational fluid dynamic simulations — Study III

Study I: Modified Blalock Taussig Shunt ROM

Case of pulmonary atresia

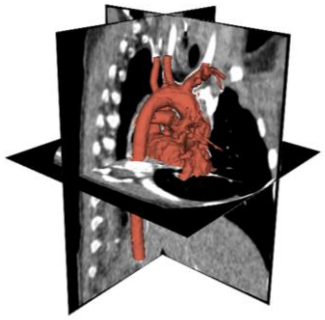

CTA data segmentation

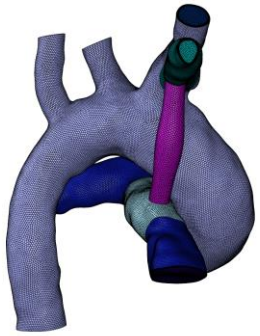

Baseline case

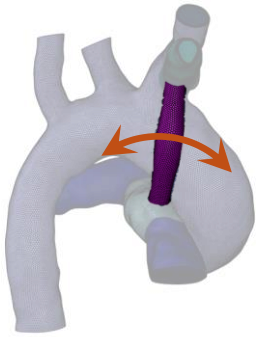

12 RBF shape modifiers

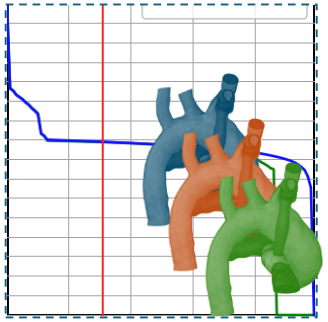

ROM Build-up

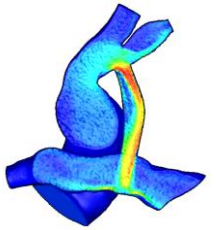

ROM Exploitation

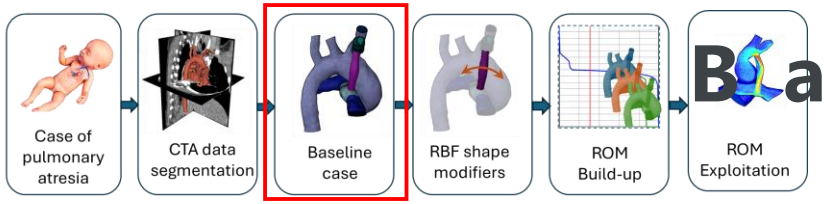

Baseline CFD case

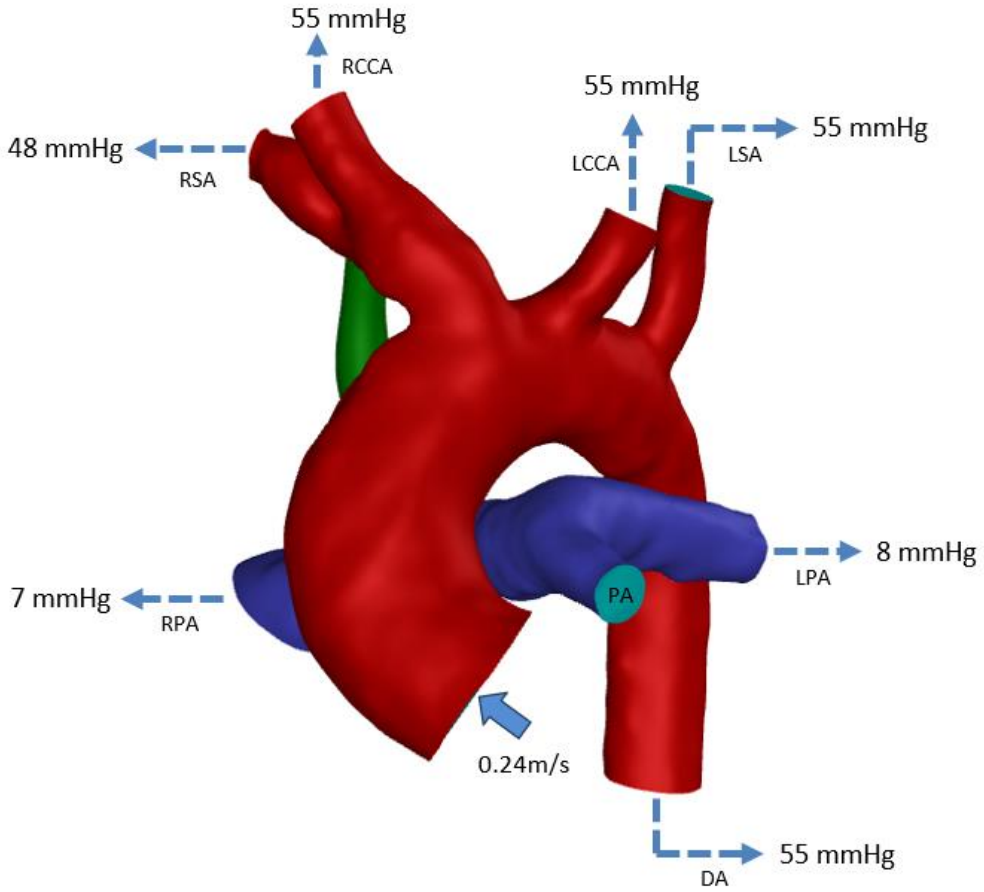

Blood properties

- Newtonian fluid
- Density $\rho=1060 kg/m^3$
- Viscosity $\eta=0.0035$ Pa s

Flow modeling

- k-ω SST model
- Steady state regime

Quantities of interest

- Surface pressure
- Surface wall shear stress (WSS)
- Volume velocity

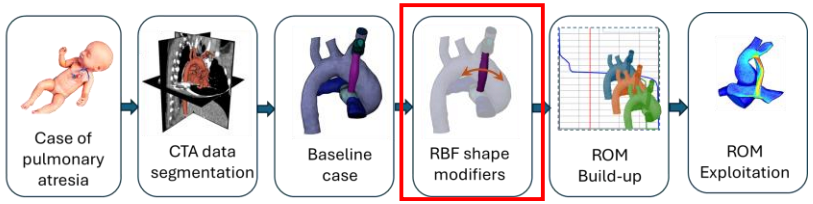

Twelve RBF Shape Modifiers

x translation

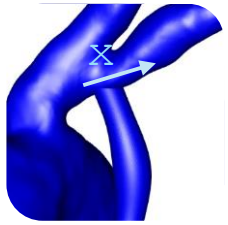

y translation

y rotation

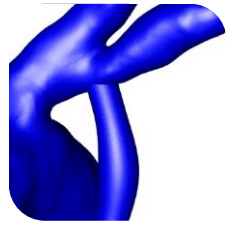

x rotation

Superior MBTS boundary SP

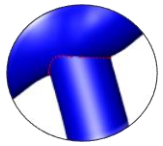

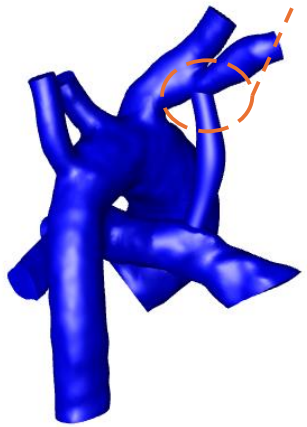

Cylindrical periphery SP

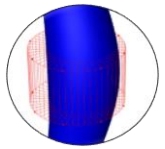

Maximum diameter SP

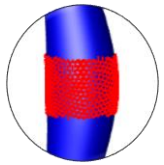

Inferior MBTS boundary SP

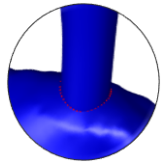

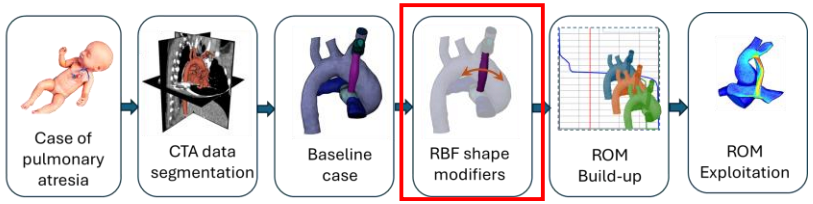

Twelve RBF Shape Modifiers

x translation | y translation | y rotation | x rotation

Superior MBTS boundary SP

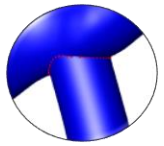

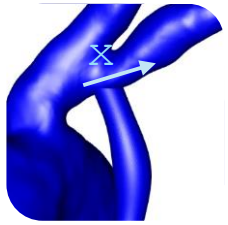

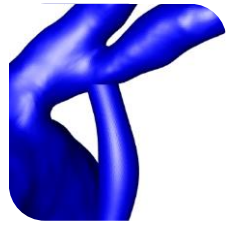

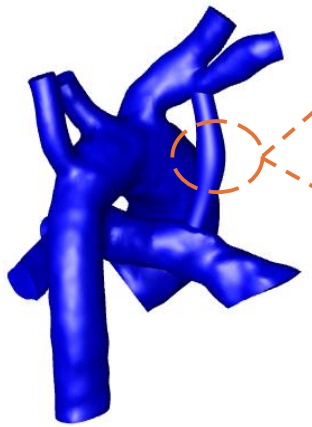

Cylindrical periphery SP

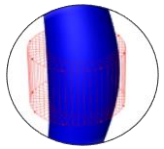

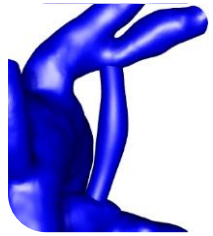

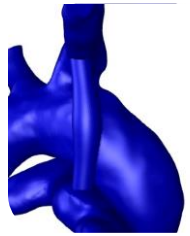

Maximum diameter SP

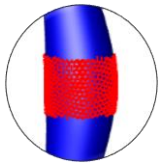

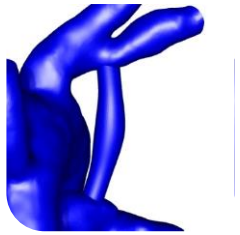

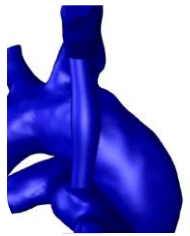

Inferior MBTS boundary SP

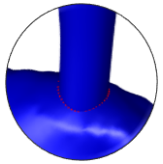

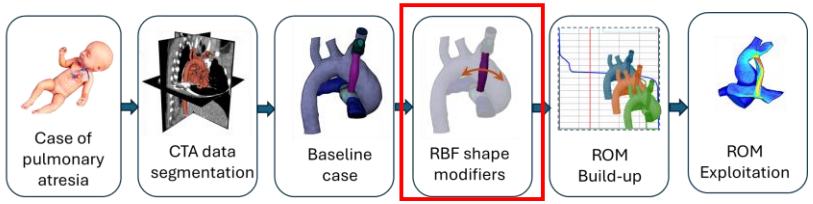

Twelve RBF Shape Modifiers

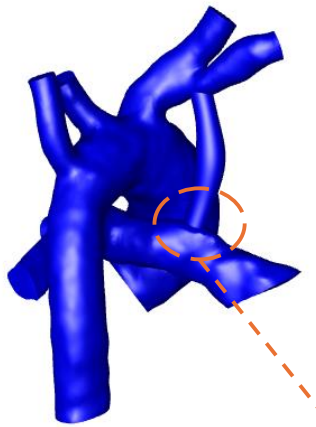

x translation | y translation | y rotation | x rotation

Superior MBTS boundary SP

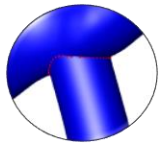

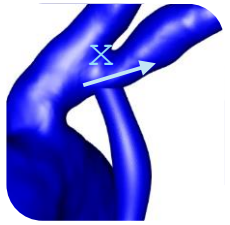

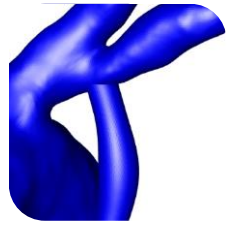

Cylindrical periphery SP

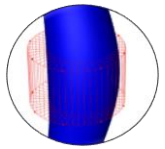

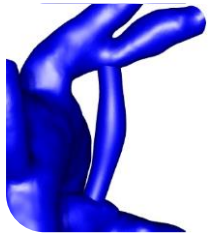

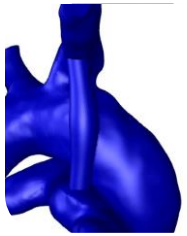

Maximum diameter SP

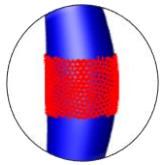

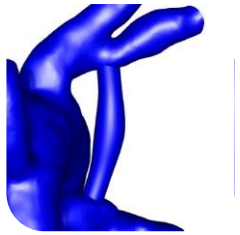

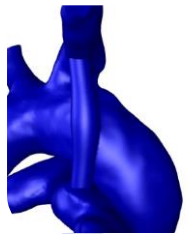

Inferior MBTS boundary SP

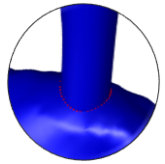

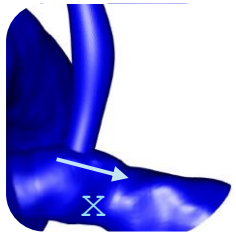

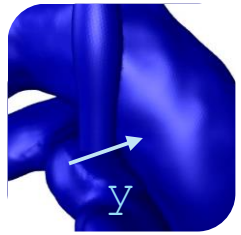

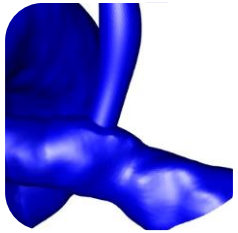

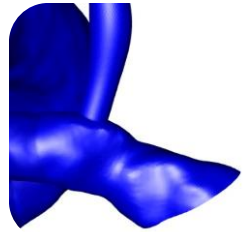

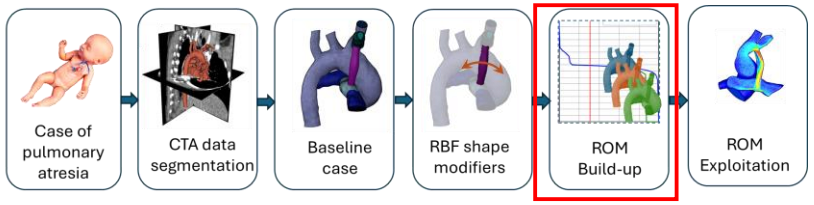

ROM Build-up: General Concept

$$\mathbf{A}_r^* = \mathbf{U}_r^* \, \mathbf{S}_r^* \, \mathbf{V}_r^{\mathrm{T}*} = \mathbf{U}_r^* \, \mathbf{C}$$

$$\mathbf{C} = [\alpha_1, \alpha_2, \ldots, \alpha_r]$$

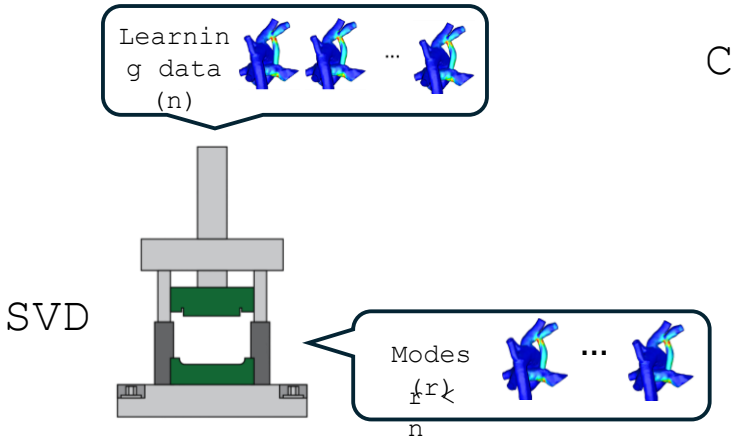

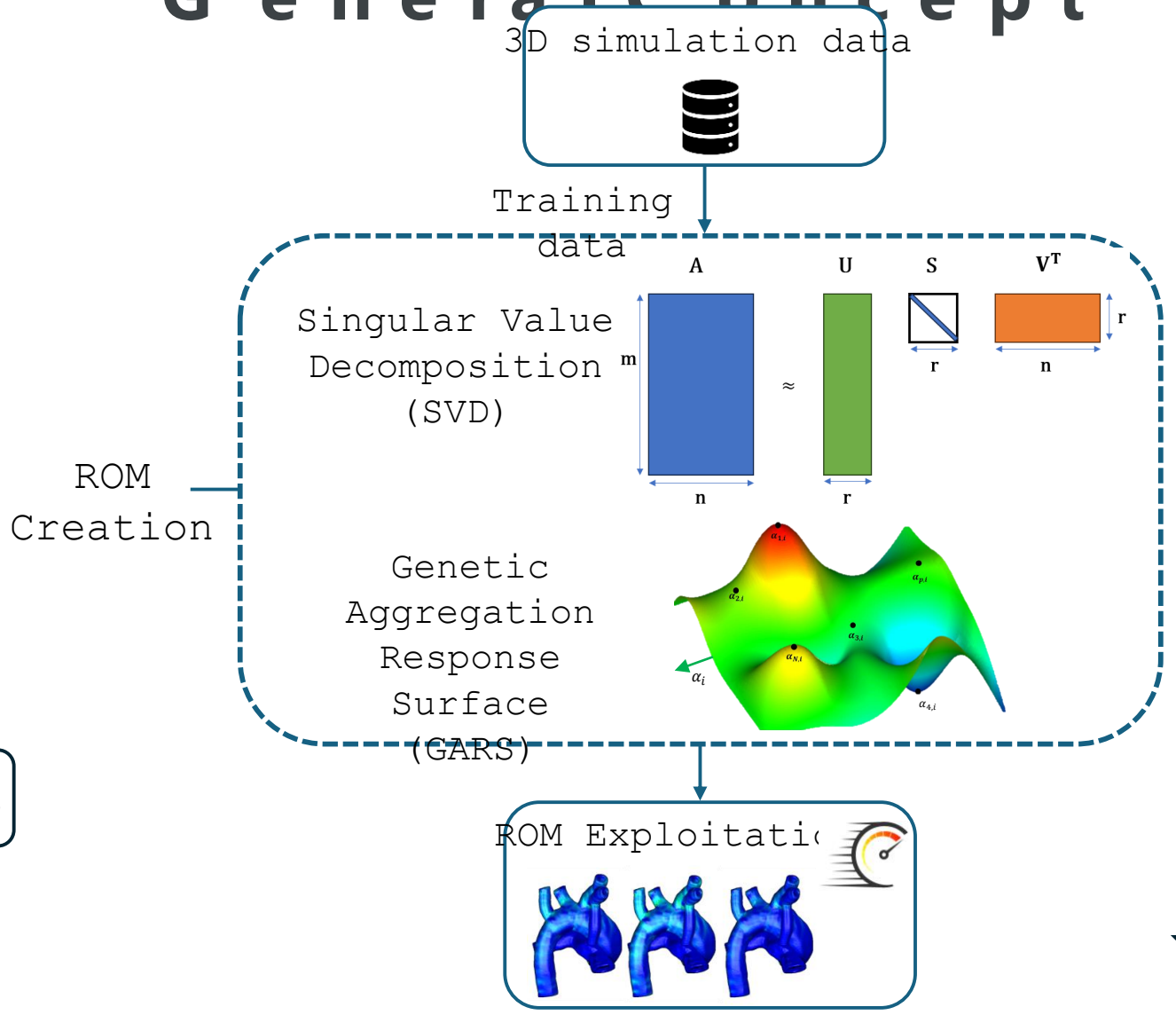

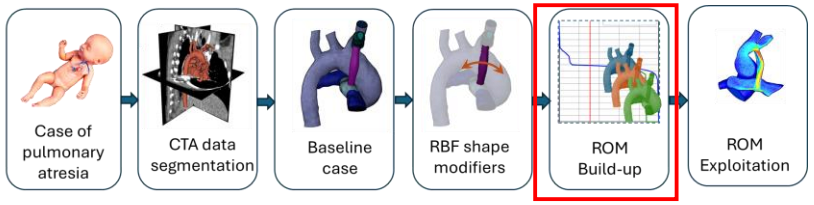

ROM Build-up: MBTS Study

$$e_{\text{red}}^{\text{RMS}} = \frac{\|\mathbf{A} - \mathbf{A}_r^*\|}{\|\mathbf{A}\|}$$

Scenarios generation:

- Optimal-Space Filling a

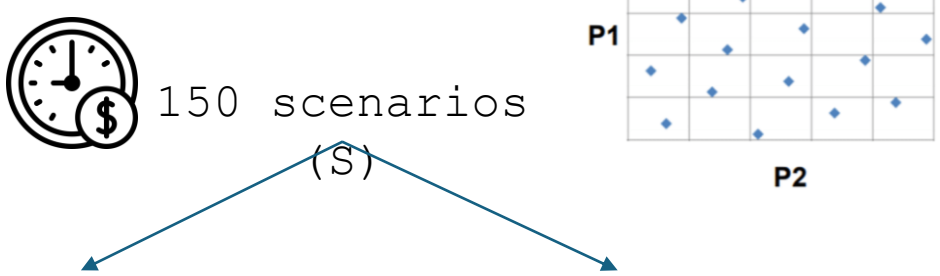

150 scenarios (S)

120 scenarios for the ROM build-up

30 scenarios for ROM verification

Flow field variable	Number of modes (r)	$e_{\text{red}}^{\text{RMS}}(\%)$
Pressure	27	0.2
Wall Shear Stress (WSS)	22	6
Velocity	18	7.4

Why so big differences?

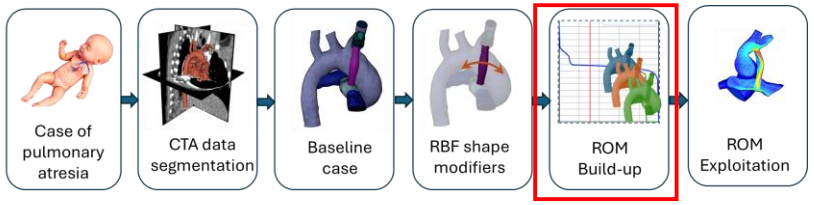

ROM Build-up: MBTS Study

$$e_{\text{red}}^{\text{RMS}} = \frac{\|\mathbf{A} - \mathbf{A}_r^*\|}{\|\mathbf{A}\|}$$

Scenarios generation:

- Optimal-Space Filling a

150 scenarios (S)

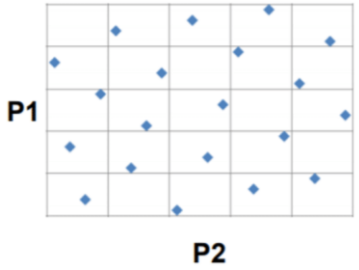

120 scenarios for the ROM build-up

30 scenarios for ROM verification

Flow field variable	Number of modes (r)	$e_{\text{red}}^{\text{RMS}}(\%)$
Pressure	27	0.2
Wall Shear Stress (WSS)	22	6
Velocity	18	7.4

Pressure: scalar + surface calculated
WSS: vector + surface calculated
Velocity: vector + volume calculated

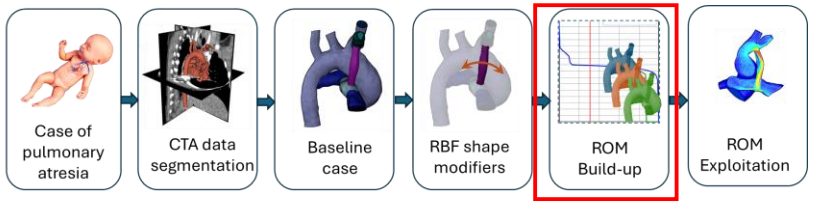

ROM Verification: Velocity

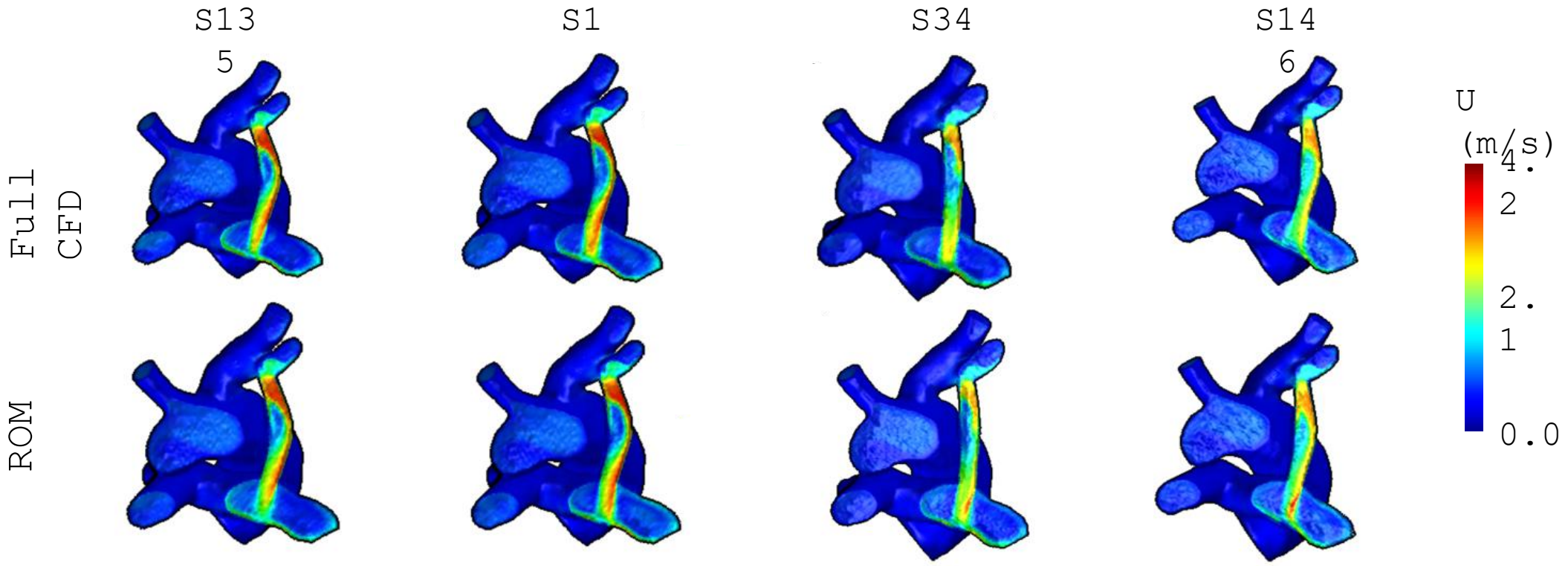

- Velocity maps on MBTS cross-section
- Results on exemplificative scenarios report agreement between ROM results and full CFDs
- Higher discrepancies limited to inferior section of MBTS

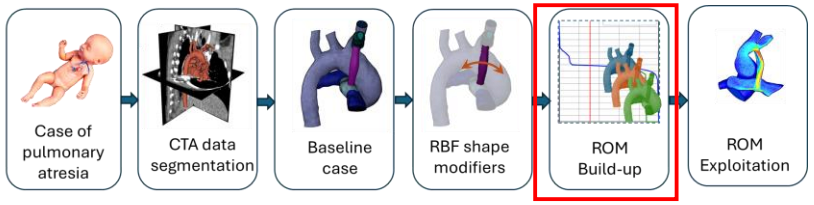

ROM Verification: Velocity

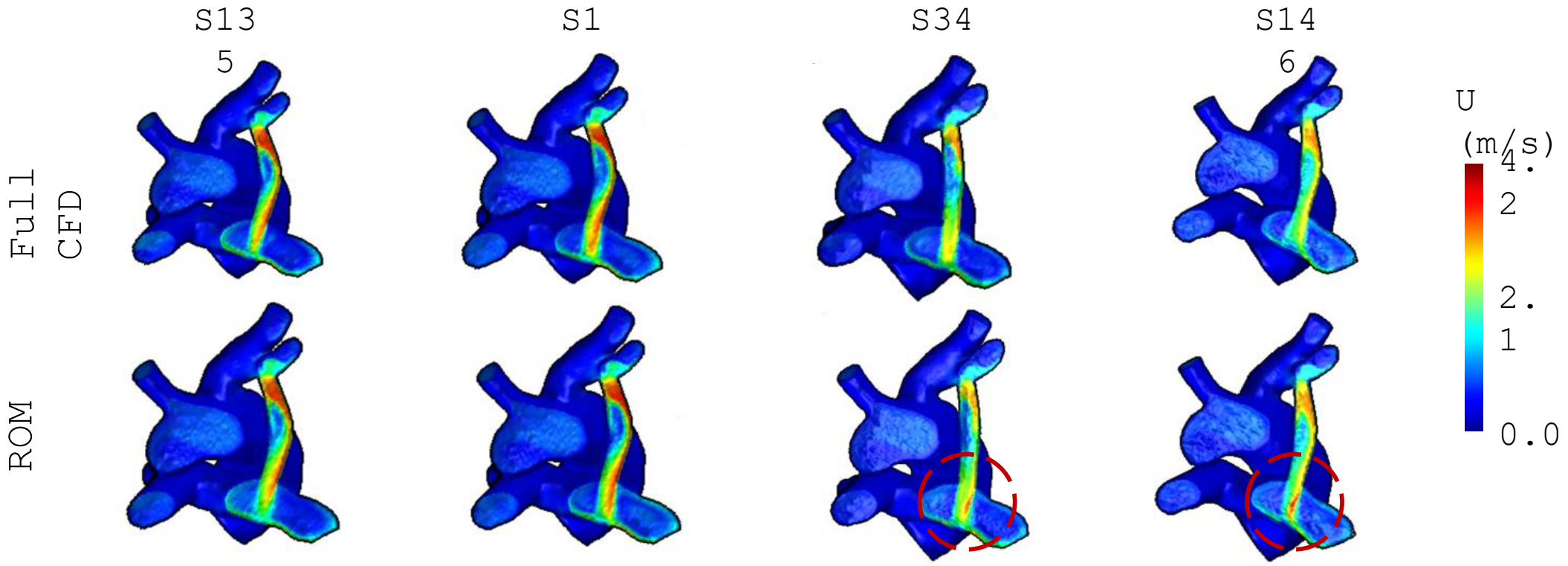

- Velocity maps on MBTS cross-section
- Results on exemplificative scenarios report agreement between ROM results and full CFDs
- Higher discrepancies limited to the inferior section of MBTS

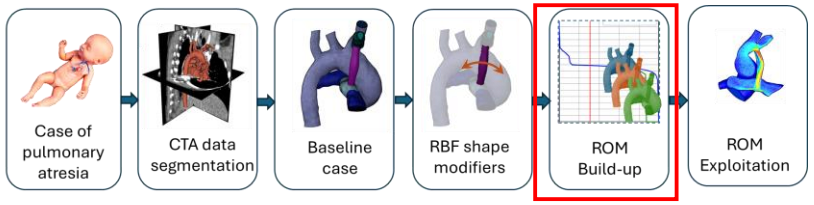

ROM Accuracy: Maximum errors

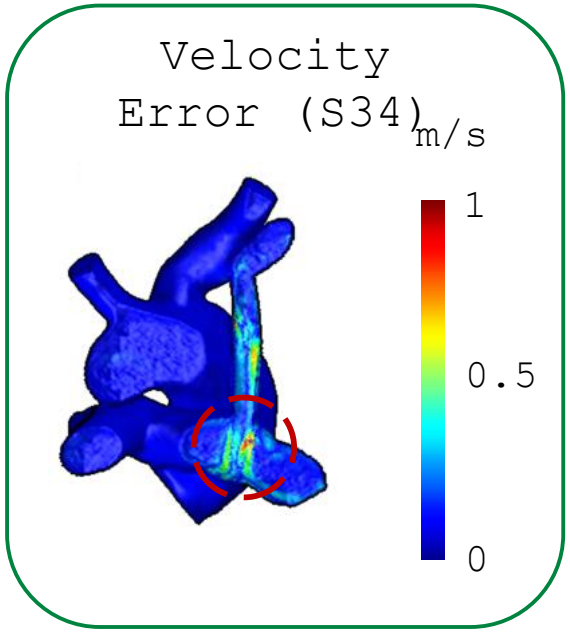

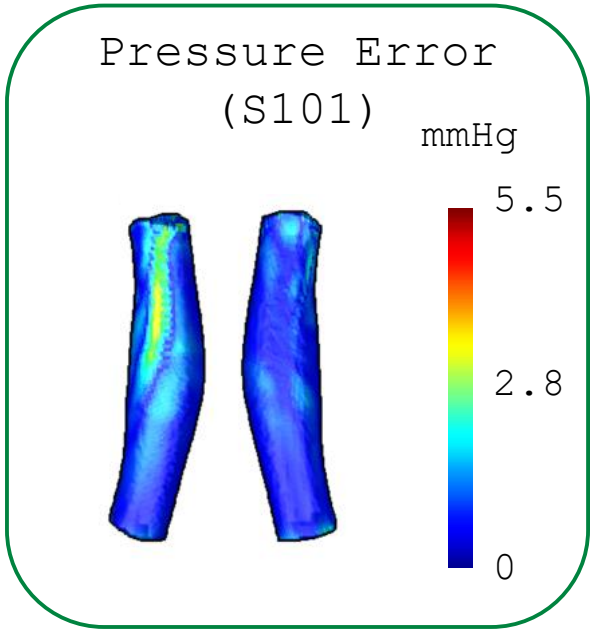

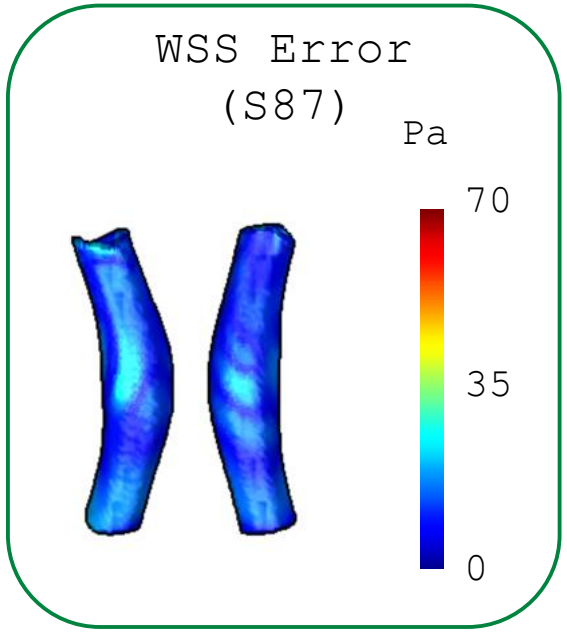

- Worst scenario reported for each field
- Maximum velocity errors limited to pulmonary
- Error ranges negligible with respect to phys range

Average absolute error	
Velocity	0.03 m/s
WSS	3.83 Pa
Pressure	1.92 mmHg

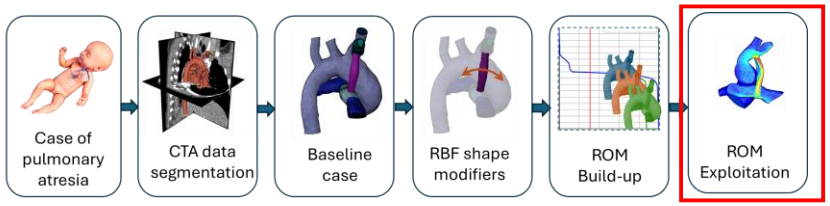

Velocity ROM Exploitation

Working Directory: .../EKA01/Desktop/rbp-output-FINAL/velocity-magnitude | 150 Snapshots - 12 Parameters | Browse | Set Geometry ROM | Auto

Check | Build | Validate | Evaluate

Available ROM:

velocity

Delete | Rename

ROM Information

Name :	velocity
Parameters :	12
Learning Snapshots :	120
Modes :	18
Version :	2022R1

Export to Twin builder

Evaluate Roms

Input parameters :

Parameter	Value
dl_1_vol	-1.50000e-01
dl_2_vol	-3.40000e-01
dr_1_vol	4.90000e+00

Points Size: 0.00 | Views : | Parts : all | CutPlane 0

velocity

Velocity Magnitude (m/s)

1.88
1.74
1.59
1.45
1.31
1.16
1.02
0.873
0.729
0.584
0.44
0.296
0.151
0.00701

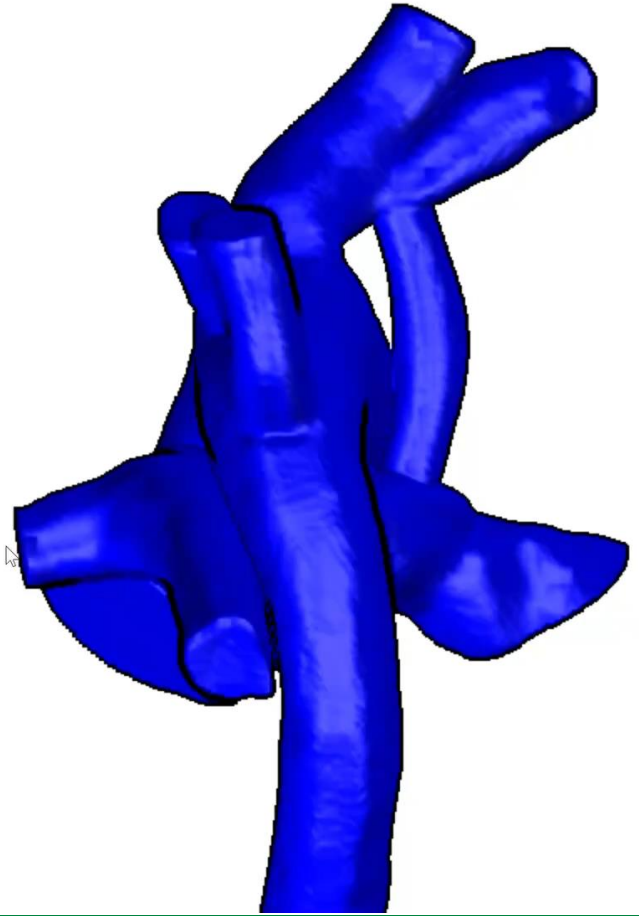

Study I: Time Comparison

CFD workflow

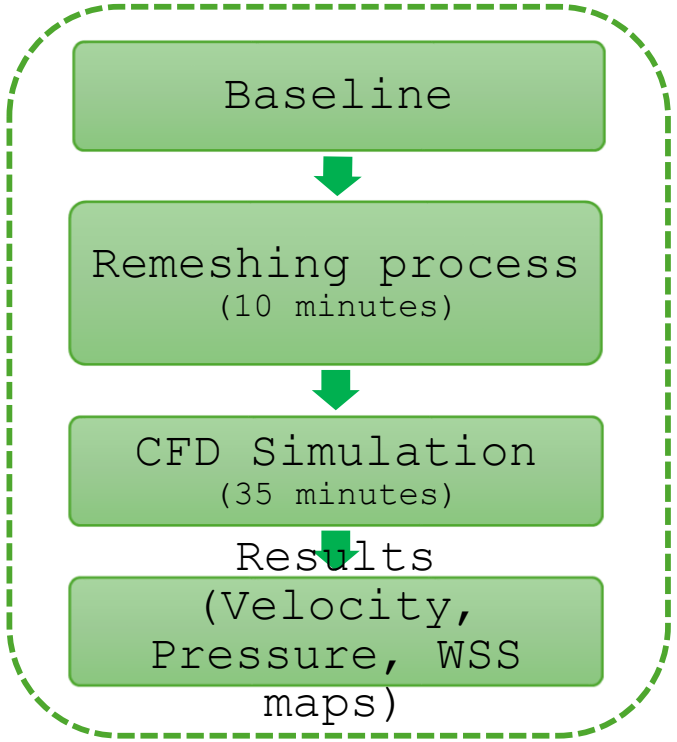

45 minutes on 8-cores laptop

ROM workflow

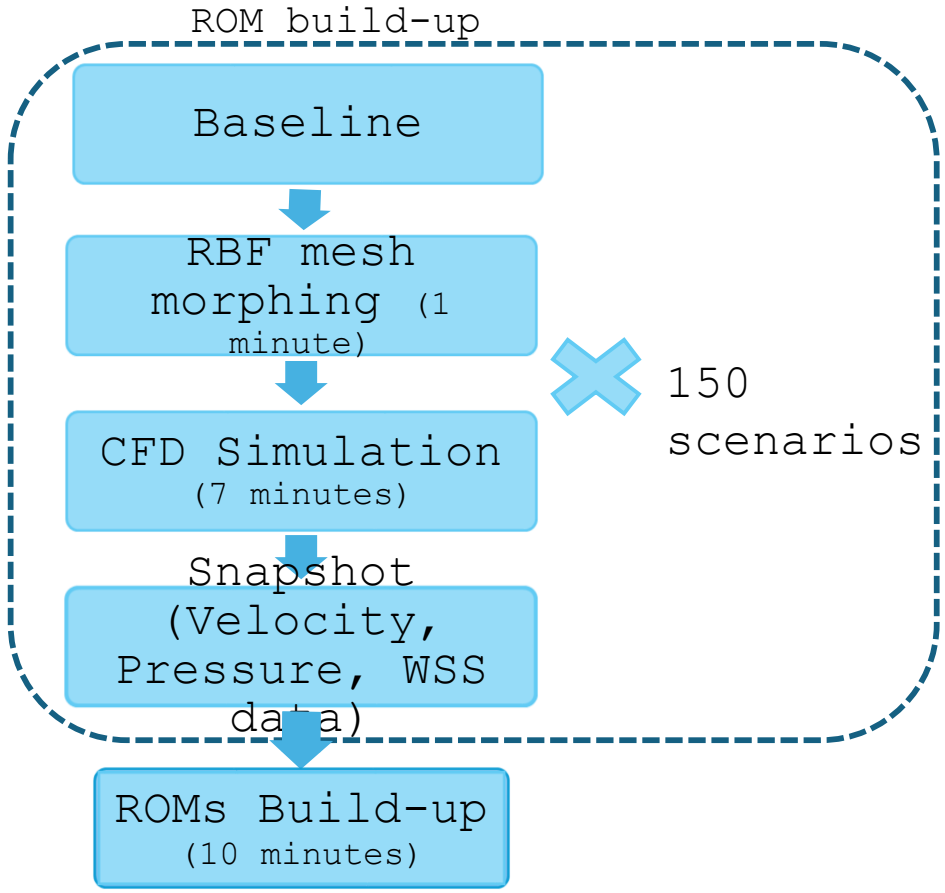

20 hours & 10 minutes on 28-cores workstation

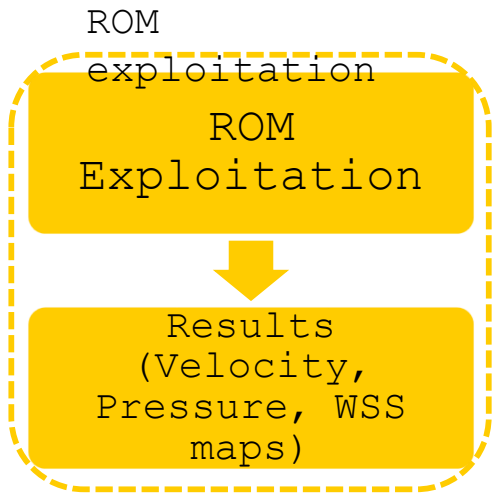

Several seconds on 8-cores laptop

Study I: Conclusions

A comprehensive framework which fuses the **ROM approach** and the **RBF mesh morphing** for the **exploration** of the effect of the shunt's shape on the fluid flow was presented.

Research Highlights

- Confirmed high ROM accuracy in velocity, pressure, and WSS fields.
- Significant reduction of the computational time using ROM vs CFD
- Wide spectrum of investigated possible shunt configurations

Future Developments

- Inclusion of more scenarios
- Application of the adopted workflow to additional MBTS patient cases
- Adoption of time-variant boundary conditions
- Inclusion of the cardiac motion

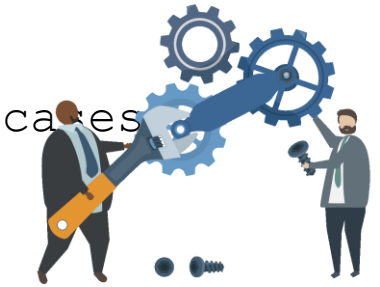

Overview of the performed studies

- Development of Reduced Order Model for the support of modified Blalock Taussig shunt (MBTS) procedures

Study I

- Development of Reduced Order Model for the assisting of the pre-operative planning and intra-operative EVAR navigation

Study II

- Investigation of the post-EVAR thrombotic events on simplified abdominal commercial stent grafts, through computational fluid dynamic simulations

Study III

Study II: Endovascular Aneurysm Repair ROM

AAA patient case

ST. OLAVS HOSPITAL
UNIVERSITETSSYKEHUSET I TRONDHEIM

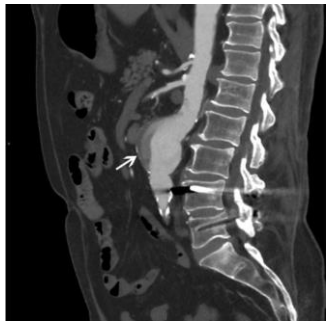

CT scan segmentation

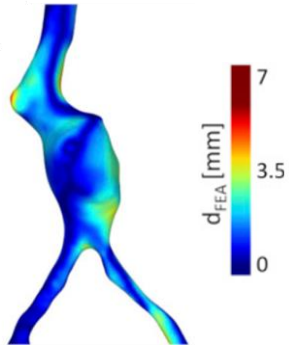

Baseline Finite Element case

Ansys
LS - DYNA

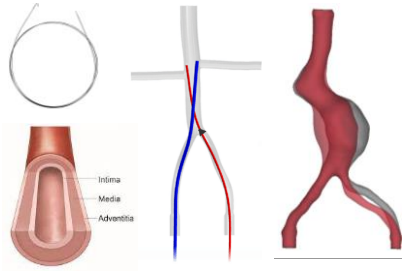

Morphological, clinical, mechanical parameterization

rbf™

python™

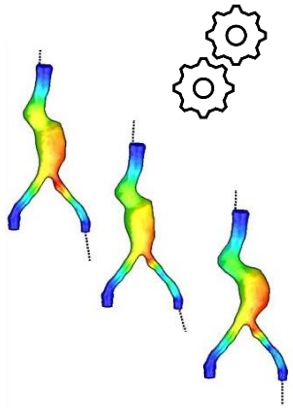

ROM Build-up

Ansys
TWIN BUILDER

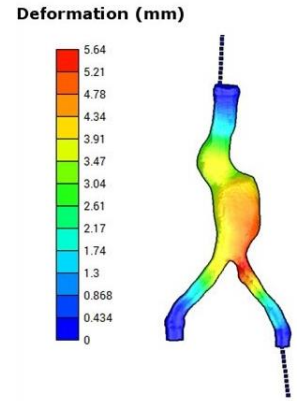

ROM exploitation

Ansys
TWIN BUILDER

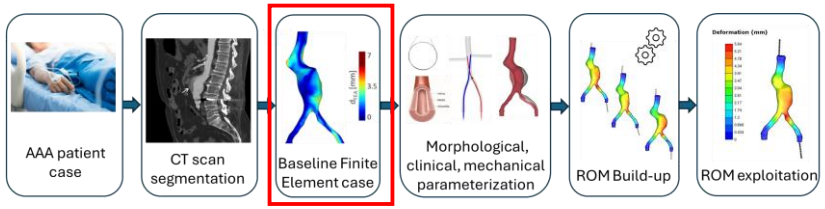

ContactMechanics Baseline Case

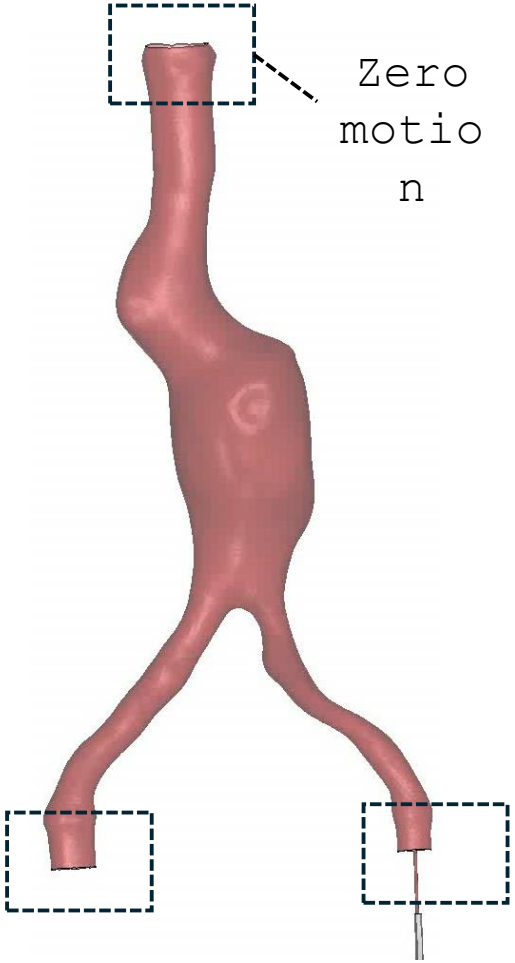

Representation of EVAR navigation inside the aorta

Model validated against experimental data[1].

[1] Emendi, Monica, et al. "Prediction of guidewire-induced aortic deformations during EVAR: a finite element and in-vitro study." *Frontiers in Physiology* 14: 1098867.

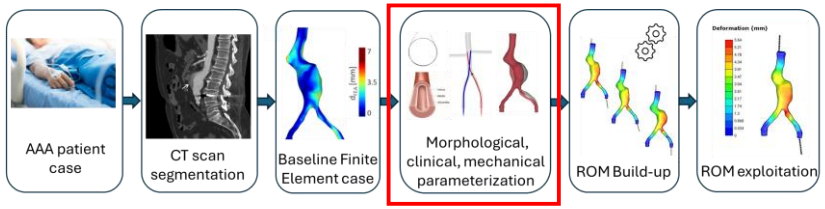

Case Parameterization

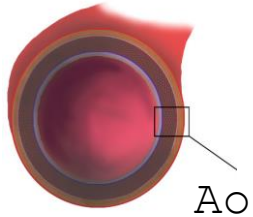

Aortic Sublayers

Mechanical parameters	
Aortic elasticity	$0.8\ MPa \leq E_{aorta} \leq 3\ MPa$
Guidewire's stiffness	$60\ GPa \leq E_{wire} \leq 200\ GPa$

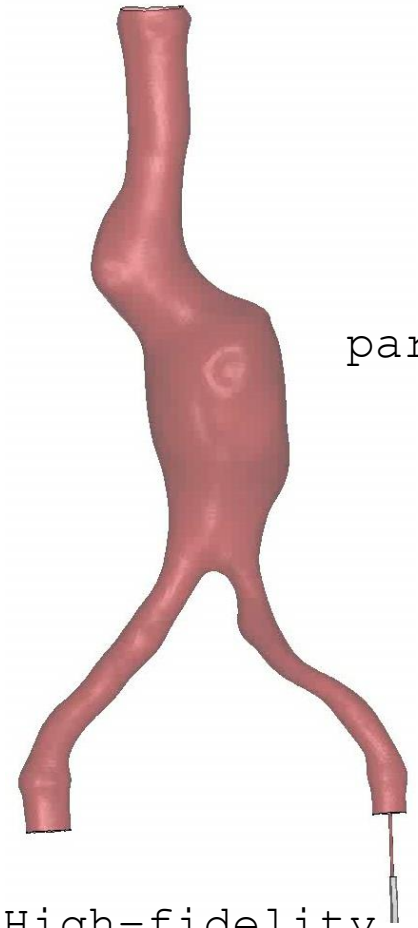

Problem parameterization

High-fidelity Finite Element simulation

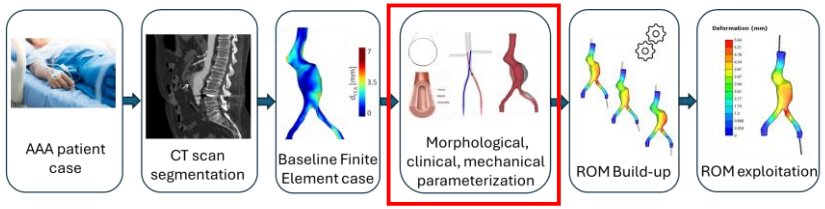

Case Parameterization

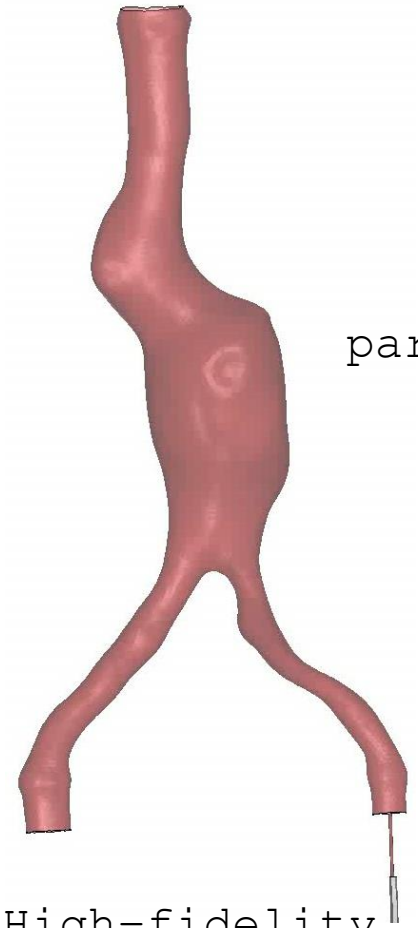

High-fidelity Finite Element simulation

Problem parameterization

Mechanical parameters
Aortic elasticity
Guidewire's stiffness
Clinical parameters
Insertion angles

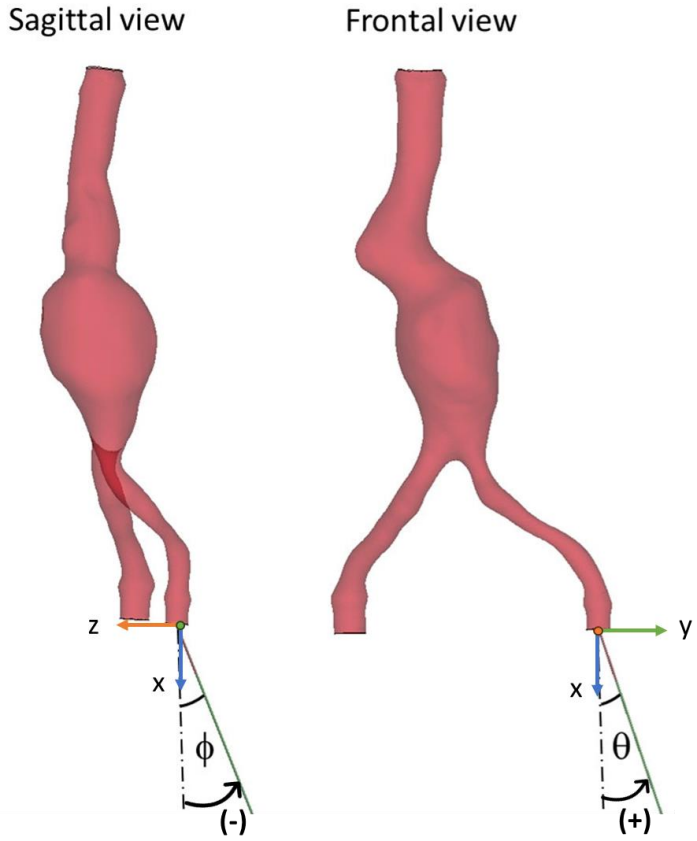

$-25^0 \leq \varphi \leq 0^0$ $0^0 \leq \theta \leq 20^0$

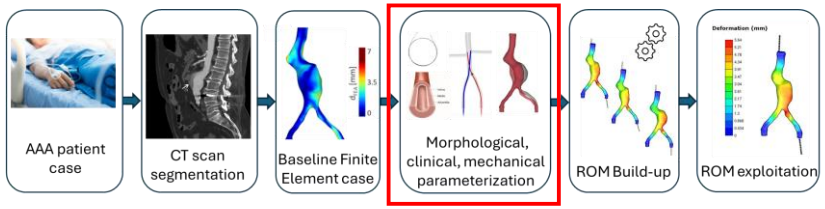

Case Parameterization

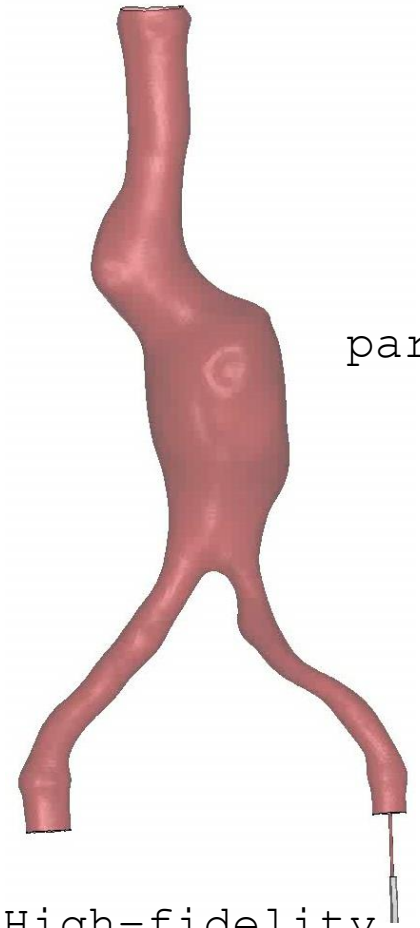

High-fidelity Finite Element simulation

Problem parameterization

Mechanical parameters
Aortic elasticity
Guidewire's stiffness
Clinical parameters
Insertion angles
Morphological parameters
Supra-renal neck angle **α**
Infra-renal neck angle **β**
Left iliac artery tortuosity **τ**

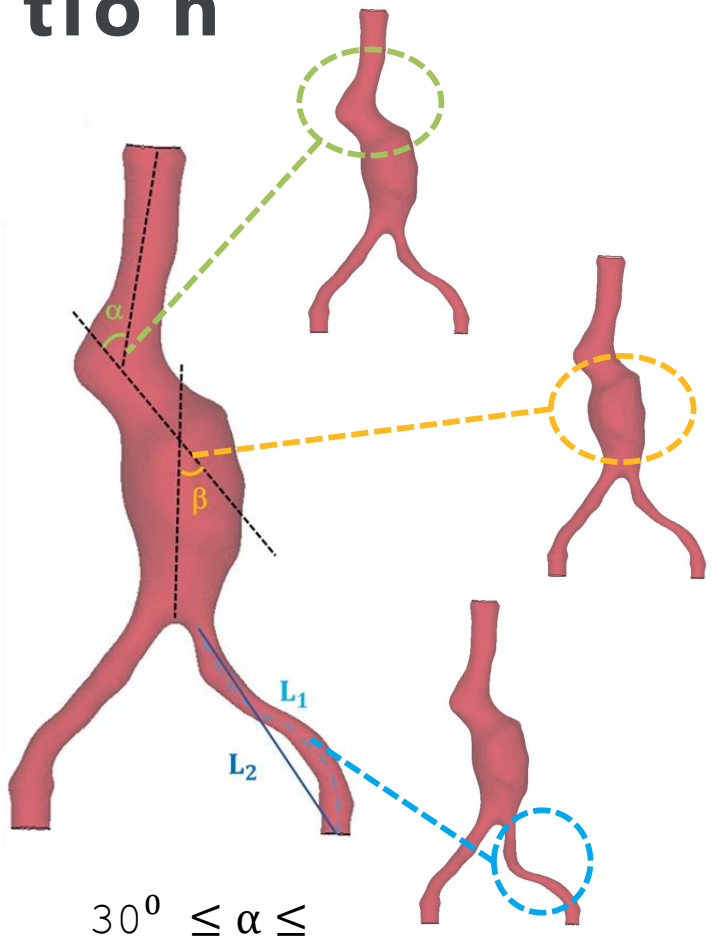

$30^0 \leq \alpha \leq 55^0$

$25^0 \leq \beta \leq 60^0$

$0.09 \leq \tau \leq 0.15$ $\quad \tau = \frac{L_1}{L_2} - 1$

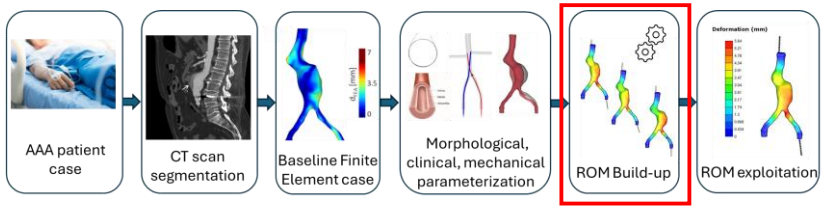

Study II: ROM Build

300 scenarios (S)

- 200 scenarios for the ROM build-up
- 100 scenarios for ROM verification

$$e_{\text{red}}^{\text{RMS}} = \frac{\|\mathbf{A} - \mathbf{A}_r^*\|}{\|\mathbf{A}\|}$$

Relative Reduction Error: $e_{\text{red}}^{\text{RMS}} = 0.2\,\%$

Number of modes: $r = 38$

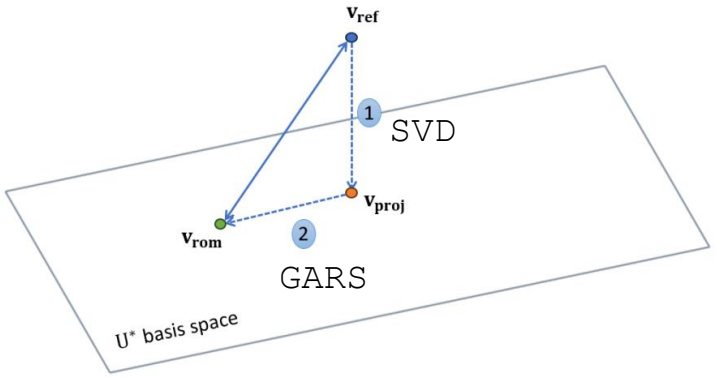

$$e_{\text{red}}^{\text{rel}} = \frac{\|\mathbf{v}_{\text{ref}} - \mathbf{v}_{\text{proj}}\|}{\|\mathbf{v}_{\text{ref}}\|}$$

$$e_{\text{ROM}}^{\text{rel}} = \frac{\|\mathbf{v}_{\text{ref}} - \mathbf{v}_{\text{rom}}\|}{\|\mathbf{v}_{\text{ref}}\|}$$

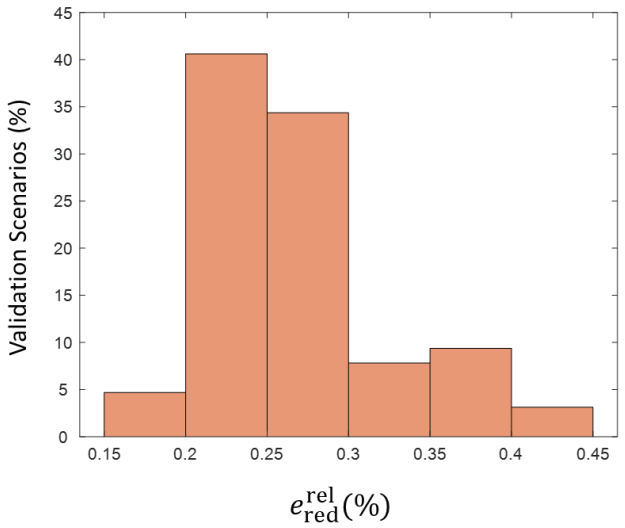

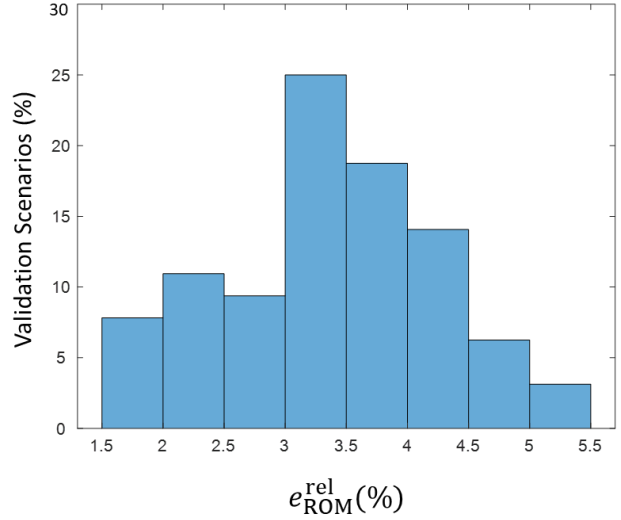

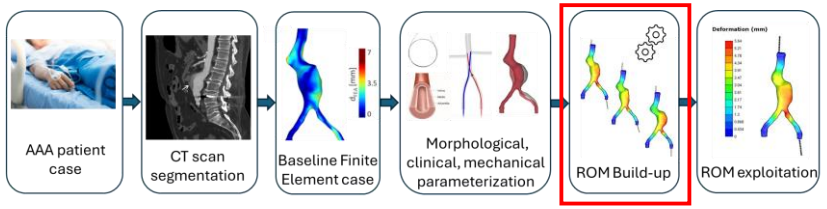

Study II: ROM Accuracy

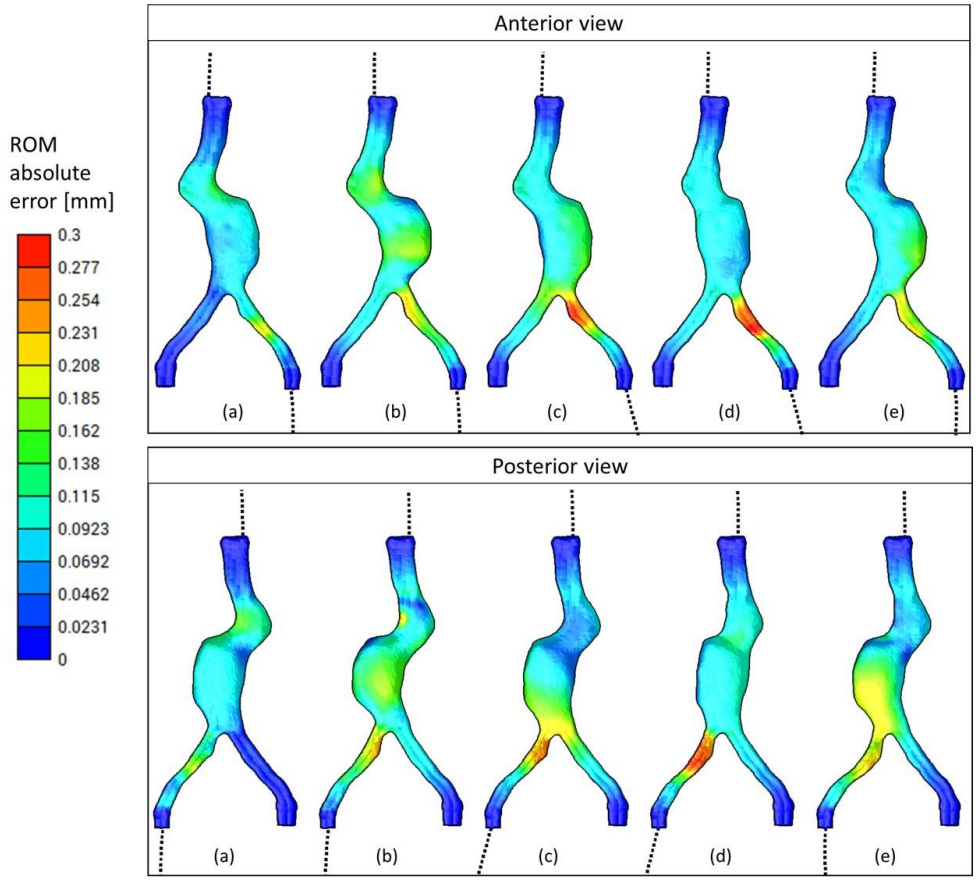

ROM absolute error = $|FE_{sol} - ROM_{pred}|$

- Highest discrepancies at the root of the common iliac artery (c, d)
- Final ROM errors less than 0.3mm

Digital Subtraction Angiography (DSA) precision ≈ 0.5mm

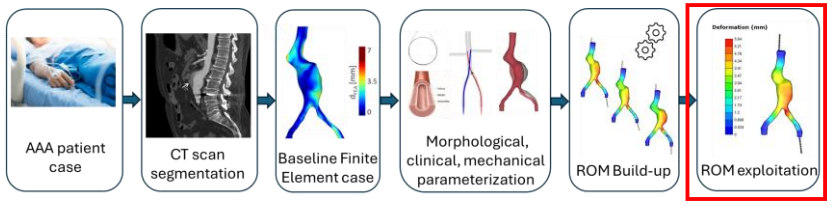

R O M
E x p lo ita tio n

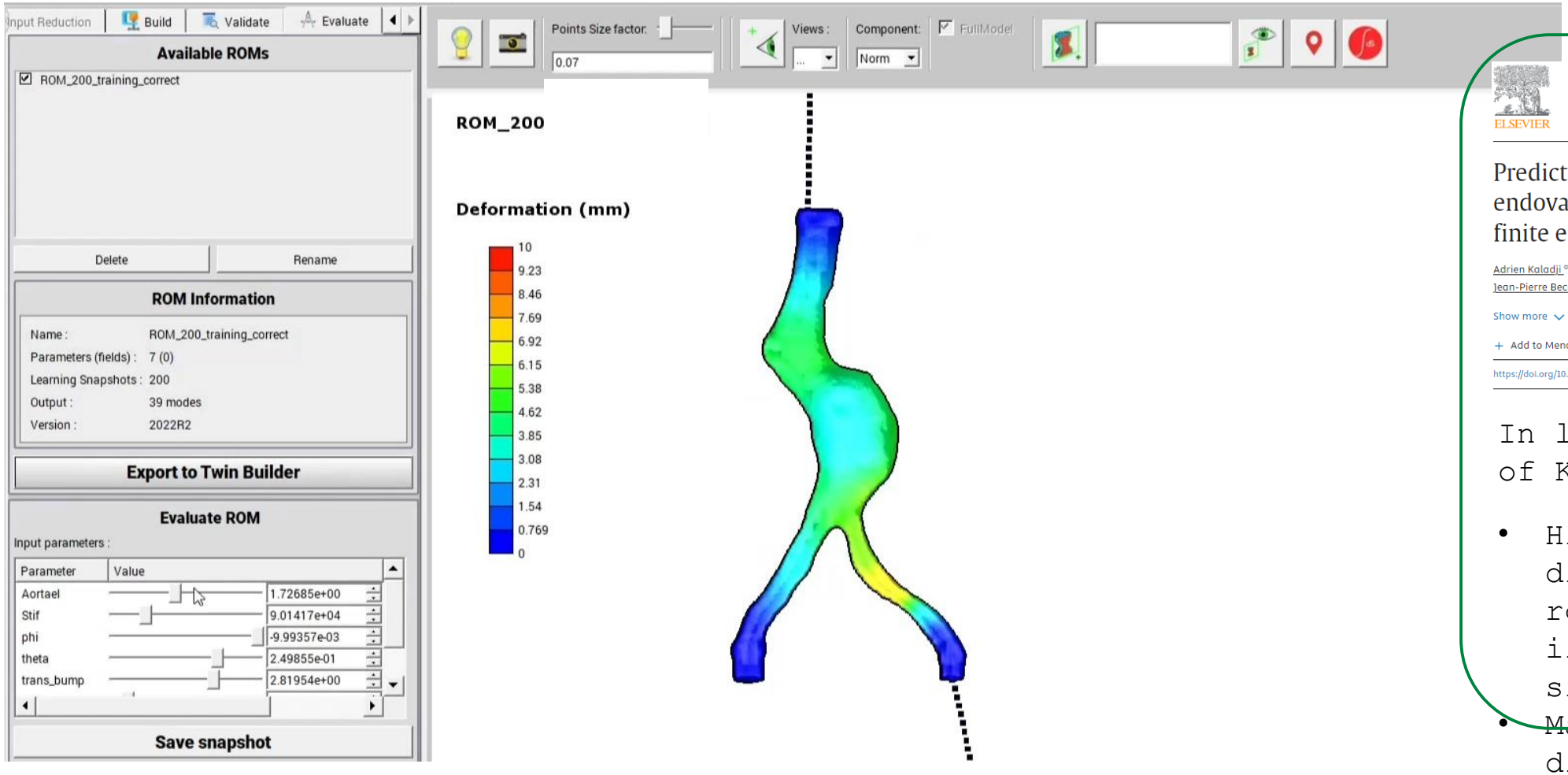

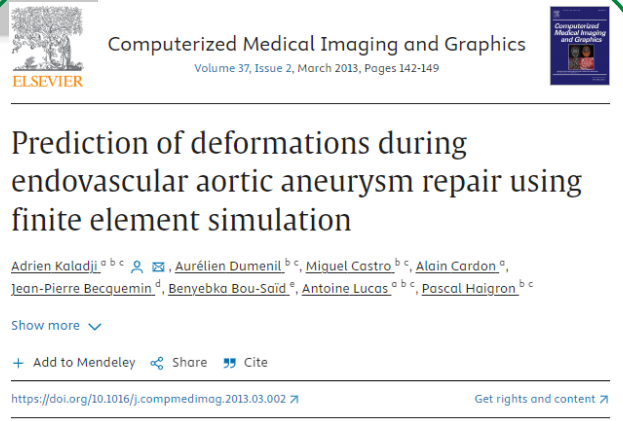

In line with observations of Kaladji et al.:

- Highest values of displacement at the root of the common iliac artery on the side of insertion
- Magnitude of displacement equal to 10.2 ± 3.3 mm

Study II: Timeframe Comparison

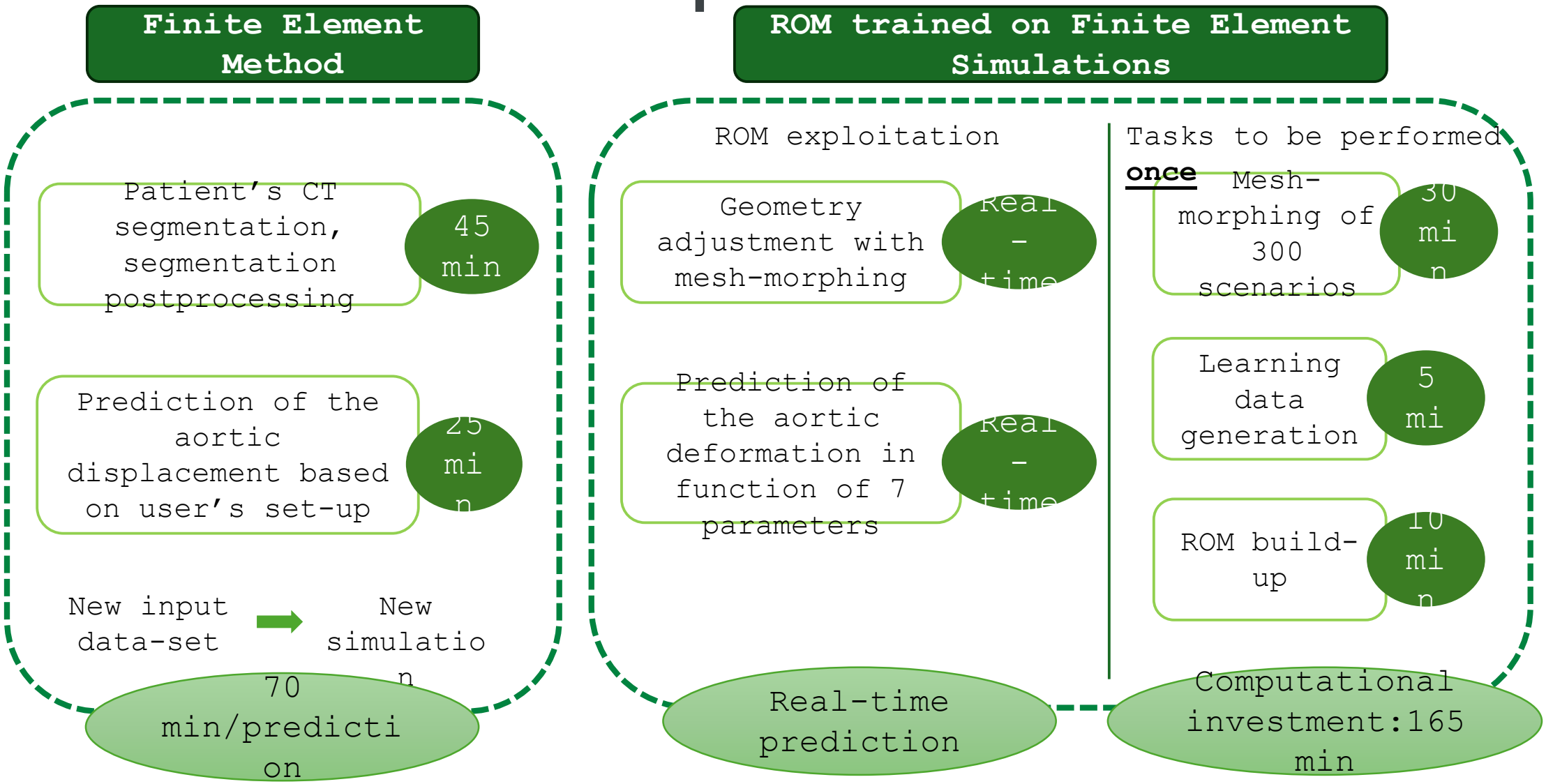

Study II: Conclusions

A comprehensive framework which fuses the **ROM approach** and the **RBF mesh morphing** for the **prediction of the guidewire-induced deformations** was presented.

Research Highlights

- ✓ ROM build-up within **3 hours and 15 minutes** starting from CT images.
- ✓ Exploration of a wide spectrum of scenarios, varying 7 **mechanical, morphological and clinical parameters**.
- ✓ Fast ROM execution compatible with **pre- and intra-operative** timeframe.

Limitations & Future Directions

- ➢ Inclusion of more **learning scenarios**
- ➢ Application of the workflow to more **challenging anatomies**
- ➢ Adoption of more **realistic boundary conditions** and **material model** for aortic tissue

Overview of the performed studies

- Development of Reduced Order Model for the support of modified Blalock Taussig shunt (MBTS) procedures — Study I
- Development of Reduced Order Model for the assisting of the pre-operative planning and intra-operative EVAR navigation — Study II
- Investigation of the post-EVAR thrombotic events on simplified abdominal commercial stent grafts, through computational fluid dynamic simulations — Study III

Study III: Stent Graft Thrombosis

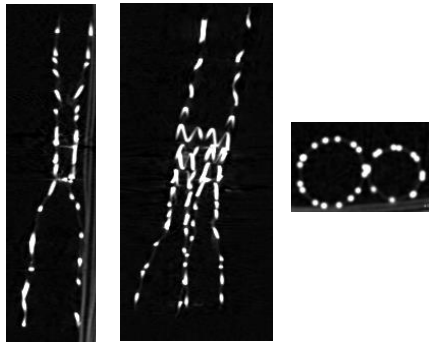

CT scans of 3 commercial grafts

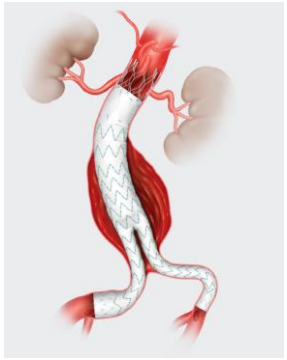

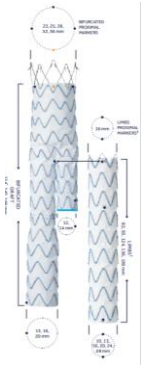

Stent Graft Geometrical Models

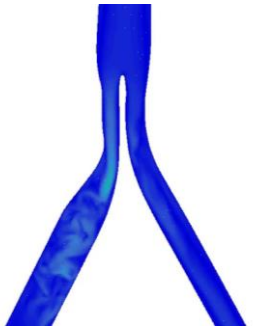

CFD simulations

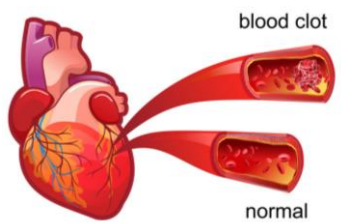

Quantities of interest

Results analysis

ST. OLAVS HOSPITAL
UNIVERSITETSSYKEHUSET I TRONDHEIM

AUTODESK MESHMIXER

Ansys SPACECLAIM

Ansys FLUENT

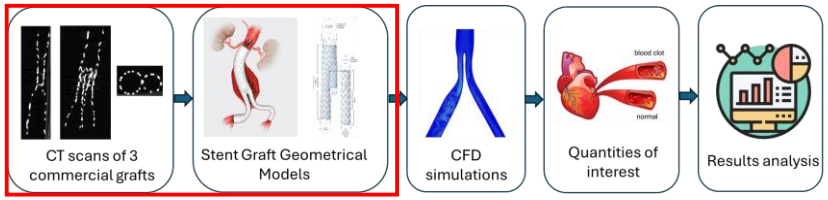

StentGraftCAD Modeling

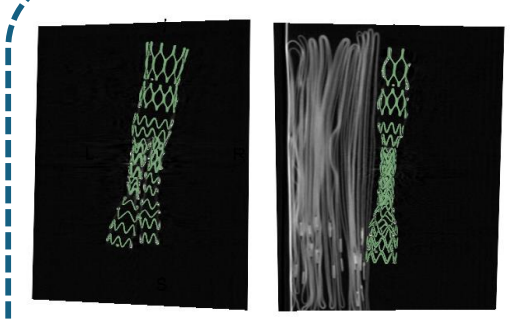

Segmentation Result

Basic CAD models

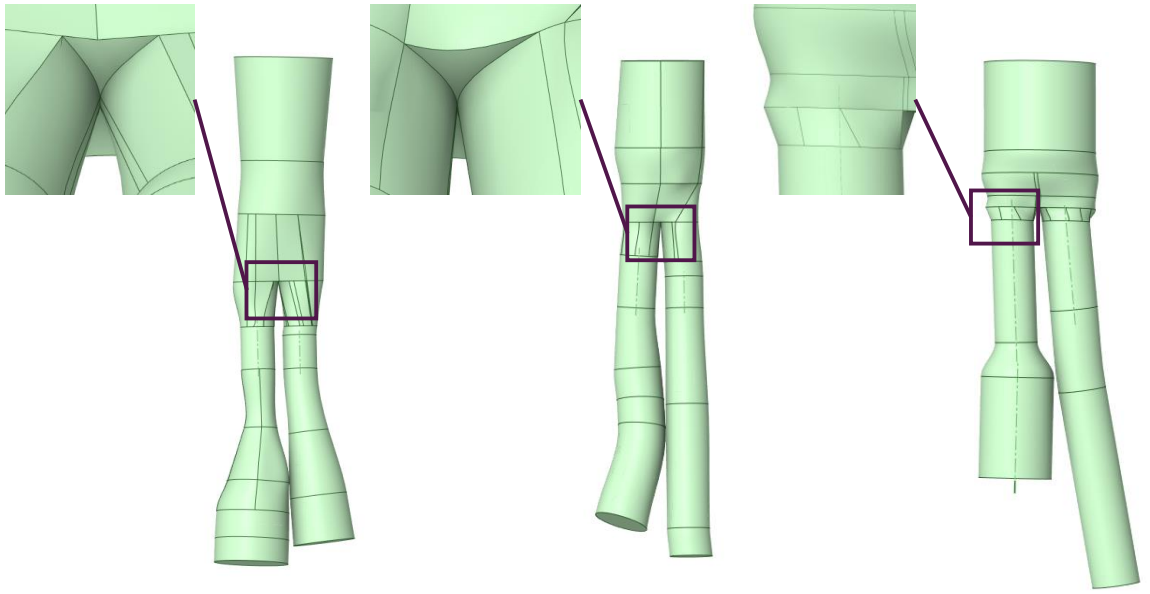

Zenith Alpha

Excluder

Endurant II

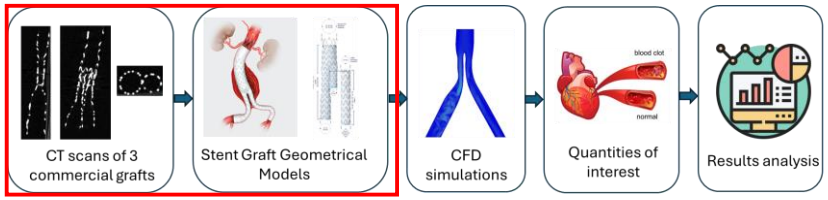

StentGraftCAD Modeling

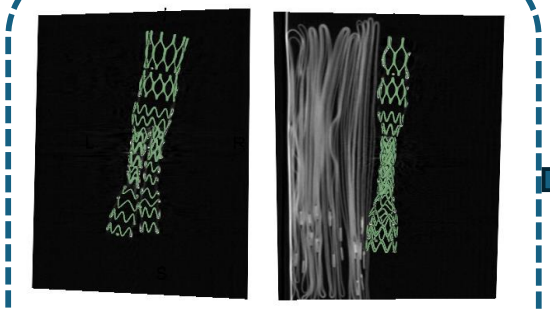

Segmentation Result

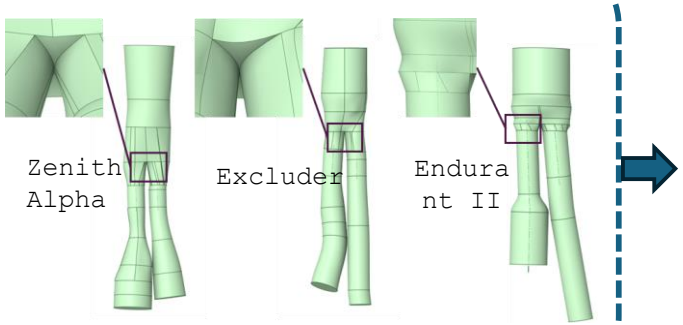

Basic CAD models

Precise CAD models

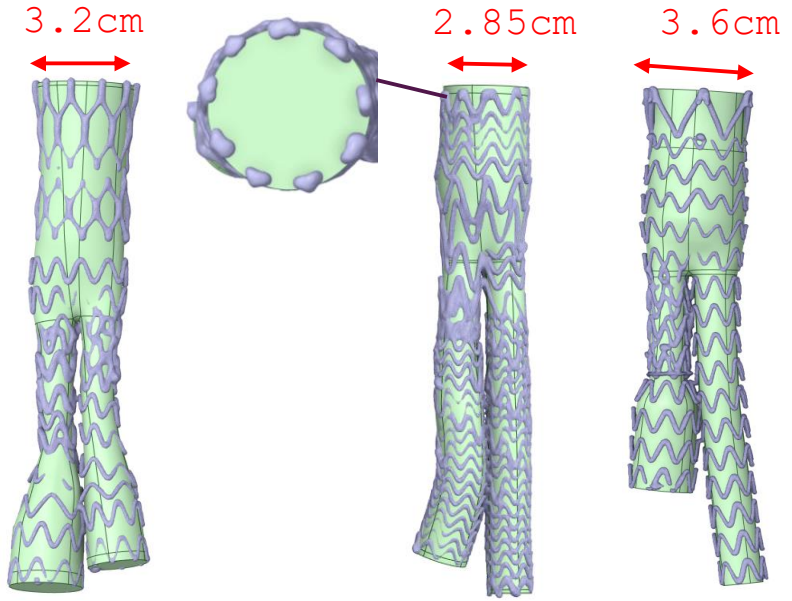

Zenith Alpha

Excluder

Endurant II

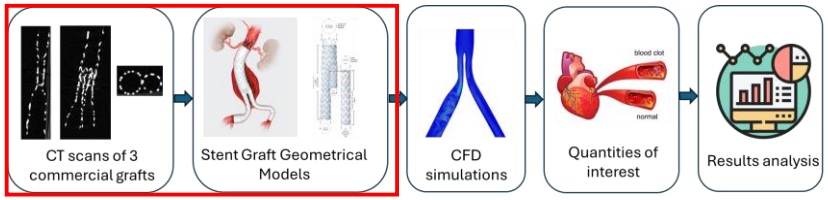

StentGraftCAD Modeling

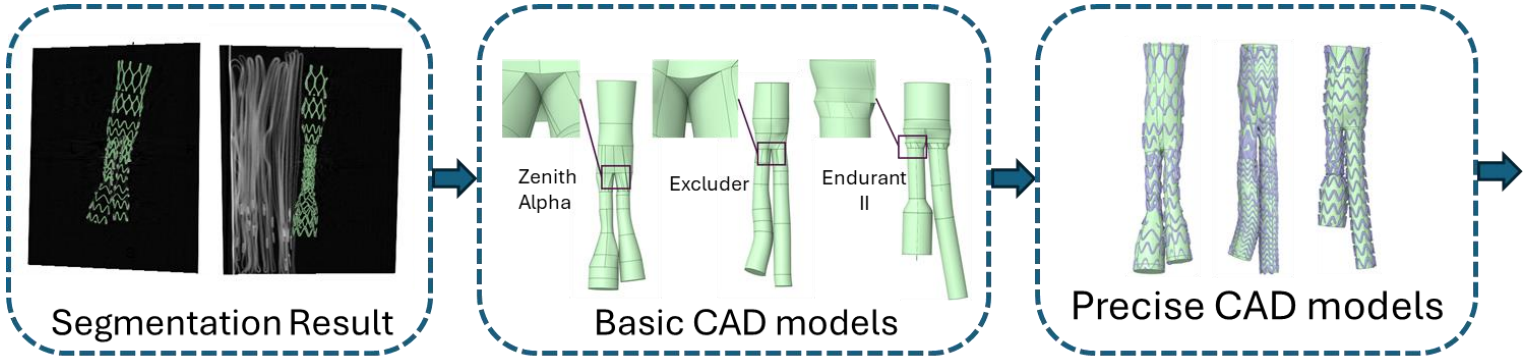

(cm)	d_n	d_s	d_c	d_f	d_i
Zenith Alpha	28	11	16	11	24
Excluder	28.5	13	14.5	13	23
Endurant II	28	16	16	13	24

Uniform graft sizing

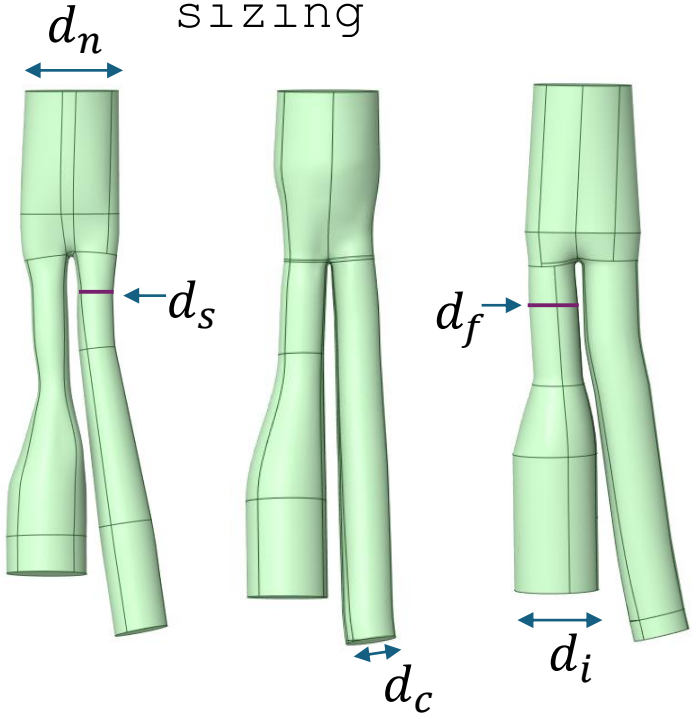

Zenith Alpha | Excluder | Endurant II

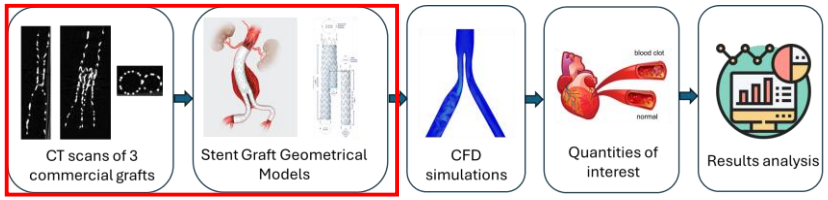

StentGraftCAD Modeling

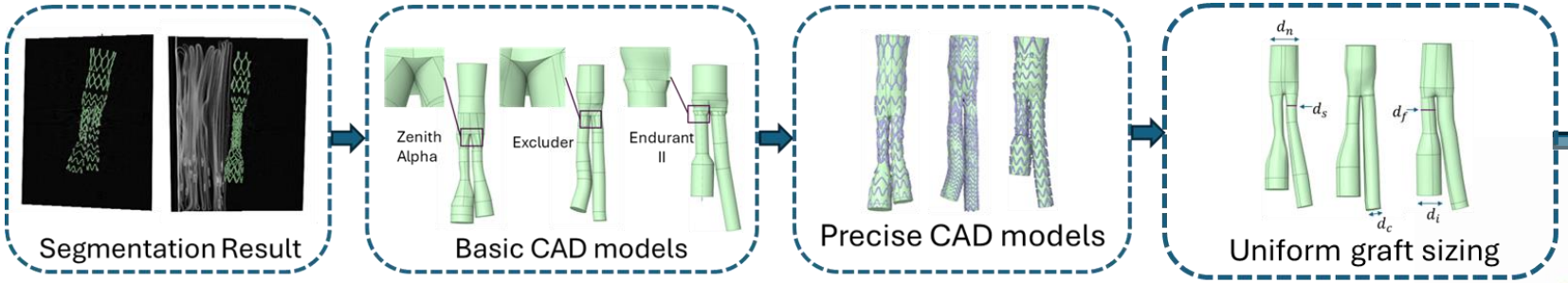

Final simplified graft configurations

Extensive CAD changes → Uncertainty ↗

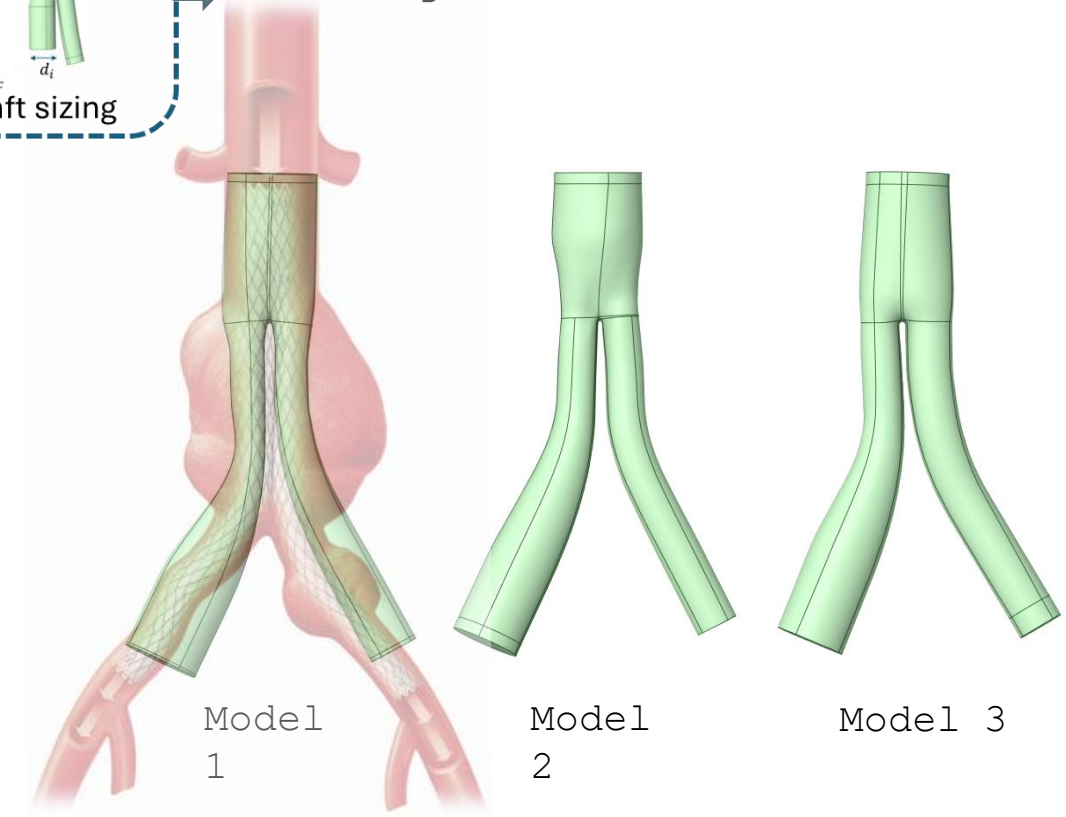

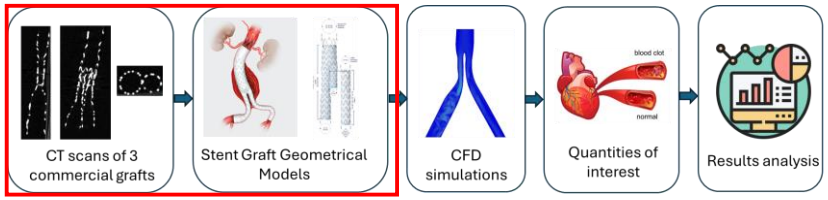

StentGraftCAD Modeling

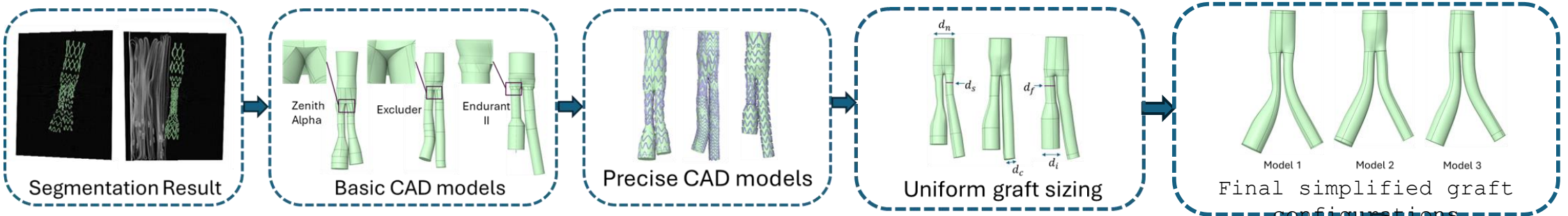

Division of blood flow domain

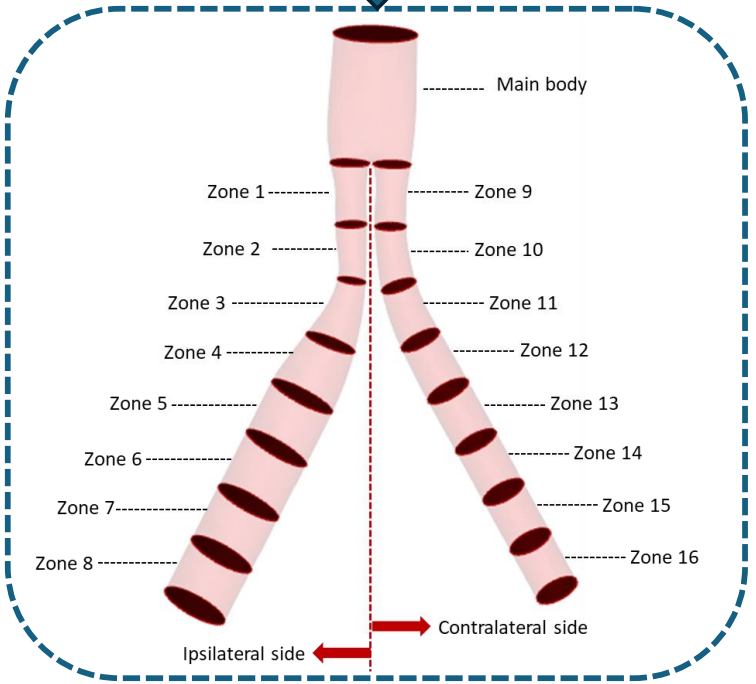

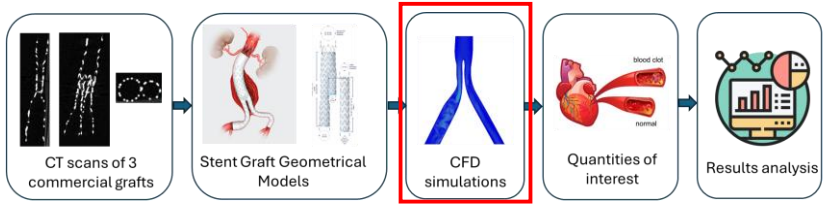

Study III: CFD set-up

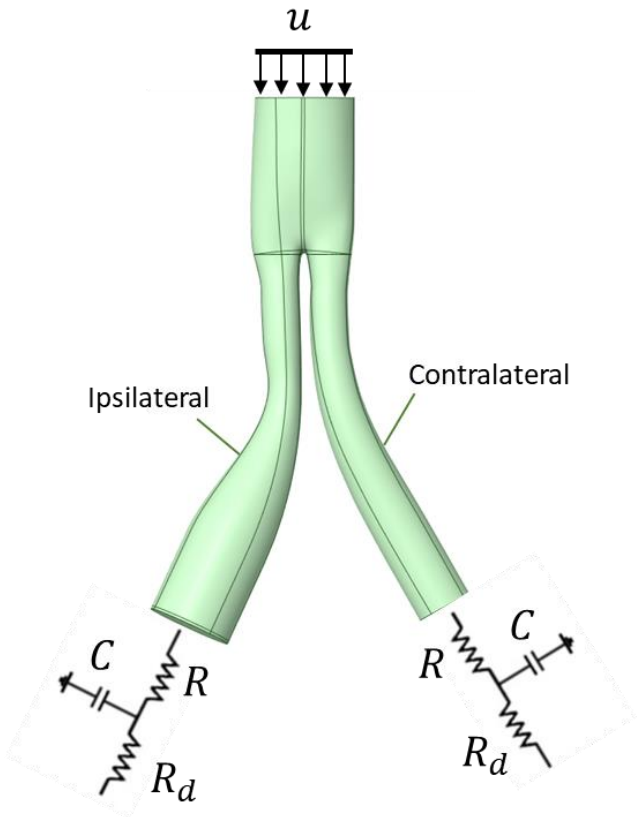

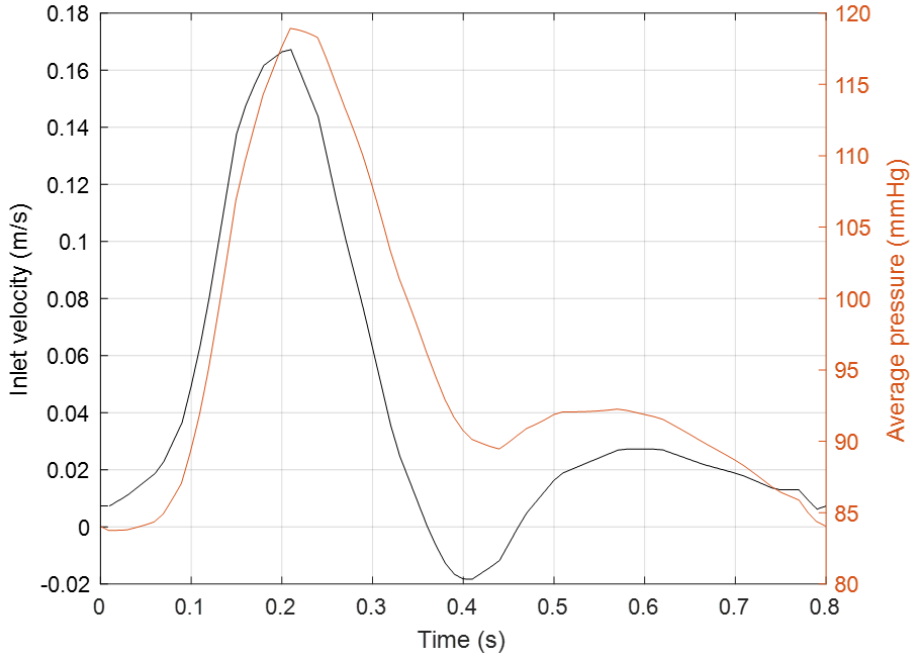

Comparative Study > J Vasc Surg. 2003 Jan;37(1):118-23. doi: 10.1067/mva.2002.107.

Comparison of abdominal aortic hemodynamics between men and women at rest and during lower limb exercise

Christopher P Cheng [1], Robert J Herfkens, Charles A Taylor

Affiliations + expand

PMID: 12514587 DOI: 10.1067/mva.2002.107

Free article

Blood properties

- Newtonian fluid
- Density $\rho=1060 kg/m^3$
- Viscosity $\eta=0.0035$ Pa s

Flow modeling

- Laminar
- Transient Simulation

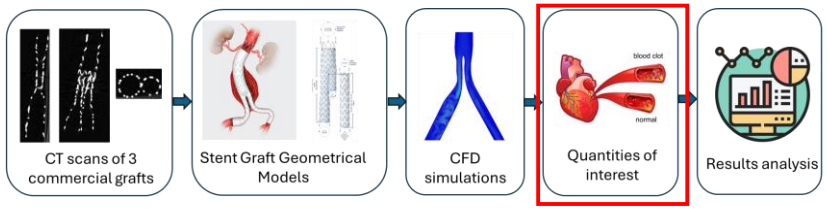

Shear Strain Rate & Blood clots

1 Shear Strain Rate (SSR)

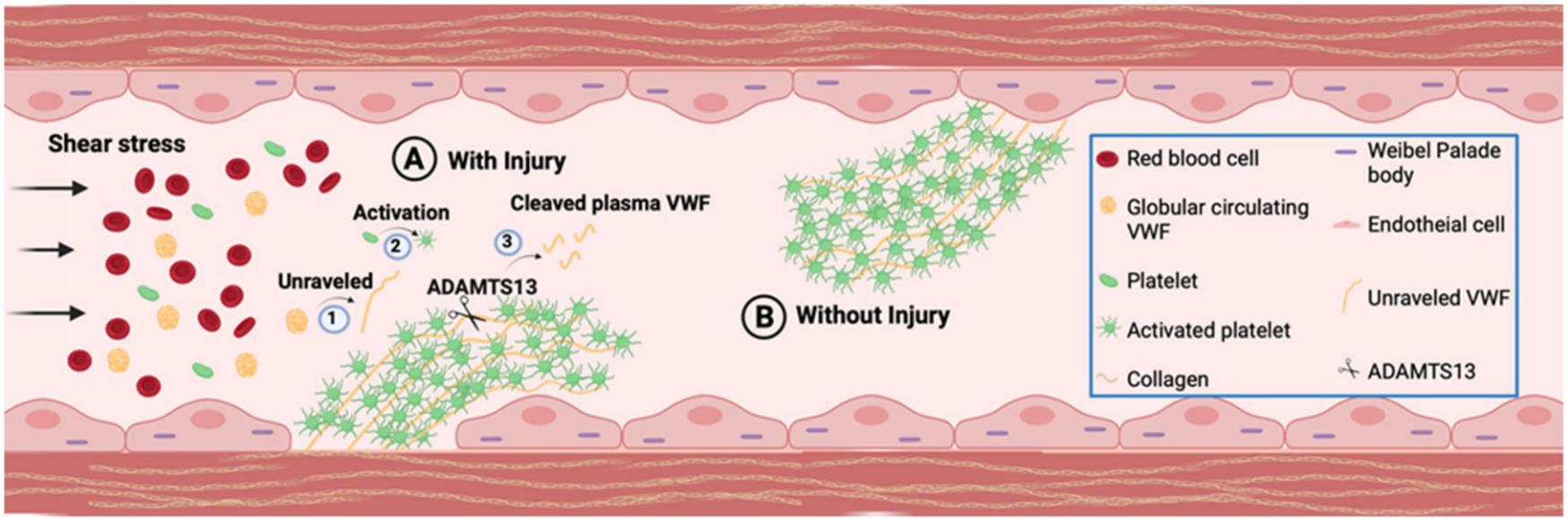

VWF is unraveling in high SSR.

What do we mean with high SSR?

$SSR > 5000s^{-1}$

Casa, L. D. & Ku, D. N. Thrombus formation at high shear rates. *Annu. Rev. Biomed. Eng.* **19**, 415–433 (2017).

$SSR > 4000s^{-1}$

Sakariassen, K. S., Orning, L. & Turitto, V. T. The impact of blood shear rate on arterial thrombus formation. *Future Sci. OA* **1**, fso.15.28 (2015).

$SSR > 3000s^{-1}$

Ruggeri, Z. M. The role of von Willebrand factor in thrombus formation. *Thromb. Res.* **120**, S5–S9 (2007).

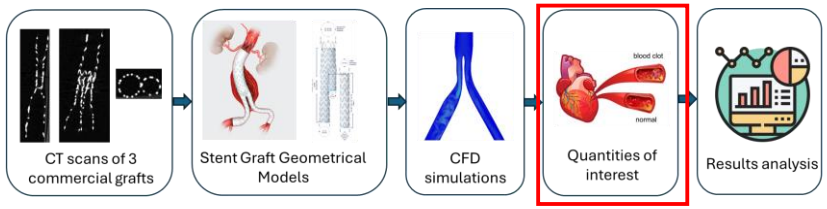

Shear Strain Rate & Blood clots

1 Shear Strain Rate (SSR)

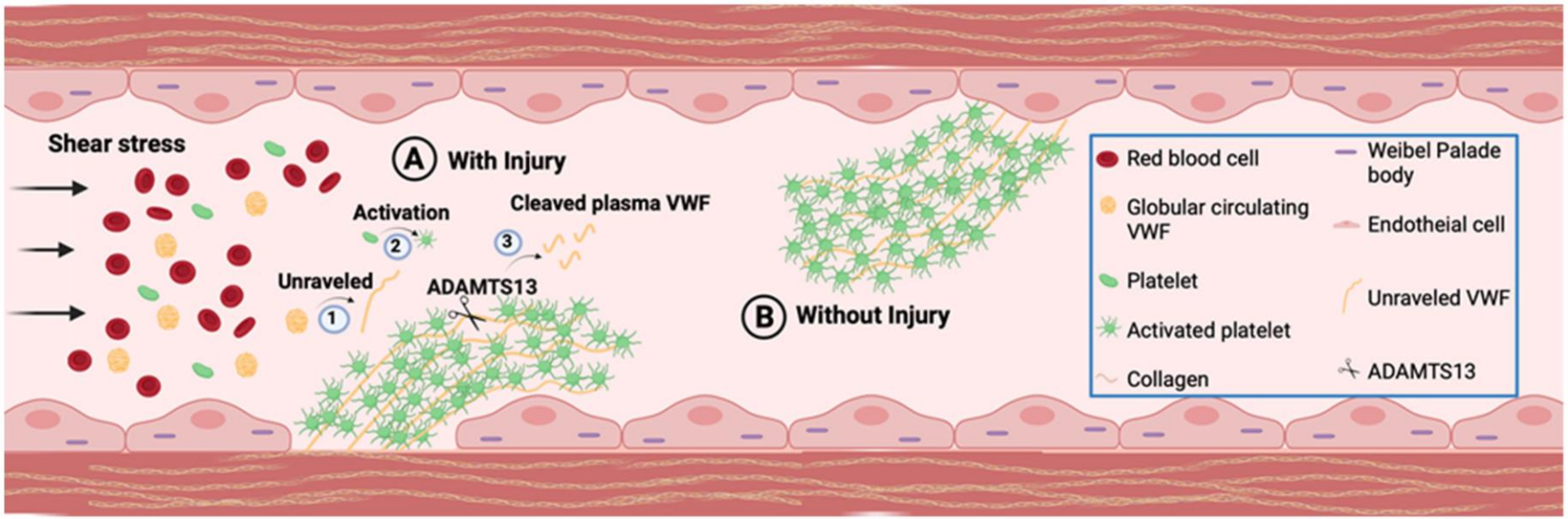

Measurement of the volume of each zone, V_{SSR}, that is exposed to SSR > 3000 s^{-1}

VWF is unraveling in high SSR.

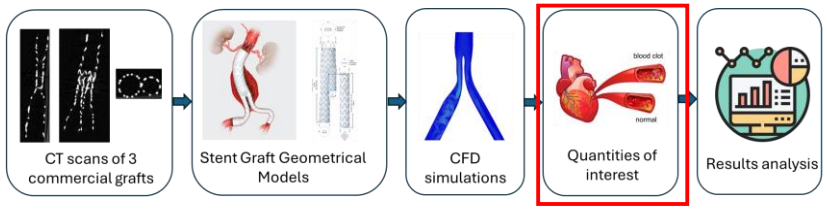

Recirculation & Blood clots

2 Recirculation
- Reverse flow monitoring
- Velocity vectors analysis

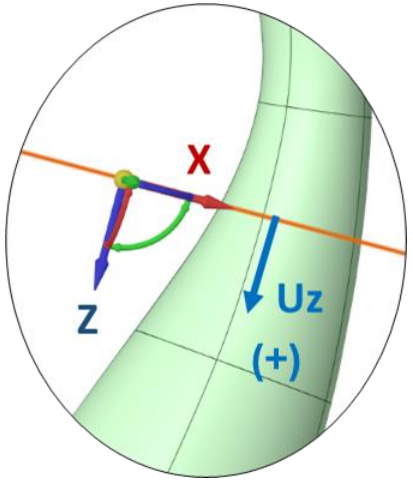

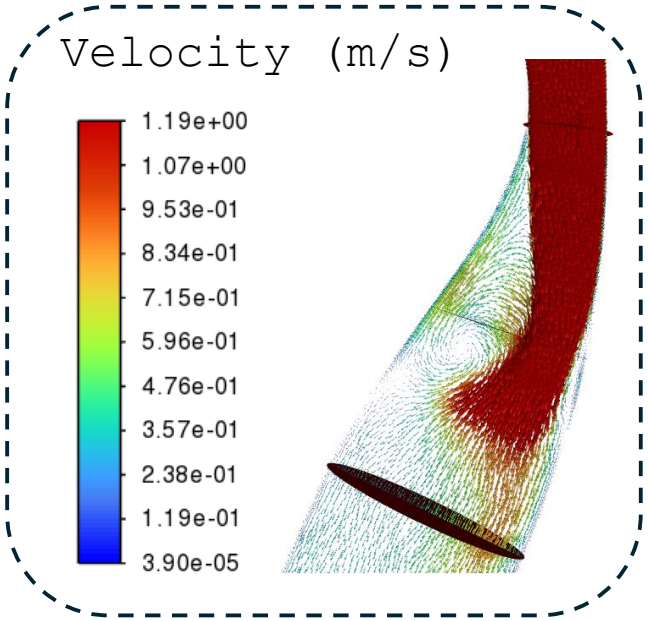

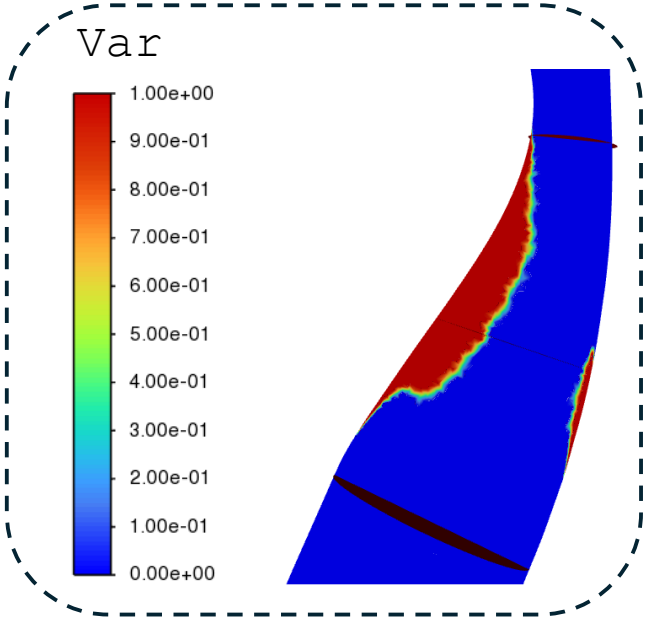

$$V_{back} = \frac{\sum v_{cell}}{V_{zone}} \; 100\% \; of \; U_z < 0$$

$$\text{Var} = \begin{cases} 1, & U_z < 0 \\ 0, & U_z > 0 \end{cases}$$

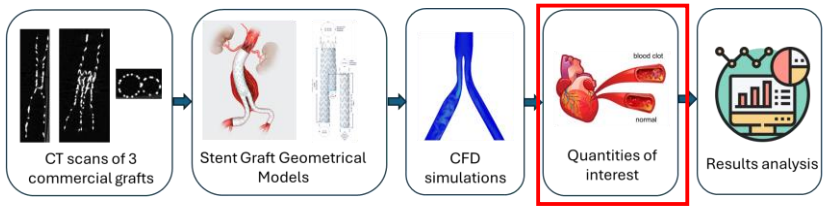

Wall Shear Stresses & Blood clots

3 Wall Shear Stress indices

"The endothelium responds to changes in the applied shear stress by altering its anti-inflammatory and anti-thrombogenic properties[1]."

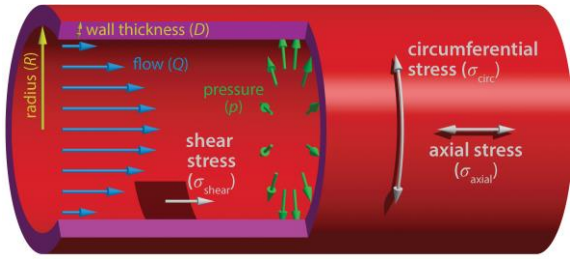

		Thrombus prone range
Time-Averaged WSS	$TAWSS = \frac{1}{T}\int_0^T \lvert \boldsymbol{WSS} \rvert \, dt$	$0.2 - 0.3 \ Pa$
Oscillatory Shear Index	$OSI = \frac{1}{2}\left(1 - \frac{\left\lvert \int_0^T \mathbf{WSS} \, dt \right\rvert}{TAWSS}\right)$	> 0.3
Endothelial Cell Activation Potential	$ECAP = \frac{OSI}{TAWSS}$	$> 1.4 \ Pa^{-1}$

[1] Davies, Peter F. "Hemodynamic shear stress and the endothelium in cardiovascular pathophysiology." *Nature clinical practice Cardiovascular medicine* 6.1 (2009): 16-26.

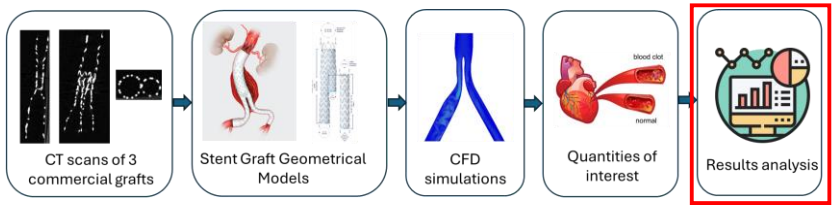

S S R Results

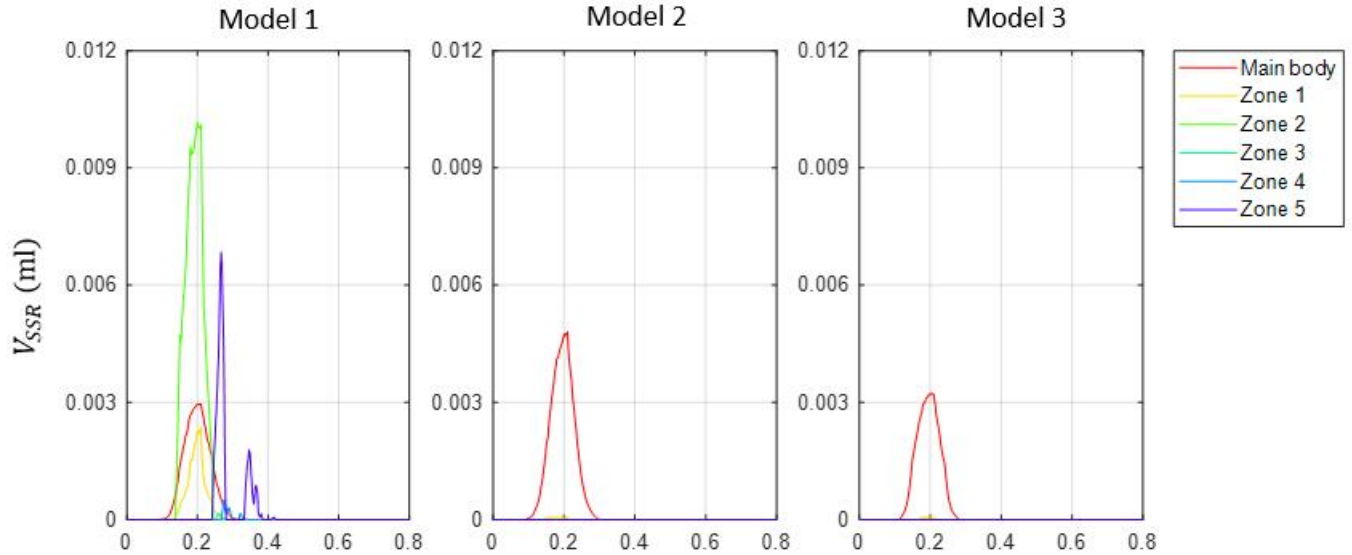

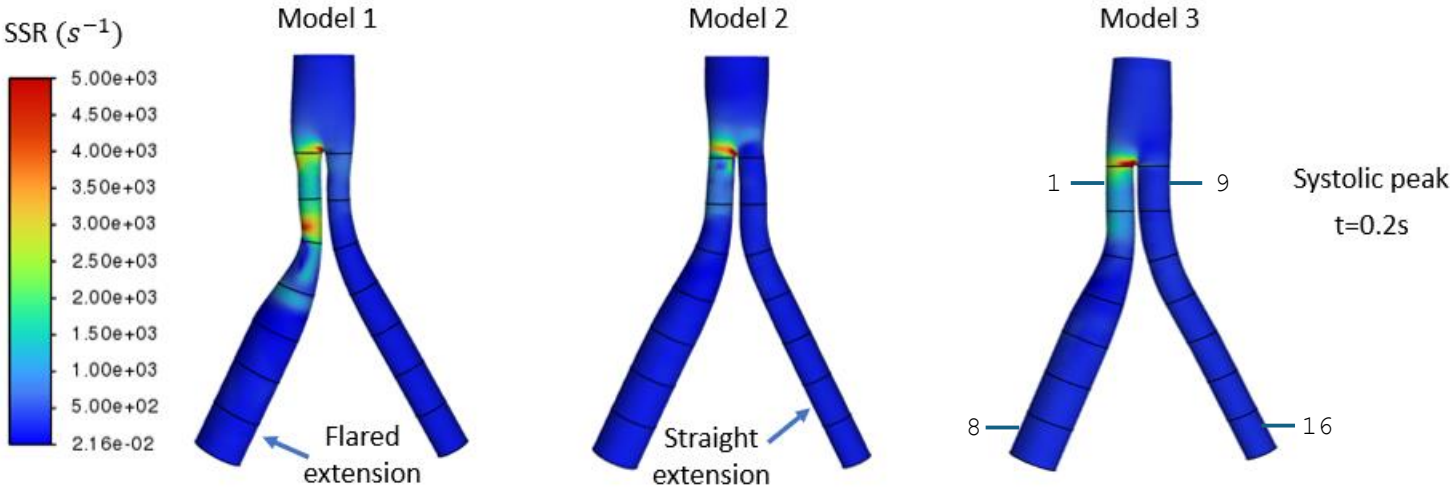

- The bifurcating area of all grafts seems prone to blood clots.
- Model 1 has an increased likelihood of developing a thrombus in its flared extension.

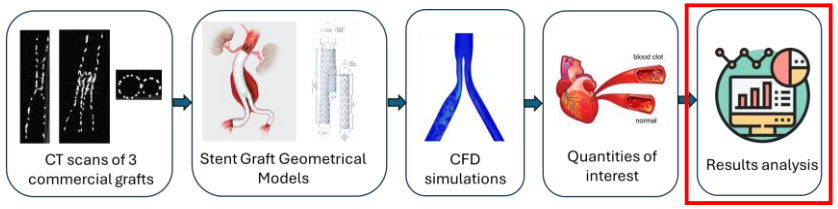

Recirculation Results: Reverse flow

- Backflow for 90% of the heart cycle in Model 1
- Smaller backflows, with less duration in Models 2, 3

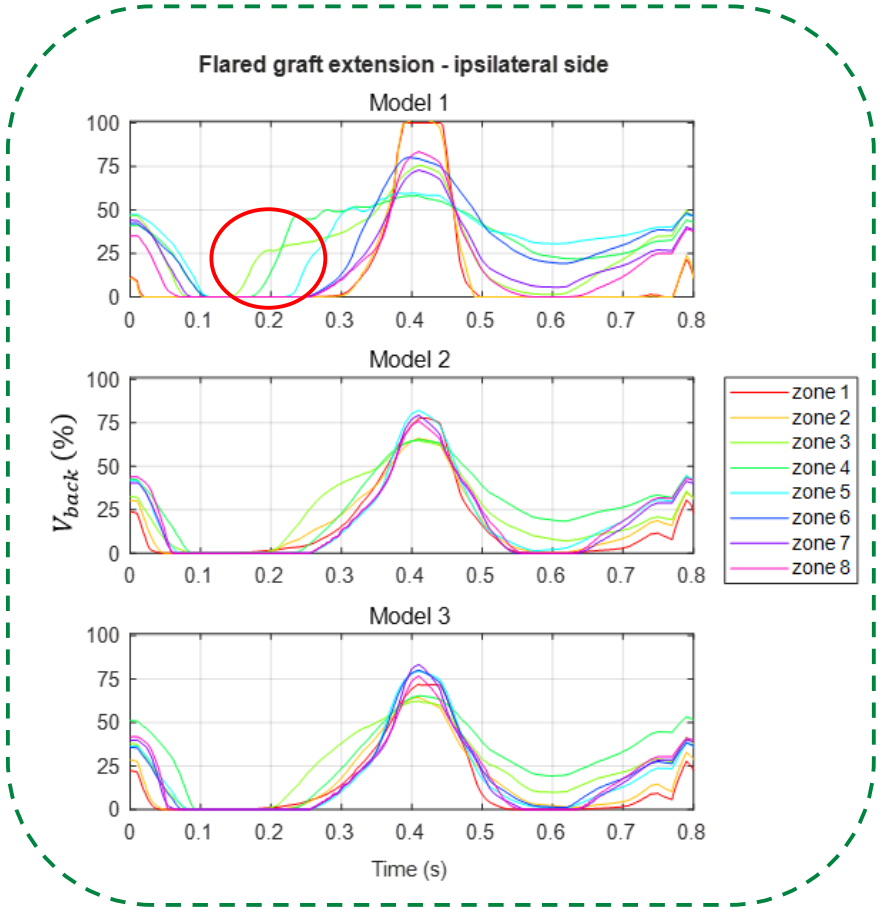

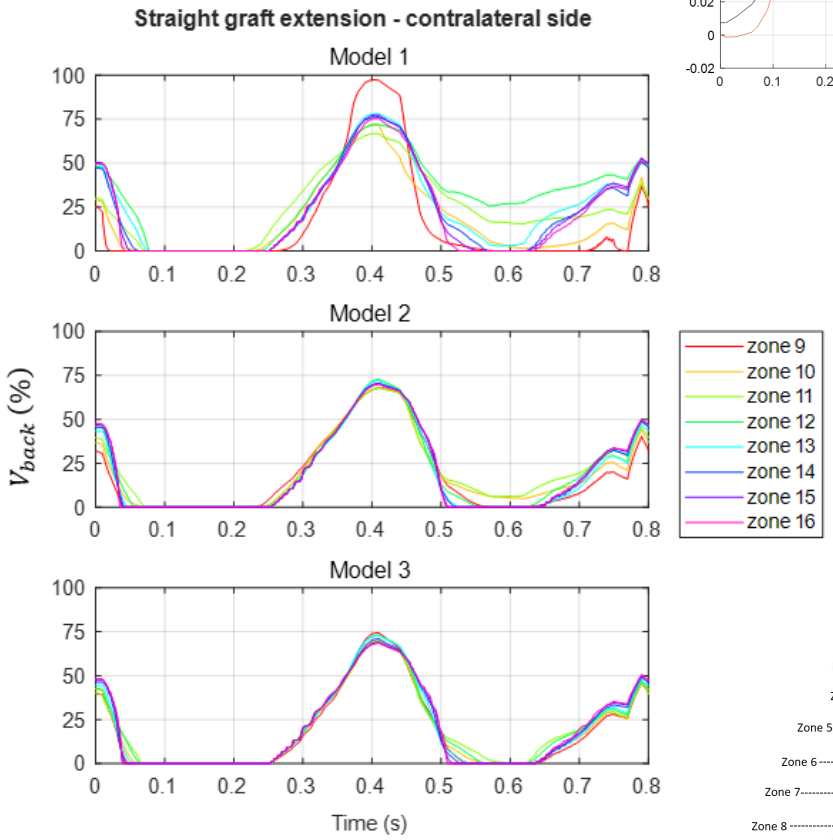

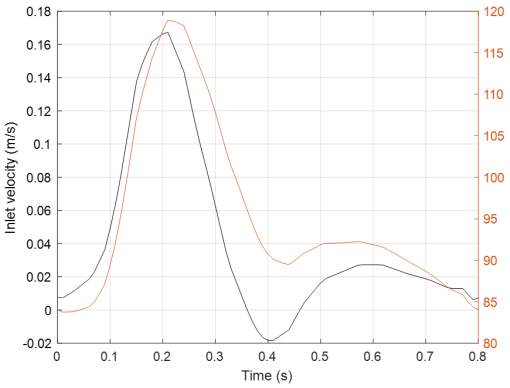

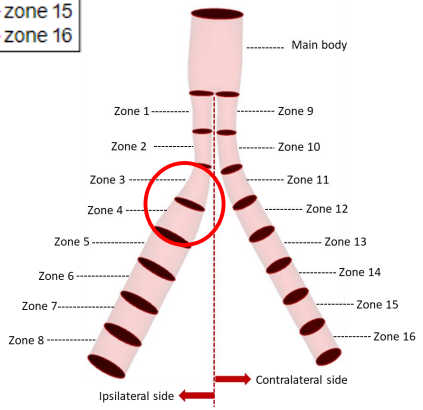

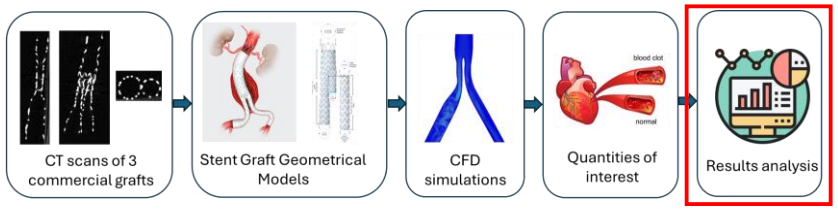

Recirculation Results: Velocity Analysis

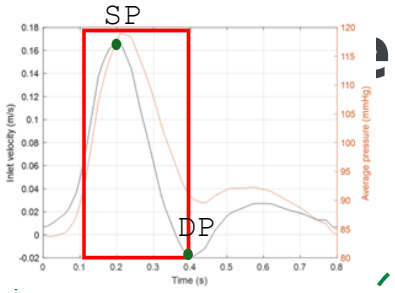

Velocity Vector Analysis

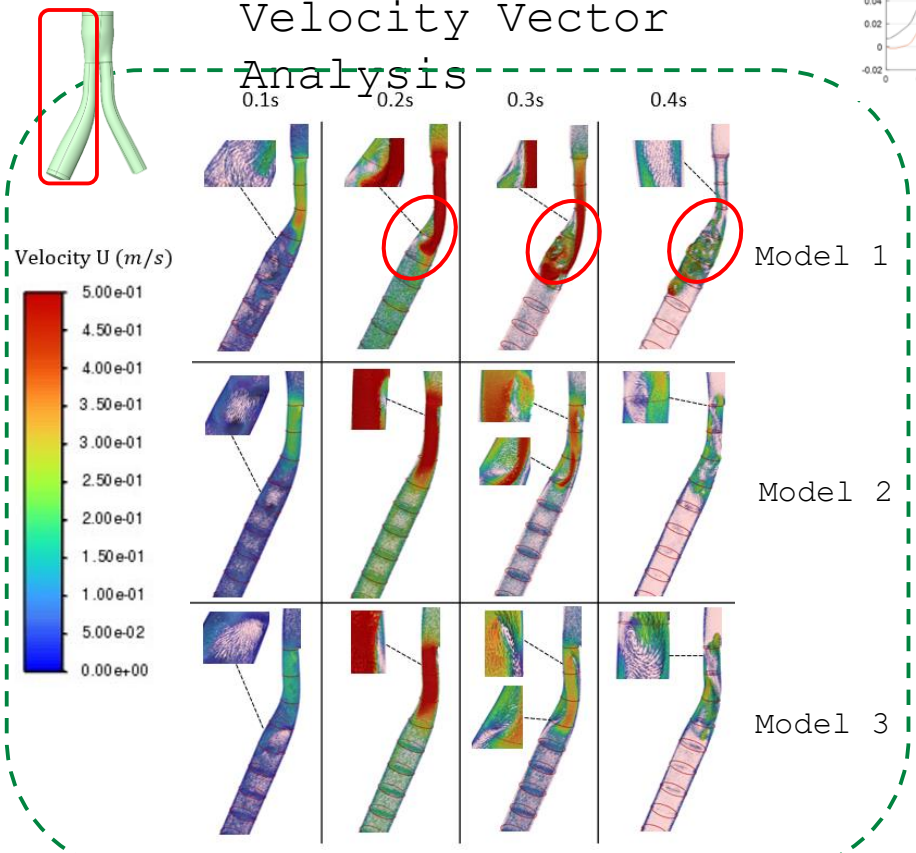

Velocity Blood Flow Simulation

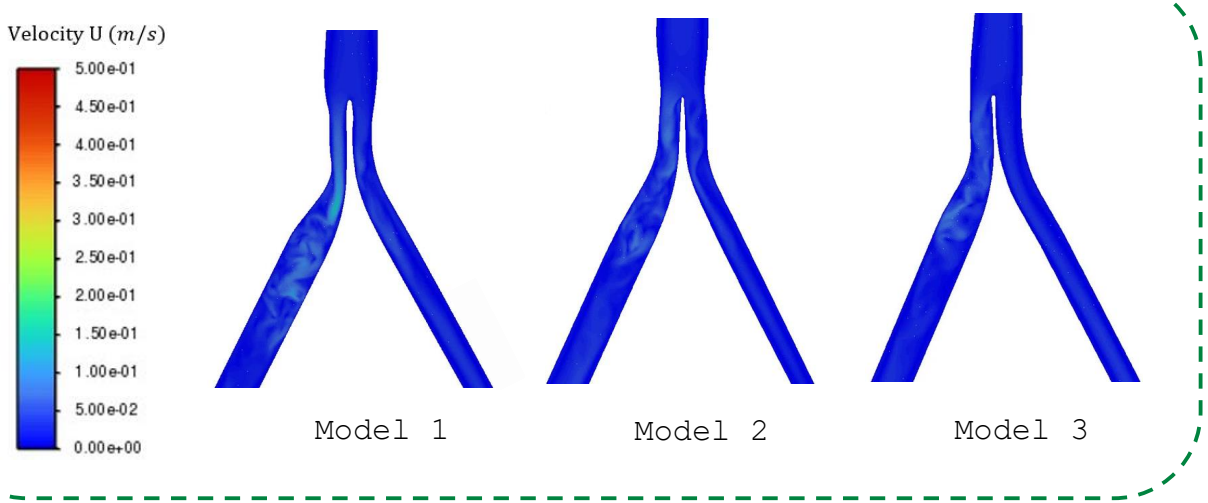

- Distinctive swirl in areas 3-5 of Model 1
- High flow disturbance in the flared extension of Model 1

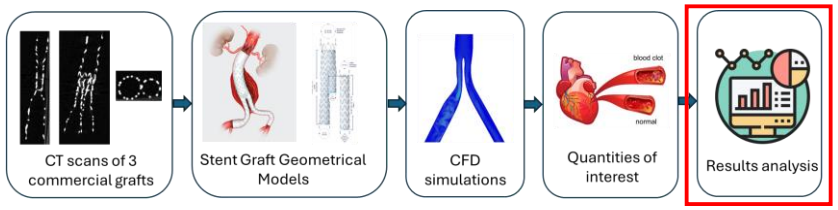

WSS-related Indices

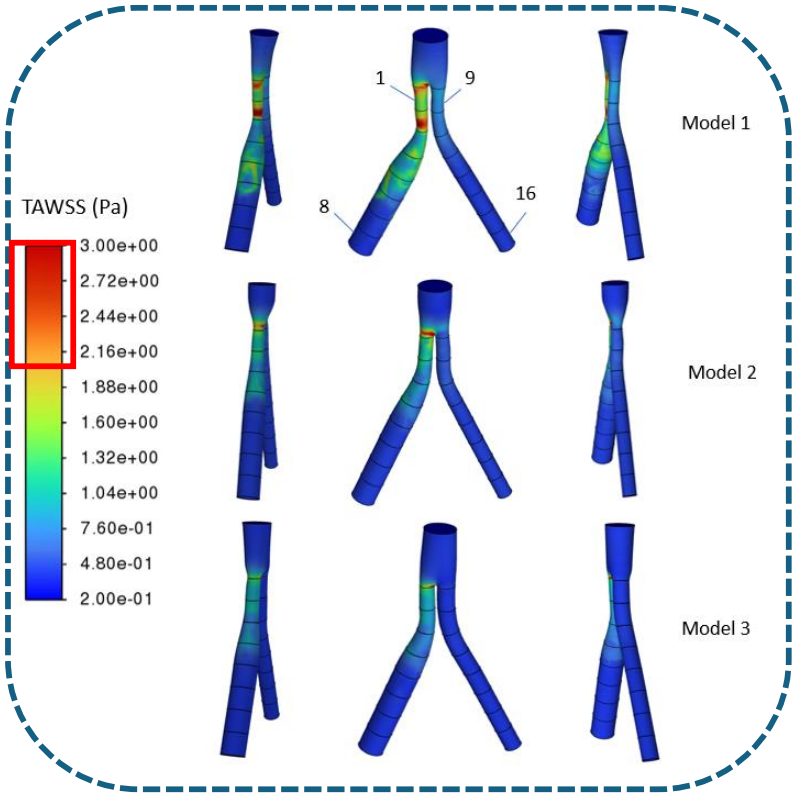

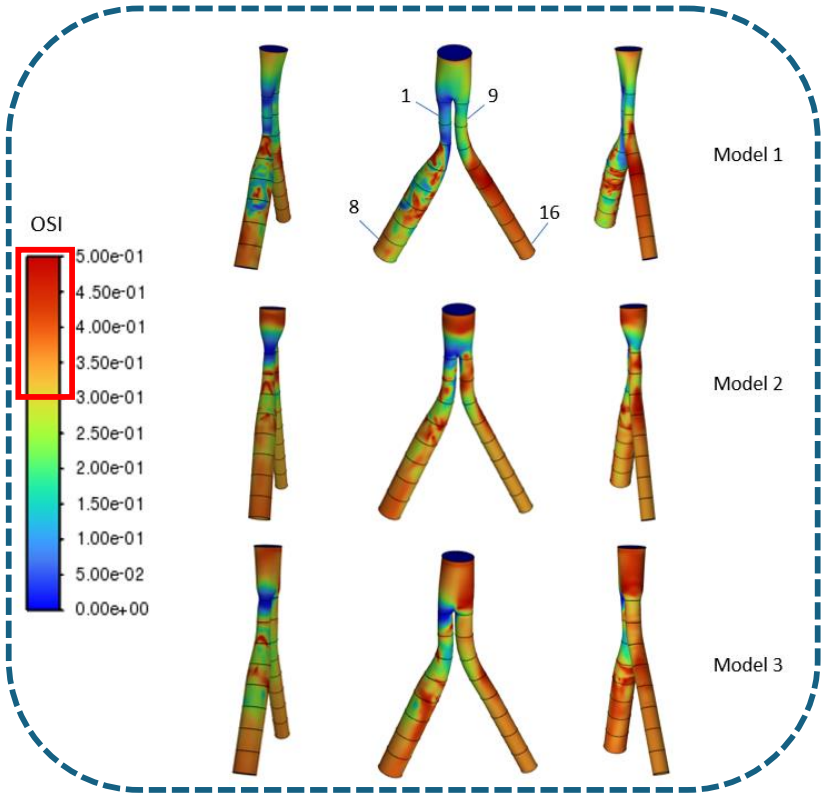

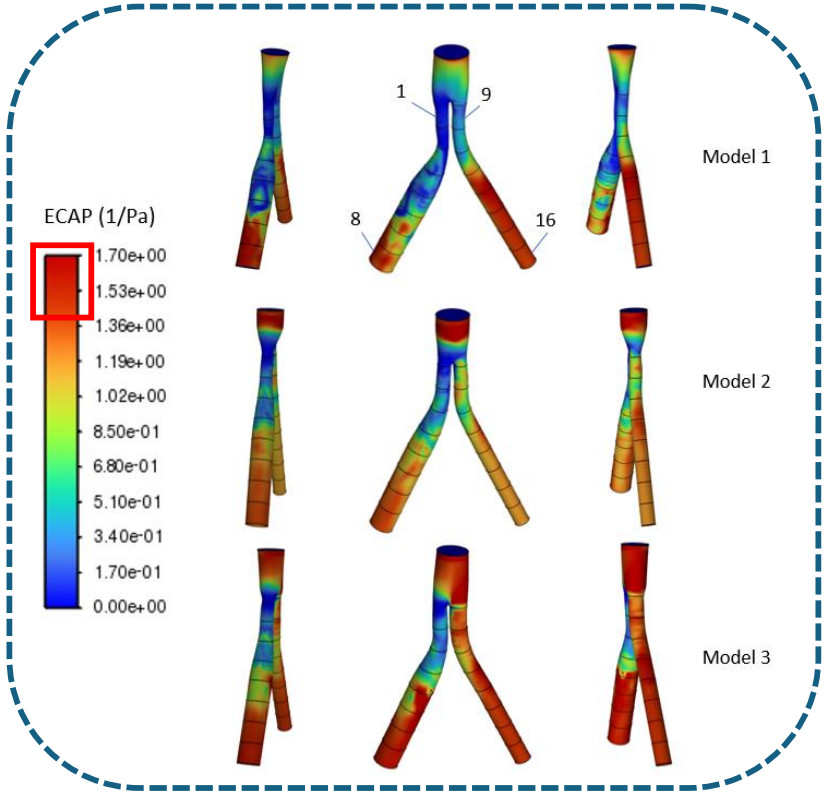

Controversial results
Challenging interpretation

Study III: Conclusions

A holistic examination of three simplified abdominal commercial stent grafts was presented to assess their thrombus proneness through a comprehensive blood flow analysis.

Research Highlights

- ✓ Stent graft CAD reconstruction can be challenging.
- ✓ SSR and recirculation analysis: flared extension of Model 1 is susceptible to blood clotting.
- ✓ WSS analysis: mixed results

Limitations & Future Directions

- ➢ Adoption of more precise geometrical models in the future
- ➢ Exploration of more complex implanted stent graft configurations
- ➢ Investigation of the impact of the adopted boundary conditions

Final Conclusions

Numerical Simulation

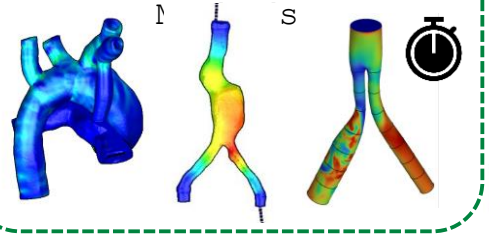

ROMs

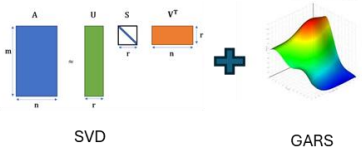

Patient-personalized pre-operative planning and

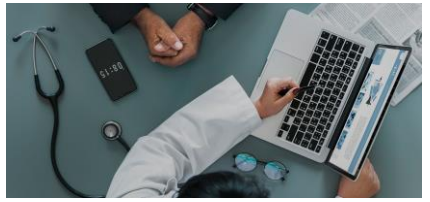

High-Performance Computing (HPC)

RBF mesh morphing

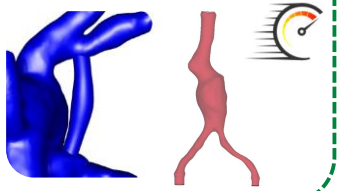

WSS-related indices

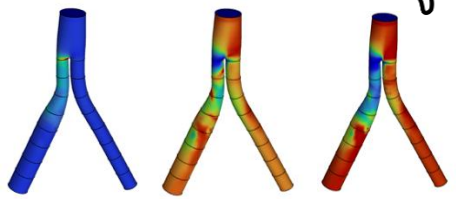

Shear Strain Rate & [illegible]culation

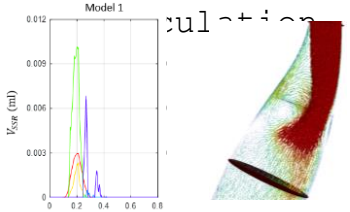

Thrombus Formation Mechanism

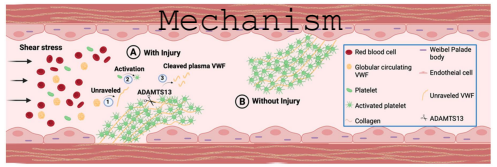

"ROMs seem a promising tool for supporting patients' preoperative planning and treatment."

"RBF mesh morphing enables rapid and efficient exploration across a wide spectrum of shape configurations."

"The conventional examination of WSS parameters might fall short of information."

"Parameters, tightly linked to the nature of the problem, appear to provide enlightening results"

T h a n k y o u a ll!









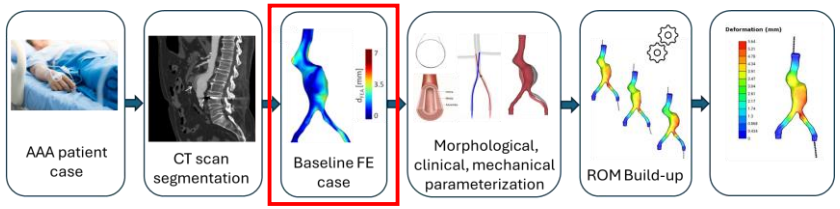

ContactMechanics Baseline Case

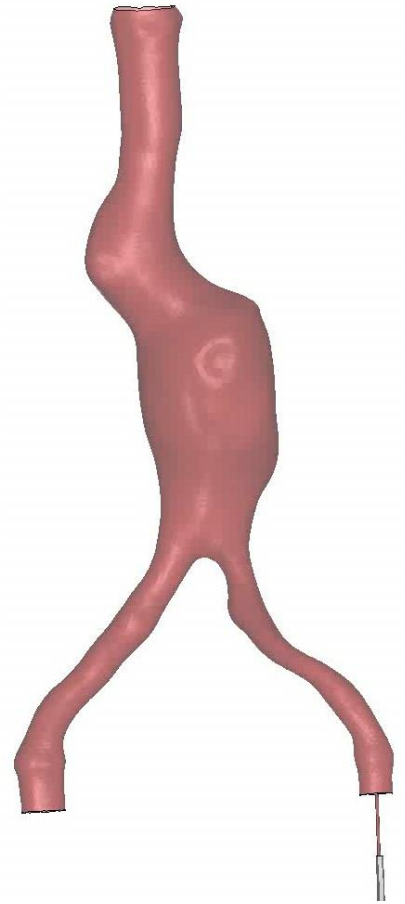

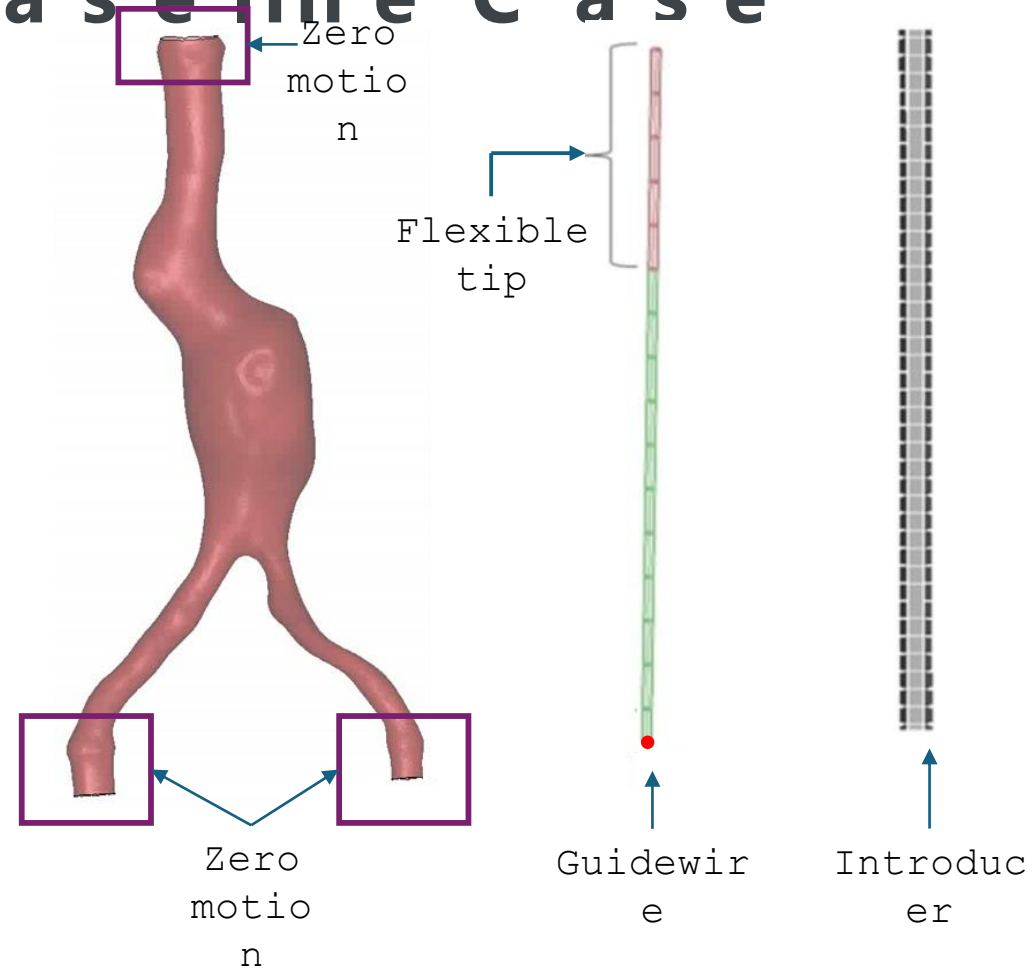

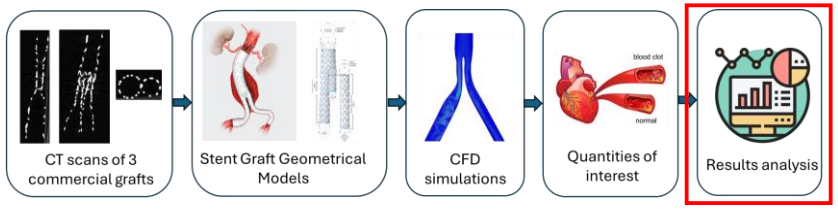

Recirculation Results

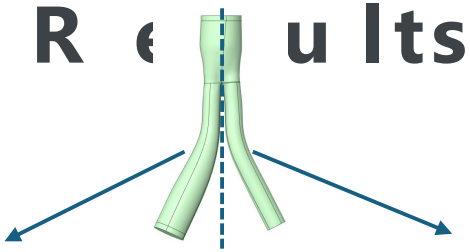

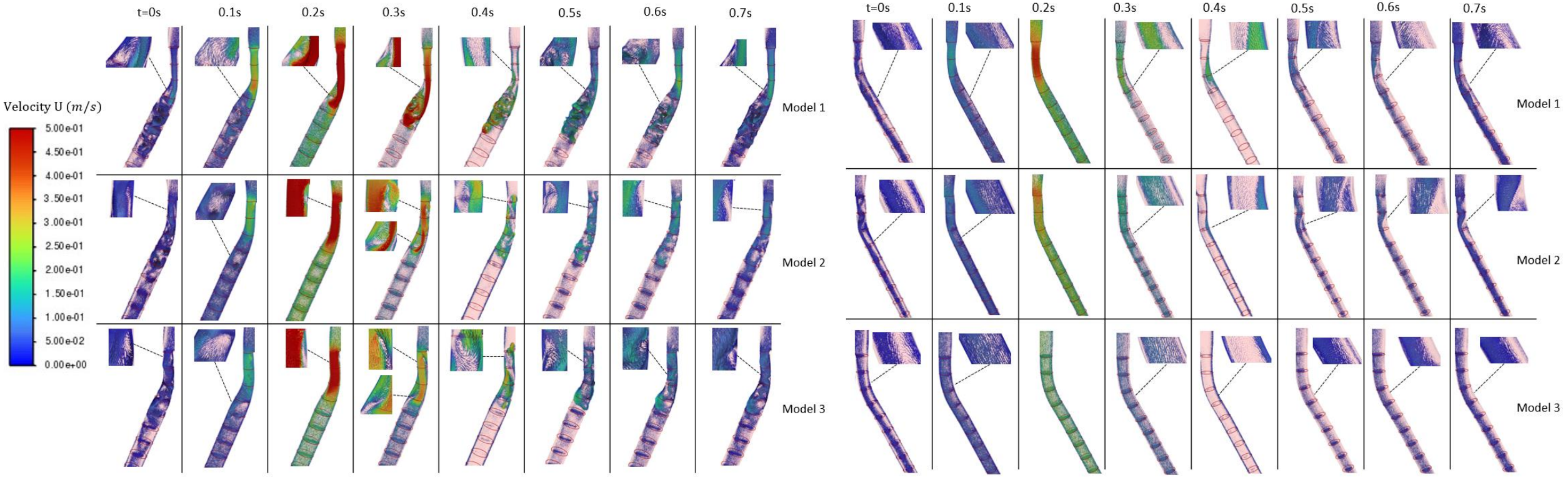

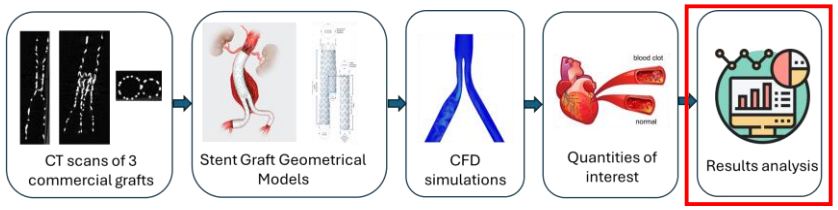

Recirculation Results

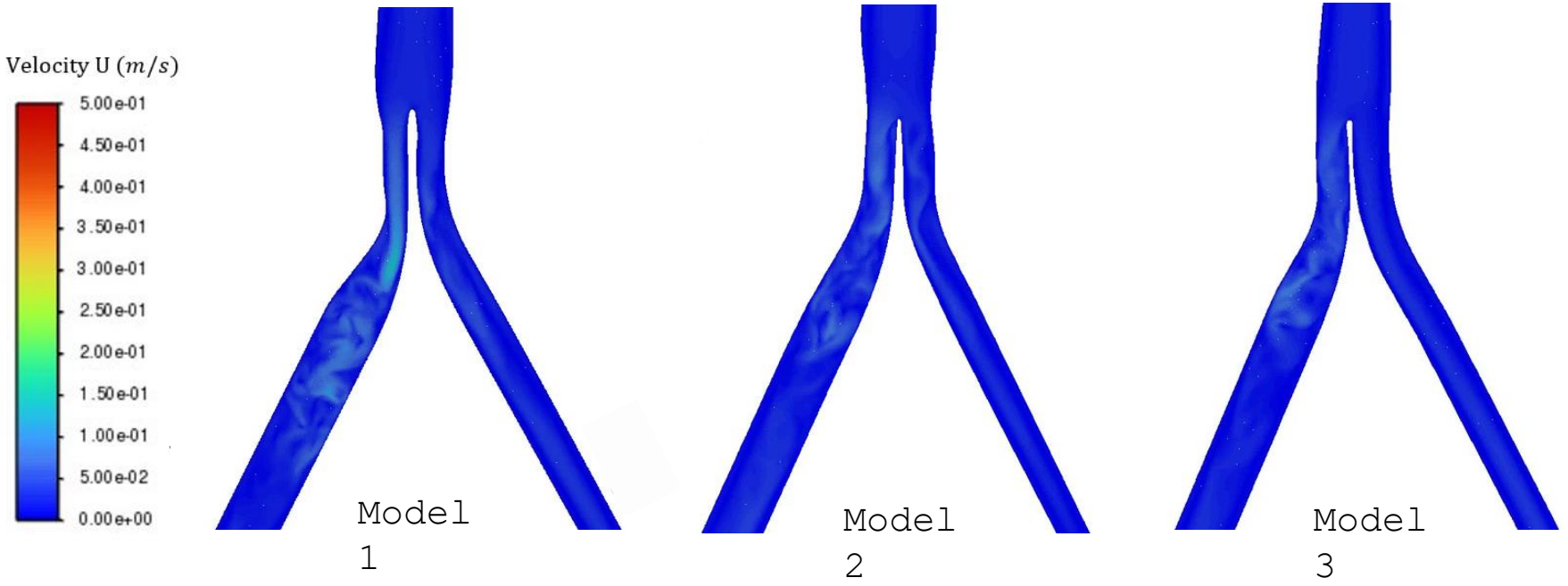

- Bigger jet on model 1
- People that support it

Final Conclusions

Numerical Simulation Methods

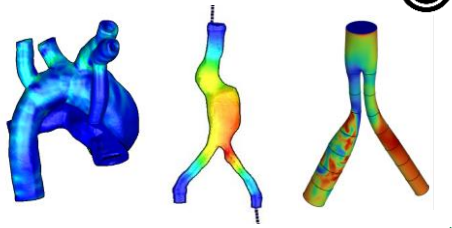

ROMs

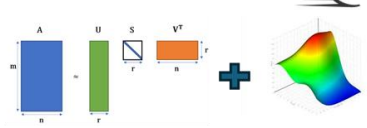

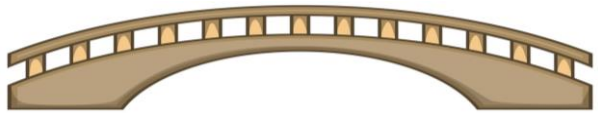

Patient-personalized pre-operative

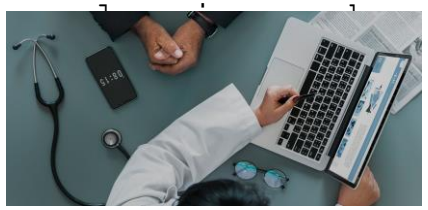

High-Performance Computing (HPC)

RBF mesh morphing

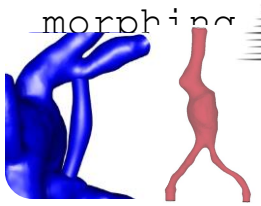

"ROMs seem a promising tool for supporting patients' preoperative planning and treatment."

"RBF mesh morphing enables rapid and efficient exploration across a wide spectrum of shape configurations."

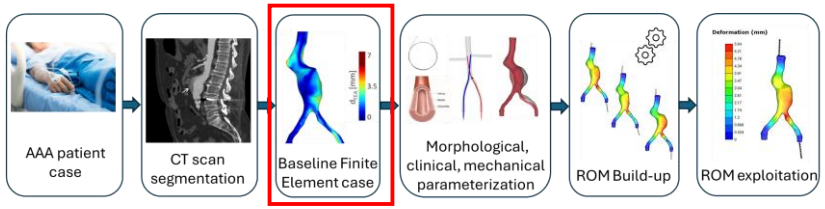

ContactMechanics FE Baseline Case

- Flexible tip: gradually decreasing elastic modulus, ranging from 1 to 50 GPa.
- Imposed velocity v(t) to the most distal node of the guidewire
- Frictionless contact algorithm between the guidewire and the vessel
- Standard penalty formulation contact type between the guidewire and the introducer

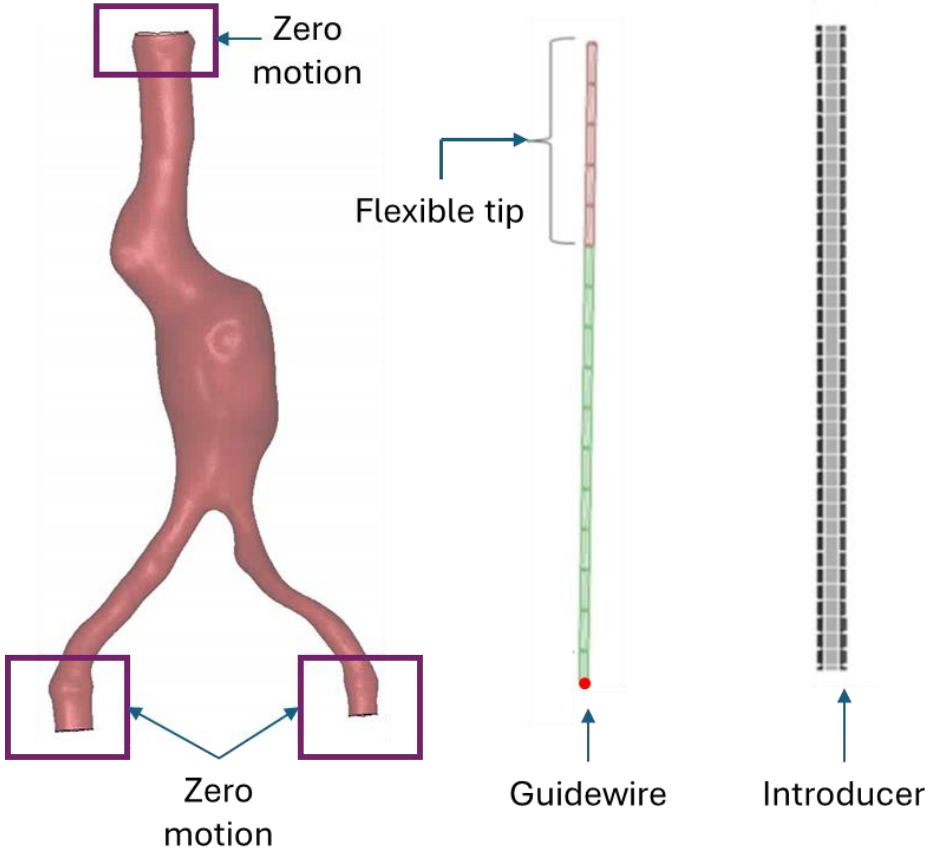

Thrombus formation and stentgrafts

Popular commercial AAA grafts
- Zenith Alpha by Cook Medical
- Excluder by W.L. Gore
- Endurant II by Medtronic

Jan, 2020 — Urgent field safety notice by Cook Medical Europe

Oct, 2021 — Zenith Alpha has an increased risk of limb graft occlusion (LGO) compared to Endurant and Excluder devices (Bogdanovic et al.)

Oct, 2022 — No relationship between COOK safety guidelines and LGO (Broda et al.)

IPT occurrence of Zenith Alpha graft is not significantly different compared to the rates of other commercial grafts (Draper et al.)

Nov, 2023 — The incidence rate of LGO was significantly higher in patients treated with Zenith Alpha than Endurant II (Ulsaker et al.)

The singular values in the diagonal matrix $\mathbf{S}$ are arranged in descending order. By exploiting this mathematical property, the matrix $\mathbf{A}$, which contains all the training data, can be approximated by a linear combination of the first r left singular vectors i.e. $\mathbf{U}_i^*$ with $i = 0, r$. The vectors included in $\mathbf{U}^*$ are referred to as modes.

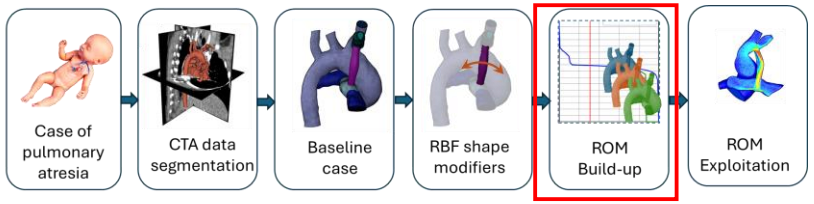

ROM Build-up: General Concept

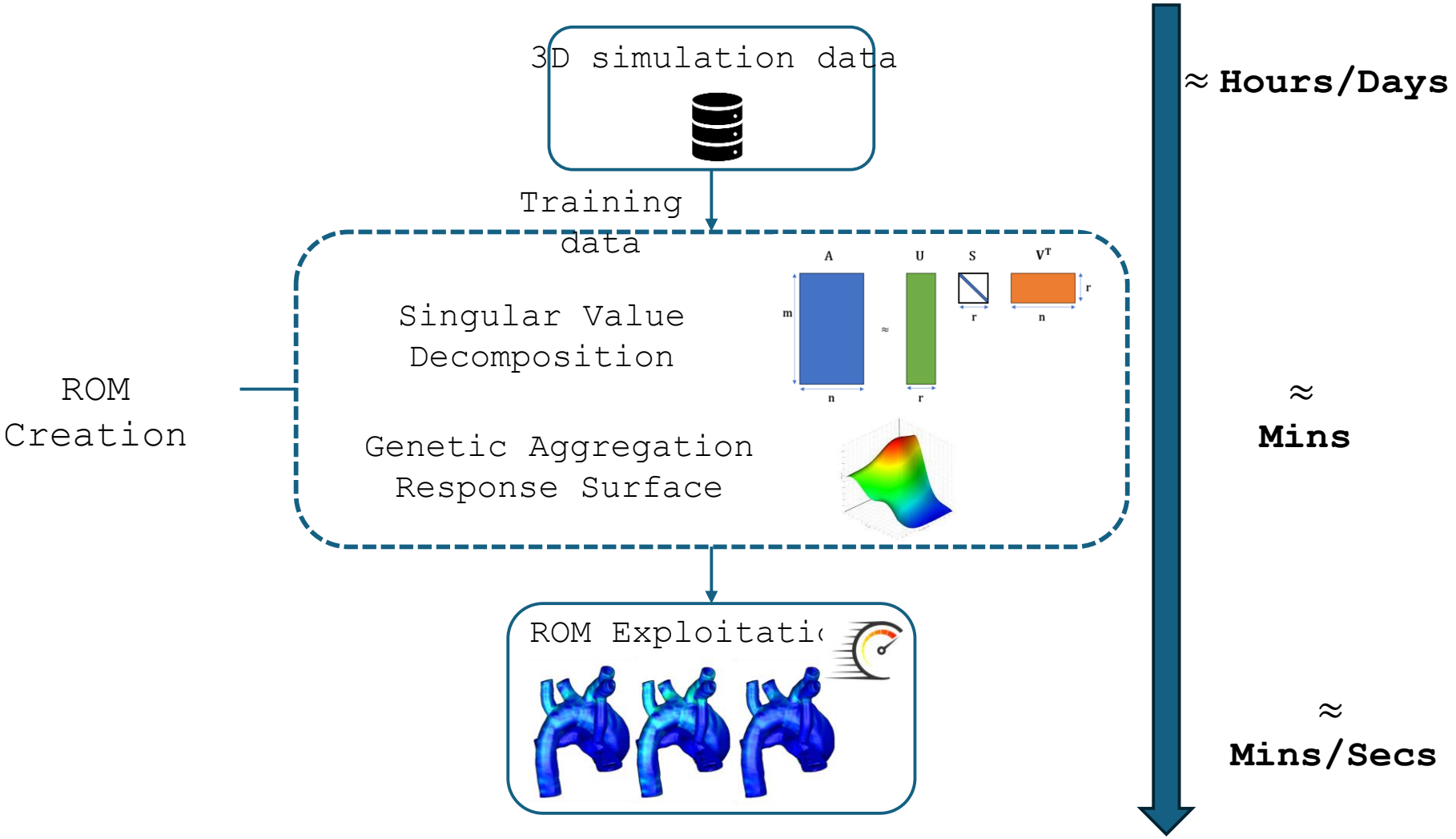

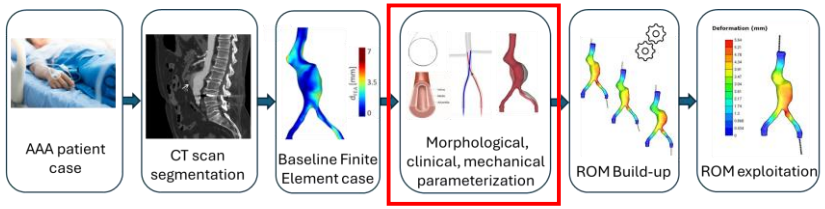

Morphological Parameterization

- 3 Shape modifiers
- 3 categories of source points (SP)
- 3 categories of domains (D)

The combination of the shape modifiers enabled us to explore a broad spectrum of possible aortic configuration

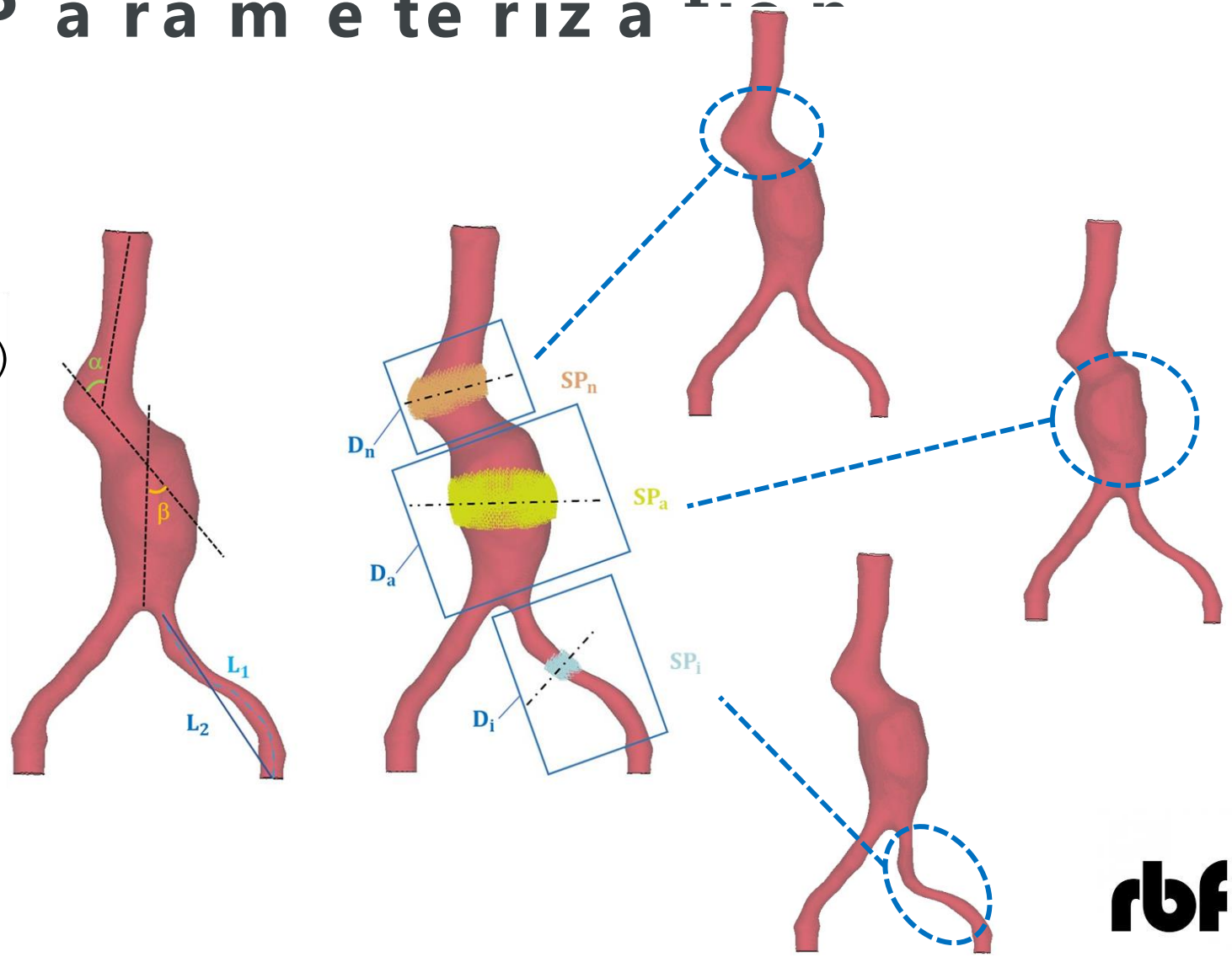

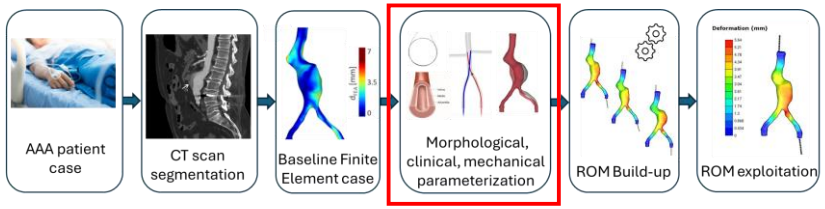

Morphological Parameterization

- 3 Shape modifiers
- 3 categories of source points (SP)
- 3 categories of domains (D)

The combination of the shape modifiers enabled us to explore a broad spectrum of possible aortic configuration

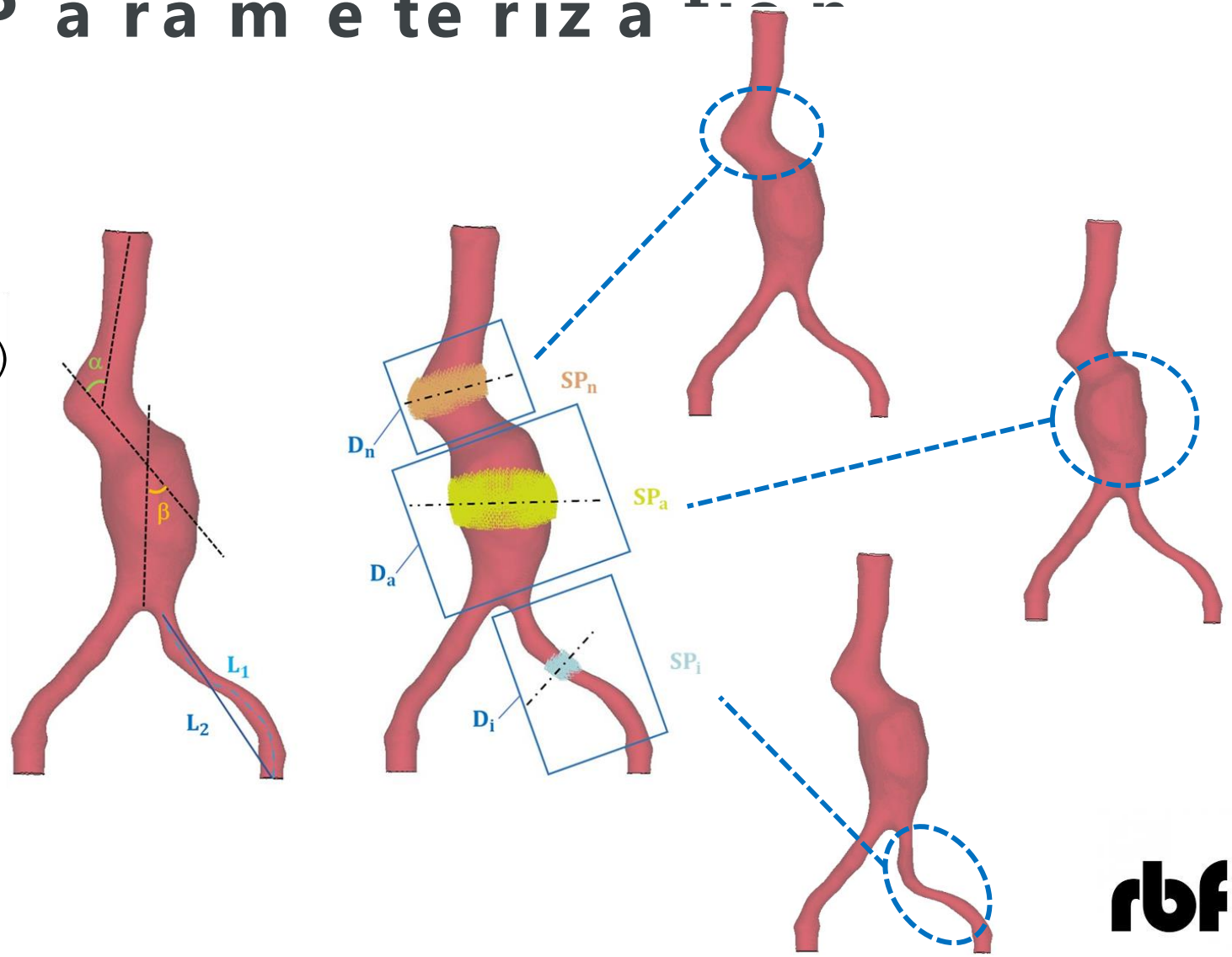

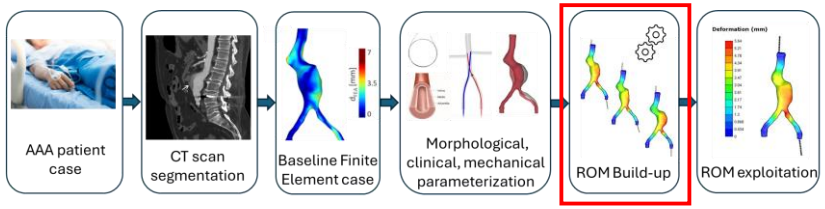

Parametric Data Generation

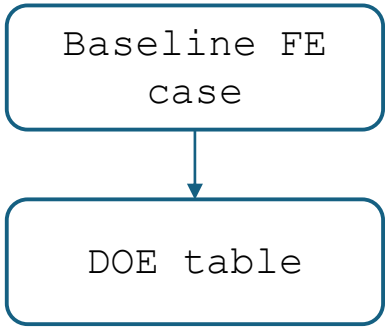

No. Scenario	E_{aorta}	E_{wire}	…	T
1	1.0	80	…	0.10
2	2.1	120	…	0.09
…	…	…	…	…
300	0.9	190	…	0.13

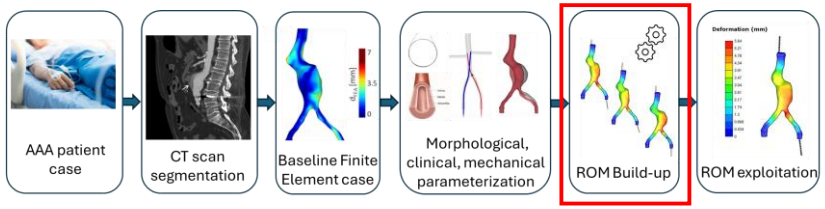

Parametric Data Generation

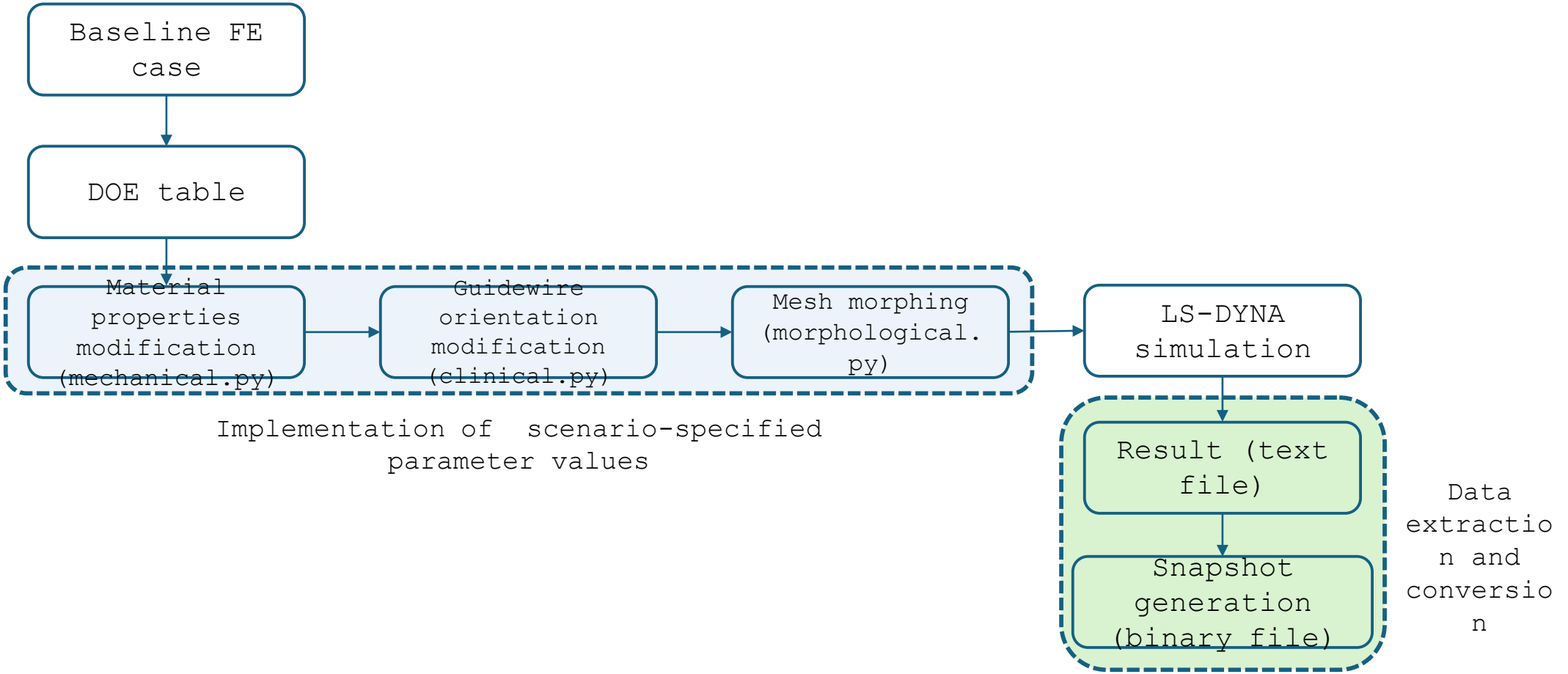

Cardiovascular diseases (CVDs)

"Cardiovascular diseases (CVDs) are the leading cause of death globally."

World Health Organization

" Responsible for 1.8 million deaths in the European Union and the United Kingdom in 2020."

"CVDs cost the EU economy 282 billion € in 2021."

Oxford Population Health's Health Economics Research Centre

CVDs causes

Popular CVD types

- Coronary heart disease
- Cerebrovascular disease
- Peripheral arterial disease
- Congenital heart disease
- Vein thrombosis and pulmonary embolism
- Aortic diseases

Post-EVAR Complications

The rate of complications is estimated to range between 16% and 30%

Endoleak 57%

Thrombosis 11%

Graft migration 15%

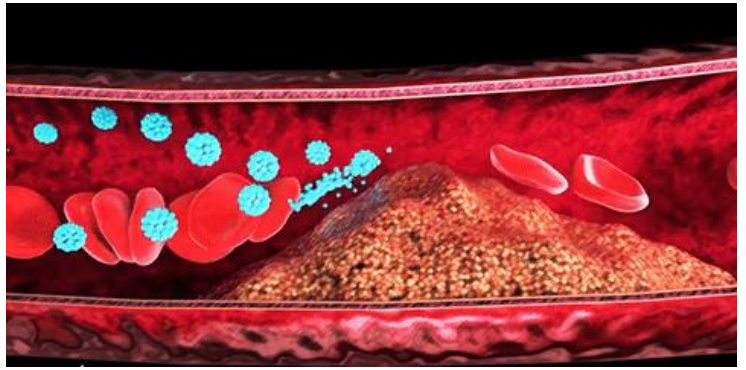

Stent Graft

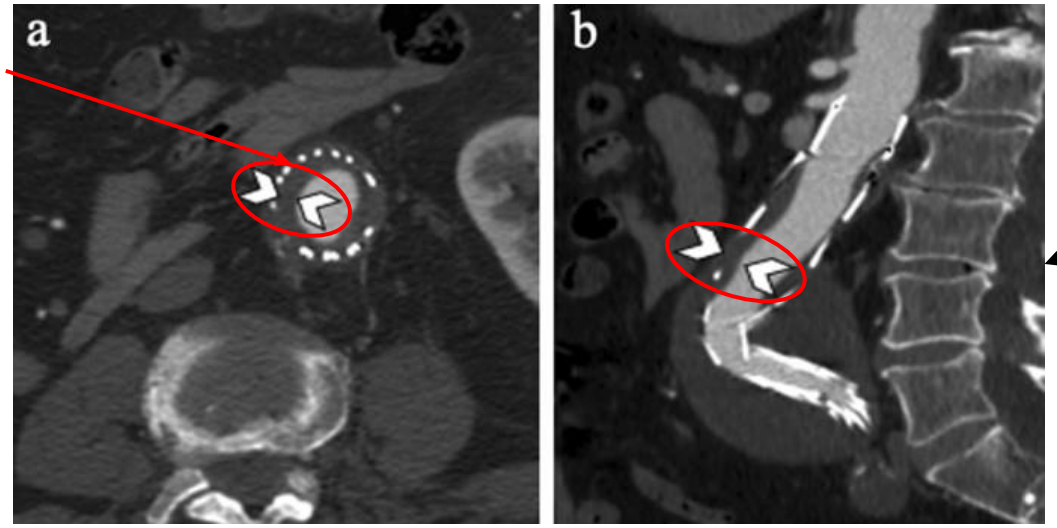

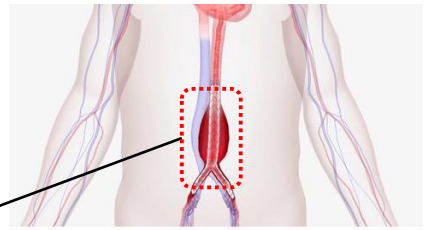

Abdominal Aortic Aneurysms (AAAs)

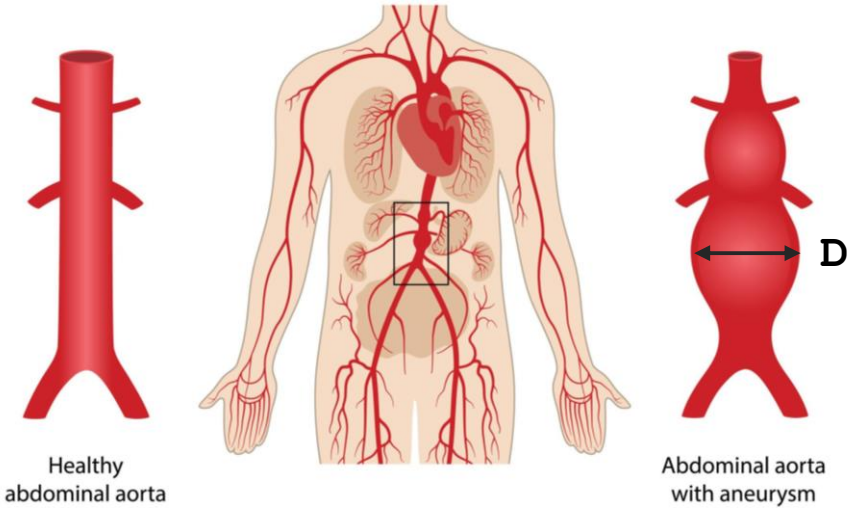

An abdominal aortic aneurysm (AAA) is the bulging or 'ballooning' of the abdominal aorta.

Surgery criterion is recommended for D > 5.5 cm

About one person in 1000 develops an AAA between the ages of 60 and 65

"Prevention is better than cure."

Around 8 out of 10 people with a rupture either die before they reach the hospital or don't survive surgery.

Cardiovascular diseases (CVDs)

"Cardiovascular diseases (CVDs) are the leading cause of death globally."

World Health Organization

" Responsible for 1.8 million deaths in the European Union and the United Kingdom in 2020."

"CVDs cost the EU economy 282 billion € in 2021."

Oxford Population Health's Health Economics Research Centre

CVDs causes

Popular CVD types

- Coronary heart disease
- Cerebrovascular disease
- Peripheral arterial disease
- Congenital heart disease
- Vein thrombosis and pulmonary embolism
- Aortic diseases

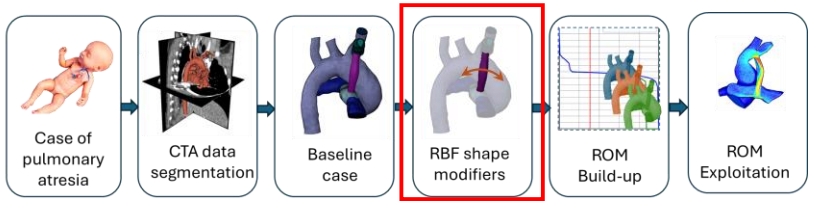

ROM Build-up

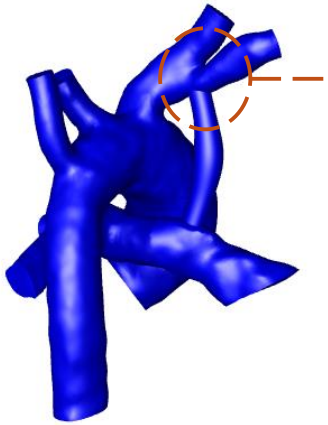

Superior MBTS boundary SP

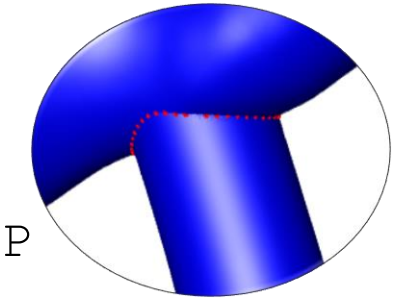

x translation

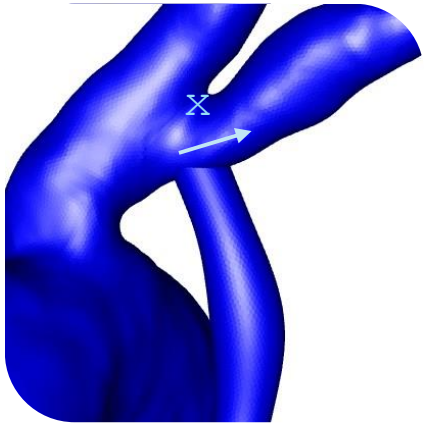

y translation

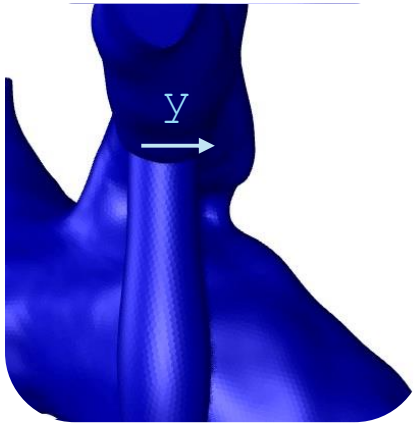

y rotation

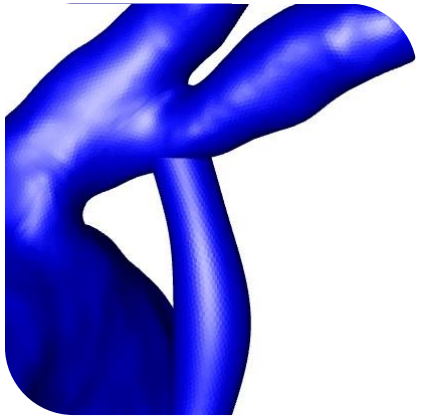

x rotation

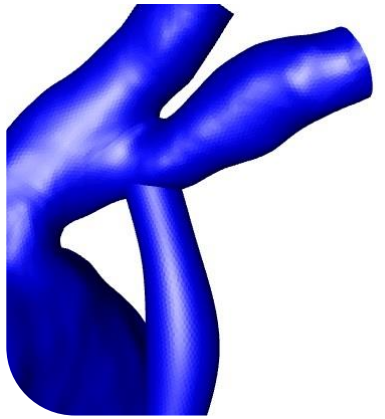

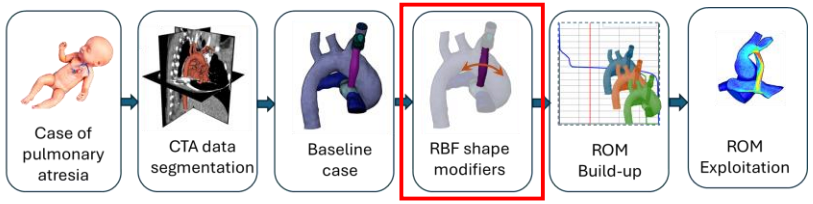

Twelve RBF Shape modifiers

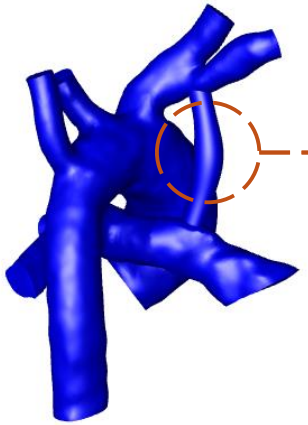

Cylindrical periphery SP

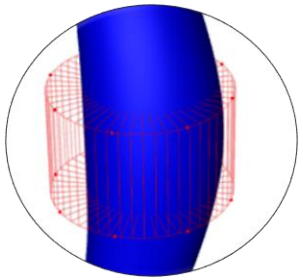

x translation

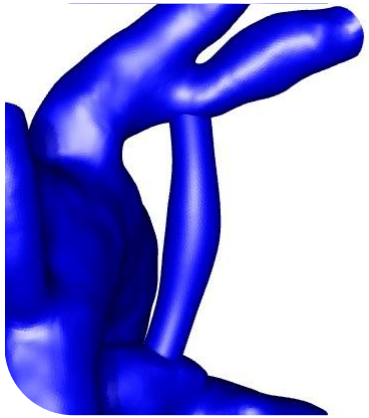

y translation

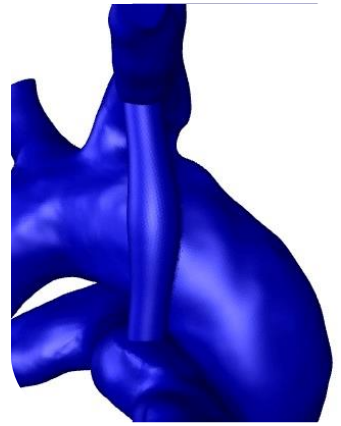

Maximum diameter SP

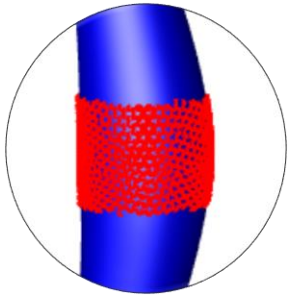

x translation

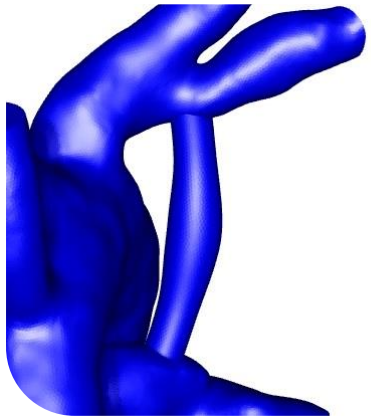

y translation

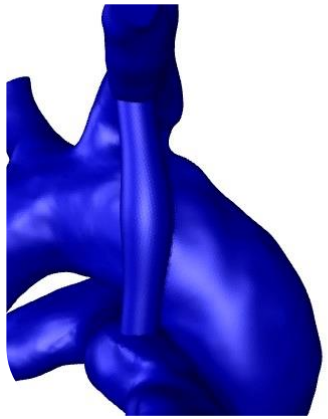

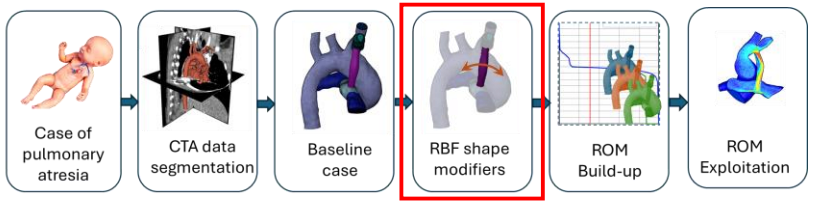

Twelve RBF Shape modifiers

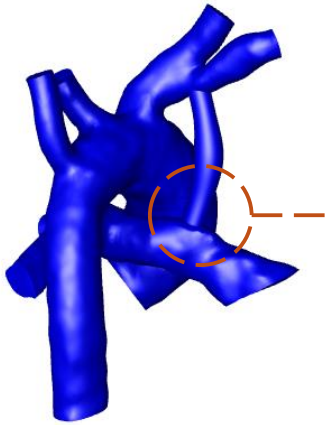

Inferior MBTS boundary SP

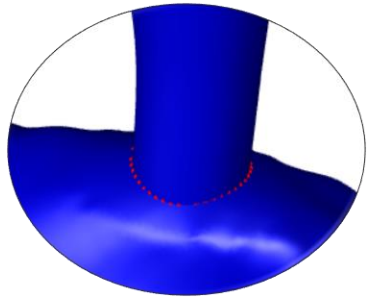

x translation

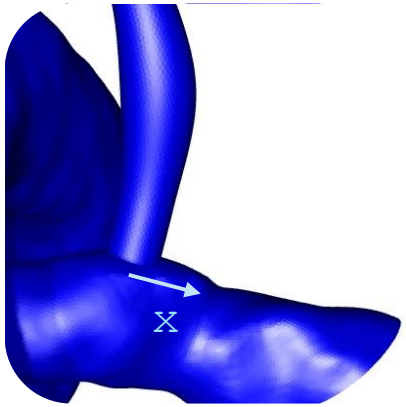

y translation

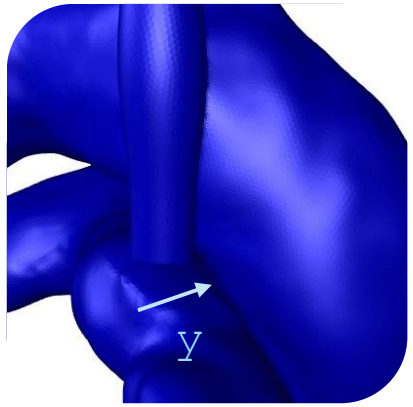

y rotation

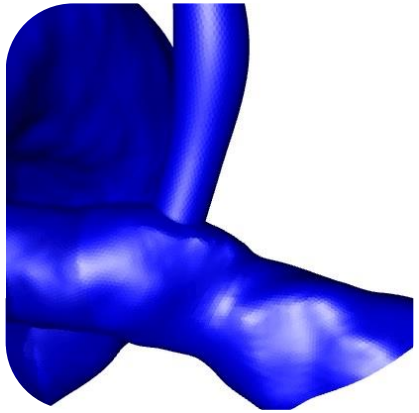

x rotation

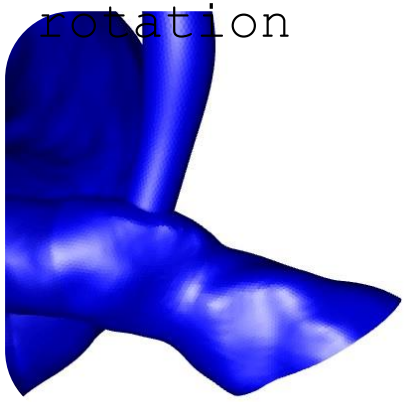

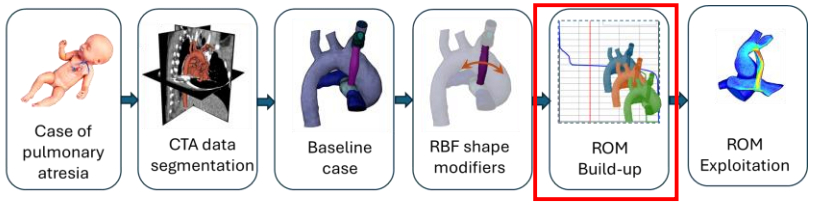

ROM Build-up: General Concept

$$\mathbf{A}_r^* = \mathbf{U}_r^* \, \mathbf{S}_r^* \, \mathbf{V}_r^{\mathrm{T}*} = \mathbf{U}_r^* \, \mathbf{C}$$

$$\mathbf{C} = [\alpha_1, \alpha_2, \ldots, \alpha_r]$$

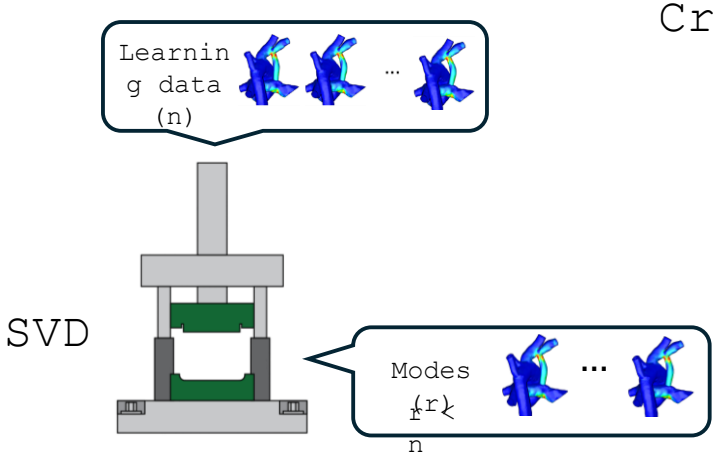

ROM Creation

Singular Value Decomposition (SVD)

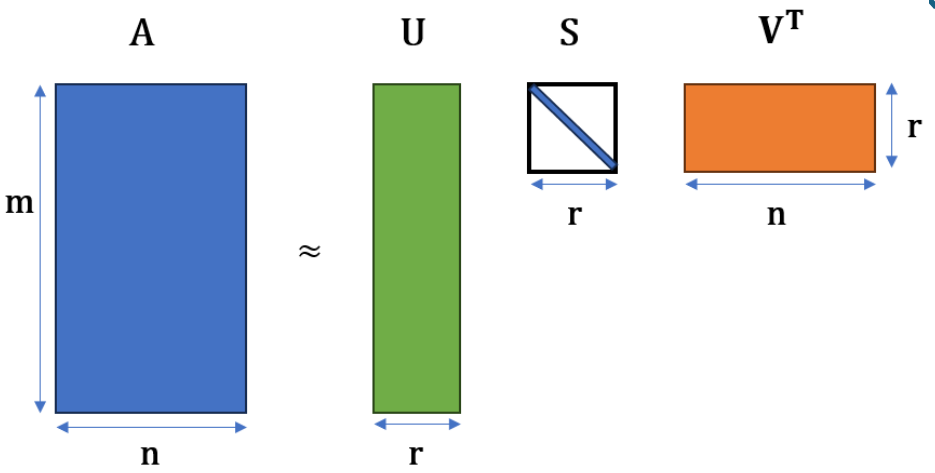

Genetic Aggregation Response Surface (GARS)

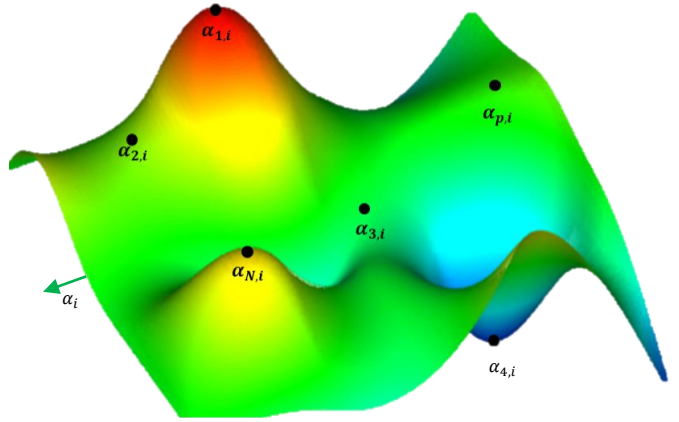

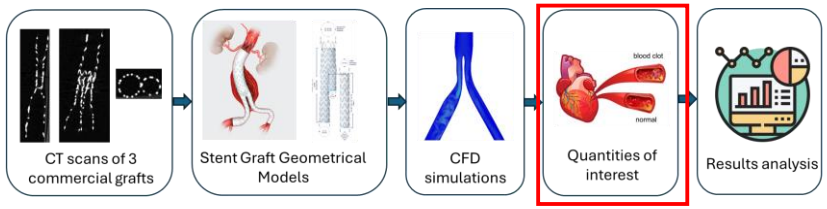

Recirculation & Blood clots

1 Recirculation → Reverse flow monitoring

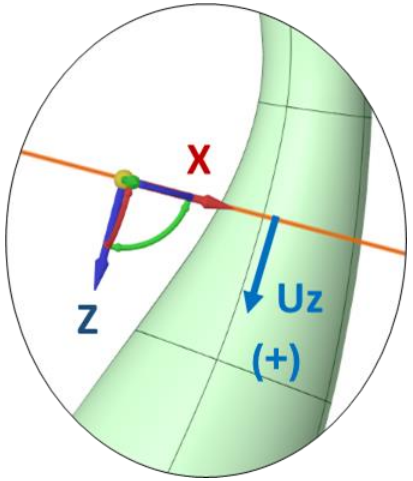

$$V_{back} = \frac{\sum v_{cell}}{V_{zone}} \; 100\% \; of \; U_z < 0$$